This is to certify that the
dissertation entitled

PATHOGENESIS AND TREATMENT OF TYPE 1 DIABETIC OSTEOPOROSIS

presented by

KATHERINE JEAN MOTYL

has been accepted towards fulfillment
of the requirements for the

Doctoral degree in Physiology

Laura P. McCabe
Major Professor's Signature

May 7, 2010
Date

DATE DUE	DATE DUE	DATE DUE

PATHOGENESIS AND TREATMENT OF TYPE 1 DIABETIC OSTEOPOROSIS

By

Katherine Jean Motyl

A DISSERTATION

Submitted to
Michigan State University
in partial fulfillment of the requirements
for the degree of

DOCTOR OF PHILOSOPHY

Physiology

2010

ABSTRACT

PATHOGENESIS AND TREATMENT OF TYPE 1 DIABETIC OSTEOPOROSIS

By

Katherine Jean Motyl

Type 1 diabetes (T1-diabetes) is a chronic condition characterized by hypoinsulinemia and hyperglycemia. Patients with T1-diabetes are susceptible to complications, including osteoporosis. Bone loss from diabetes increases risk of fracture and impairs fracture healing. Understanding the mechanism of diabetic osteoporosis is important for choosing the best therapies. Reduced bone formation (not altered resorption) is responsible for diabetic bone loss. Additionally, rodent models of T1-diabetes (streptozotocin and the non-obese diabetic mouse) have increased marrow adipocyte number compared normal, suggesting mesenchymal stem cell lineage selection favors the osteoblast over the adipocyte in diabetic conditions. In Chapter 2, we characterized the bone phenotype of mice during diabetes induction and found that markers of osteoblasts and adipocytes were altered as early as two days after blood glucose levels began to rise. Because diabetes is associated with inflammation, we measured serum and bone pro-inflammatory cytokine levels and found increases in cytokines that coincided with reduced osteoblast activity. Diabetes is also associated with reduced serum leptin, a hormone secreted by adipocytes that is capable of promoting bone formation in conditions of unloading. In Chapter 3, we treated diabetic mice with leptin and found that chronic subcutaneous leptin infusion prevented diabetic marrow adiposity but not bone loss, suggesting that

marrow adiposity is not required for diabetic osteoporosis. In Chapter 4, we induced diabetes in mice lacking CCAAT/enhancer binding protein beta (C/EBPβ), a transcription factor that promotes adiposity and prevents osteoblast differentiation. We found that under diabetic conditions, the lack of C/EBPβ actually enhanced adipocyte differentiation in bone and increased bone resorption, which is not classically observed in T1-diabetes. In Chapter 5, we found reduced Wnt10b, a strong activator of osteoblast differentiation and inhibitor of adipogenesis, in diabetic bone. To test whether Wnt10b was a factor influencing bone changes in diabetes, we induced T1-diabetes in mice with overexpression of Wnt10b in osteoblasts. Wnt10b mice were protected from bone loss but not marrow adiposity in diabetes. Finally, in Chapter 6 we examined the ability of intermittent parathyroid hormone (PTH), the only anabolic osteoporosis therapy available to patients, to promote bone formation in diabetes. We found that PTH increased osteoblast maturation and prevented osteoblast death, even under diabetic conditions. Bone density levels of diabetic mice returned to those of untreated controls, even after bone loss had already occurred. Taken together, Chapters 2-5 demonstrate that bone marrow fat is likely not necessary for diabetic bone loss. Additionally, Chapter 5 and 6 suggest that anabolic therapies targeting Wnt10b/wnt signaling could improve bone density in diabetic patients.

Dedicated to my husband Chris and our beautiful son Henry for their unconditional love and encouragement through the good times and the better times. I love you both.

ACKNOWLEDGMENTS

Dr. Laura McCabe is deserving of a very large portion of this section. I still remember the day that I met her in her office and begged her to let me rotate in the lab. She did, of course (she has trouble saying "no") and the rest is history. It has been a thrill to be a part of the research that she is so passionate about. She has always been approachable and grounded, and a source of wisdom and encouragement for life and lab. Thank you Laura.

My committee members, Dr. Ron Meyer, Dr. Narayannan Parameswaran, Dr. Gloria Perez, and Dr. Richard Schwartz have given me useful input and guidance over the past five years. Thank you for all of the time you have spent helping me to achieve this goal.

Regina Irwin and Lindsay Martin, my current lab mates, have always given me something to laugh about. Thank you for the time you have given and continue to give to this research. Also, thank you to the other graduate students, undergraduate students, volunteers and rotation students who have donated their time to these worthy projects. Thank you to the Department of Physiology for their support.

Thank you to my family Chris and Henry for keeping me smiling through this entire process. Thank you to my parents, Ken and Del Frank and to my in-laws Dave and Michelle Motyl for encouraging me to do my best and for supporting me in all of the decisions that I have made.

TABLE OF CONTENTS

LIST OF TABLES

LIST OF FIGURES

LIST OF ABBREVIATIONS

AP-1	activator protein 1
AGE	advanced glycation end product
ATP	adenosine triphosphate
BADGE	bisphenol-A-diglycidyl ether
BMC	bone mineral content
BMD	bone mineral density
BMI	body mass index
BMU	basic multicellular unit
BVF	bone volume fraction
bZIP	basic region-leucine zipper
Cbfa1	core binding factor 1
C/EBP	CCAAT enhancer binding protein
CRP	C-reactive protein
CSF1R	colony stimulating factor 1 receptor
Dkk	dickkopf
Dlx	distaless
DNA	deoxyribonucleic acid
dpi	days post injection
FABP4	fatty acid binding protein 4
Fra-1	Fos-related antigen 1
Fzd	frizzled
GDM	gestational diabetes mellitus
GLUT	glucose transporter
GSK3β	glycogen synthase kinase 3 beta
Hb A_{1C}	glycated hemoglobin
HD	homeodomain
IFN-γ	interferon gamma
Ins2	insulin 2
IRKO	insulin receptor knockout
KO	knockout
LAP	liver activating protein
LEF	lymphoid enhancer factor
LIP	liver inhibitory protein
LRP	low density lipoprotein receptor-related protein
M-CSF	macrophage colony stimulating factor
MSC	mesenchymal stem cell
Msx	meshless
NF-κB	nuclear factor kappa-B
OPG	osteoprotegrin
PICP	procollagen carboxy-terminal extension peptide
PPARγ	peroxisome proliferator-activated receptor gamma
Pref-1	preadipocyte factor 1
PTH	parathyroid hormone

RANK	receptor activator of nuclear factor kappa-B
RANKL	receptor activator of nuclear factor kappa-B ligand
ROS	reactive oxygen species
Runx2	runt related transcription factor 2
Ser	serine
sFRP	secreted frizzled-related protein
SREBP	sterol regulator element binding protein
STZ	streptozotocin
T1-diabetes	type 1 diabetes mellitus
T2-diabetes	type 2 diabetes mellitus
TCF	T-cell factor
TNFα	tumor necrosis factor alpha
TRAP	tartrate-resistant acid phosphatase
Thr	threonine
WT	wildtype

CHAPTER 1

1. LITERATURE REVIEW

1.1. BONE

Bone is the structural connective tissue comprising the skeleton of reptiles, mammals, amphibians and some fish (i.e. higher vertebrates) (1). Highly dynamic, bone is constantly remodeling in response to physiological stimuli. Remodeling (the process of bone formation and resorption) ensures that bone fulfills its basic functions of structural support and calcium homeostasis. Defects in remodeling lead to either too much or too little bone, both of which can have debilitating consequences.

1.1.1. Molecular composition of bone

Bone is made of a mineralized matrix of collagen proteins containing 99% of the calcium, 85% of the phosphate, and 50% of the magnesium in the body (2). Outside of bone, calcium is important for a variety of cellular functions including muscle contraction and neurotransmitter release and its levels are therefore tightly controlled (2). The major protein component of the bone matrix is type 1 collagen, with smaller contributions from other collagens. Non-collagenous proteins in the bone matrix include osteocalcin, which is secreted by osteoblasts

(bone forming cells), binds calcium, and is clinically used as a blood marker of osteoblast activity (2). Other proteins in the matrix are important for cell attachment, collagen fibril formation, and sensing of mechanical stress (2).

1.1.2. Cellular composition of bone

Embedded in the bone matrix are osteocytes, and on the surface of bone are bone lining cells, osteoblasts, and osteoclasts (Figure 1). Osteoblasts, bone lining cells, and osteocytes are derived from mesenchymal stem cells. Osteoblasts are responsible for the deposition of bone matrix, which is subsequently mineralized either by osteoblast derived matrix vesicles, or through processes initiated by collagen molecules themselves, although these processes of mineralization are poorly understood (1). Osteocytes are mature osteoblasts that occupy circular structures called lacunae and are thought to be responsible for some maintenance of the bone matrix (1). Bone lining cells are flat and cover the surface of the bone but do not form or resorb bone (1). Multinucleated osteoclasts are derived from hematopoietic precursors and are responsible for the resorption of mineralized bone (1). Osteoclasts, nearby osteoblasts that deposit osteoid and mineral in their wake and the more distal bone lining cells together comprise one basic multicellular unit (BMU).

In addition to the above mentioned bone cells, the interior of the bone compartment contains bone marrow, which is comprised of cells of the hematopoietic and mesenchymal lineages, and is the site of the majority of

hematopoiesis (blood production). Therefore, bone also contains blood and lymphatic vessels, leukocytes and erythrocytes, as well as nerves and adipocytes.

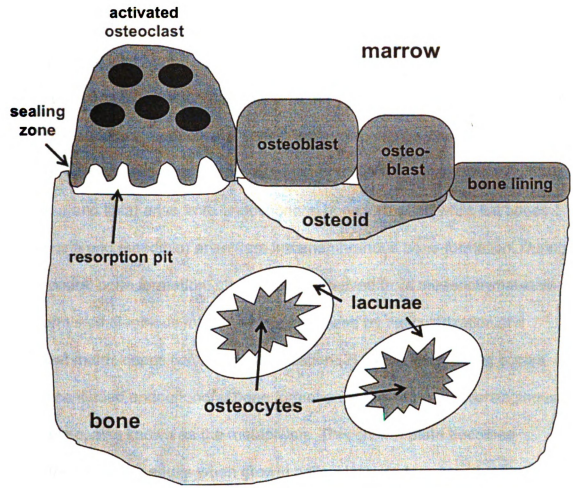

Figure 1. **Bone cells**. Cuboidal osteoblasts (bone forming), elongate bone lining cells, and multinucleated osteoclasts (bone resorbing) line the surface of the bone. Osteocytes arise from osteoblasts that have become embedded in the bone.

1.1.3. Bone development and anatomy

Bones have an outer shell of cortical (dense) bone and inner trabecular (spongy, cancellous) bone in the compartment containing bone marrow (Figure 2). The periosteum and endosteum refer to the layer of cells lining the outer and inner bone surfaces, respectively. During embryonic development, bone formation is either endochondral or intramembranous. Vertebrae and long bones (i.e. femur and tibia) arise from endochondral bone formation while flat bones (i.e. calvaria and mandible) arise from intramembranous bone formation. During endochondral bone formation, chondrocytes (derived from mesenchymal stem cells) form a cartilaginous matrix, which is followed by vascularization and osteoblast matrix deposition and mineralization (2). Bone lengthening occurs through continued endochondral bone formation at the site of the cartilaginous growth plate, also known as the metaphysis. This growth plate becomes mineralized in young adults when growth halts. Unlike in humans, the growth plates of mice never completely mineralize and bone growth continues into adulthood, albeit at a much slower rate. The diaphysis is the region of bone between both metaphyses, and the epiphyses are the ends of the bone. Intramembranous bone formation occurs when osteoblasts do not follow a cartilage matrix template and directly deposit and mineralize the bone matrix. Long bones can also have intramembranous bone formation at sites where cartilage does not provide a matrix template (i.e. in the periosteum and during remodeling in the trabeculi of adults) (2).

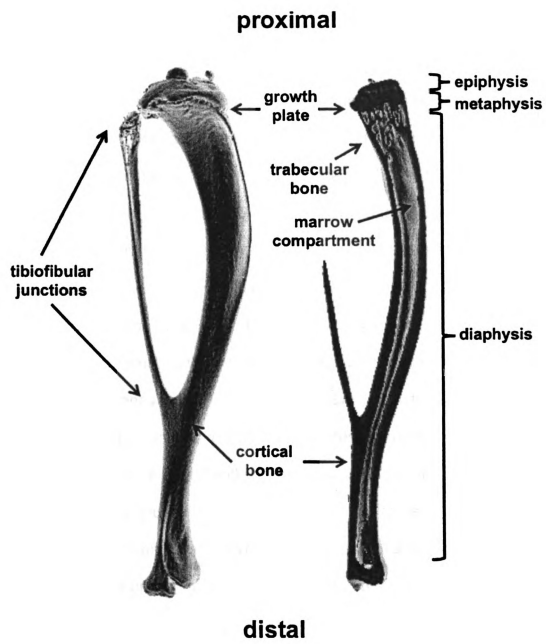

Figure 2. **Three-dimensional micro-computed tomography image of a mouse tibiofibula.** Left: complete bone, right: longitudinal section demonstrating structures of the interior of the bone.

1.1.4. Regulation of osteoblast differentiation

Differentiation of MSCs to the osteoblast lineage is completely dependent on expression of runt related transcription factor 2 (Runx2) (also known as Cbfa1, core binding factor 1) (1) which is induced by Indian hedgehog (Ihh) secretion from prehypertrophic chondrocytes (3, 4) (Figure 3). Runx2 binding sites are present in the promoters of several genes expressed in mature osteoblasts, such as osteocalcin and type I collagen (3). Activator protein 1 (AP-1) family transcription factor (i.e. c-Fos, Fos-related antigen 1 (Fra-1), and c-Jun) binding sites also exist on the promoters for osteocalcin, alkaline phosphatase and other bone genes (1, 5). The meshless (Msx) and distaless (Dlx) homeodomain (HD) proteins regulate skeletal development as well, and some (i.e. Dlx5) may work independently of Runx2 (6, 7). Activation of osteoblast differentiation may occur at the expense of other cell types that arise from the same precursors, such as adipocytes. Other transcriptional regulators (such as CCAAT enhancer binding protein beta (C/EBPβ) and T-cell factor (TCF)/lymphoid enhancer factor (LEF)) are likely crucial for understanding MSC fate and will be further discussed in the context of diabetic bone defects (See Section 1.4.3).

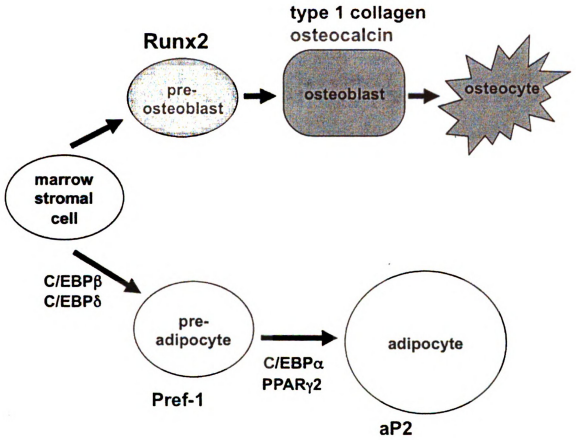

Figure 3. **Differentiation of mesenchymal stem cells to osteoblasts and adipocytes.**

1.1.5. Adipocyte differentiation

Adipocytes are also derived from mesenchymal stem cells, and are present to varying degrees in the bone marrow (depending on location, age, and other factors). The adipocyte portion of the bone marrow is often called yellow marrow, while the blood component is red marrow. C/EBPβ and C/EBPδ are transiently expressed during early adipocyte differentiation followed by expression of peroxisome proliferator-activated receptor gamma (PPARγ) 2 and C/EBPα (8-10) (Figure 3). Preadipocyte factor 1 (Pref-1) is not expressed in mature adipocytes and is therefore used as a marker for preadipocytes (11). Alternately, fatty acid binding protein 4 (FABP4, also called aP2) is a marker for mature adipocytes. Sterol regulatory element binding protein (SREBP) also plays a role in adipocyte differentiation and regulates several genes important for lipid metabolism (12).

1.1.6. Osteoclasts

Osteoclasts, responsible for bone resorption, attach to the bone surface through a ruffled border surrounded by a sealing zone (Figure 1). The membrane that is in contact with bone secretes acid and enzymes responsible for degrading mineral and matrix. Recruitment of an inactive osteoclast precursor requires both macrophage colony stimulating factor (M-CSF) and receptor activator of nuclear factor kappa-B ligand (RANKL) (1). After stimulated to differentiate by M-CSF (through the colony stimulating factor 1 receptor, CSF1R), osteoclastic

precursors express the membrane bound receptor activator of nuclear factor kappa-B (RANK), which binds RANKL to further stimulate osteoclast maturation and activity. RANKL is expressed on the cell membrane of osteoblasts, which also secrete osteoprotegrin (OPG), a decoy receptor for RANKL that inhibits it's binding to RANK and thus inhibits osteoclast maturation. Thus, the ratio of RANKL to OPG is important for regulating degree of bone resorption (Figure 4) (1). Active osteoclasts secrete tartrate-resistant acid phosphatase (TRAP) 5b into the serum, which can be quantitated and used to measure whole body bone resorption status.

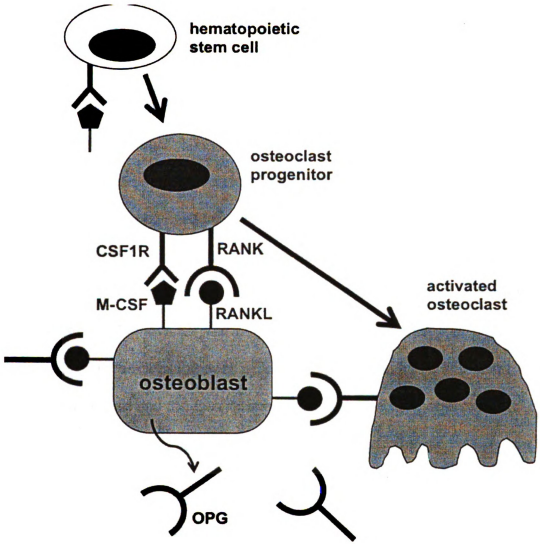

Figure 4. **Osteoclast activation through the RANKL/OPG pathway.** M-CSF embedded in the matrix or on osteoblasts stimulates hematopoetic precursors to express RANK, becoming osteoclast progenitors. RANKL and M-CSF then activate osteoclasts. OPG is the decoy receptor for RANKL.

1.1.7. Mineral homeostasis

Whole body calcium and phosphate levels are tightly regulated. Too much could cause spontaneous precipitation in the tissues and too little could result in multiple organ dysfunction (2). In its active form, parathyroid hormone (PTH) is an 84-amino acid peptide secreted from chief cells of the parathyroid gland in response to low blood calcium. PTH has an extremely short half-life of 2 minutes once it is secreted, allowing for nearly instantaneous regulation of calcium (2). PTH itself is stable for longer in solution, but in the body it is quickly metabolized by the liver and kidneys (2). Although most of the calcium entering the kidney is resorbed, PTH further stimulates active calcium resorption in the distal convoluted tubule and the connecting tubule by increasing expression of calcium transporters, as well as through increased synthesis of vitamin D ($1,25(OH)_2D$) (2, 13). Vitamin D itself promotes expression of calcium transporters in the kidney and is also necessary for intestinal calcium absorption (2).

PTH effects on bone are dependent on the method of administration and are not completely understood (2). Minute-to-minute regulation of calcium levels by PTH are thought to be primarily through its effects on osteocytes, which may be responsible for small amounts of mineral resorption (1). However, preosteoblasts, osteoblasts and bone lining cells also express PTH receptors and exhibit responses to PTH depending on conditions. Intermittent PTH (daily injections) promotes osteoblast differentiation and inhibits osteoblast and osteocyte apoptosis, perhaps through upregulation of Runx2 (14). Additionally, *in*

vitro PTH treatment activates TCF/LEF-dependent transcription, which is activated by Wnt signaling (15). A very recent report indicates that the anabolic effects of intermittent PTH are dependent on T-lymphocyte expression of Wnt10b (16). PTH may also inhibit production of sclerostin, which inhibits bone formation by inhibiting Wnt and bone morphogenic protein (BMP) signaling (17). Because no PTH receptors are present on cells of the osteoclast lineage, net bone resorption from chronic PTH treatment is likely due to secreted osteoblast factors (RANKL and M-CSF) activating osteoclast activity (1).

1.2. OSTEOPOROSIS

Osteoporosis is a severe reduction of bone mass, which leaves patients at risk for fractures. Bone remodeling is altered in osteoporosis such that there is decreased bone formation, increased resorption, or both. Clinically, osteoporosis is defined as having a bone mineral density (BMD) less than 2.5 standard deviations lower than the average population BMD for that location. This number is also referred to as the T-score. Patients are deemed osteopenic when their T-score is between -1 and -2.5, and normal if it is greater than -1 (1). Osteoporotic fractures are a serious health concern because they cost more than $18 billion annually in the United States and often leave patients hospitalized, with decreased mobility, and at higher risk for contracting secondary infections like pneumonia (18, 19). Therefore, effective diagnosis and treatment of osteoporosis is essential to the overall health of the patient. However, osteoporosis can occur

through different mechanisms depending on the cause (which can range from aging, menopause and unloading, to being secondary to diseases like diabetes and inflammatory bowel disease). Understanding the mechanism of osteoporosis is essential to developing successful therapies and preventative regimens.

1.3. GLUCOSE HOMEOSTASIS AND DIABETES MELLITUS

1.3.1. Glucose homeostasis

Glucose is the most commonly used fuel for generation of energy rich ATP in the tissues. Blood glucose levels are regulated by the hormones insulin and glucagon. High blood glucose levels (such as after a meal) stimulate insulin secretion from the pancreas into the blood. Insulin then binds insulin receptors on target tissues (liver, muscle, fat), which initiates an intracellular signaling cascade that results in increased plasma membrane expression of GLUT4, the insulin responsive glucose transporter. GLUT4 mediates the uptake of glucose into the cell, where it is stored in the form of glycogen in liver and muscle, or lipid in adipose tissue. Alternatively, low blood glucose levels (during fasting or exercise) trigger glucagon secretion from pancreatic α-cells. Glucagon stimulates liver glycogenolysis, gluconeogenesis, and subsequent increased glucose production (2).

1.3.2. Diabetes mellitus definition and classifications

Diabetes mellitus is a metabolic disease in which a defect in insulin action (either by lack of insulin or tissue insulin resistance) results in impaired glucose homeostasis. Diabetes is a broad term that encompasses type 1 diabetes mellitus (T1-diabetes), type 2 diabetes mellitus (T2-diabetes) and gestational diabetes mellitus (GDM).

T1-diabetes is characterized by hypoinsulinemia and subsequent hyperglycemia caused by death of insulin-secreting pancreatic β-cells. Depending on the etiology of the disease, T1-diabetes has been divided into type 1A (immune mediated and more prevalent) and type 1B (not immune-mediated and less prevalent). In type 1A diabetes, immune destruction of pancreatic β-cells is confirmed by the presence of anti-islet autoantibodies in humans (2). Type 1A diabetes is heterogeneous, with several loci linked to the disorder (20). The only environmental factor demonstrated to induce type 1A diabetes in humans is congenital rubella infection, although other factors may contribute and could be difficult to identify (2, 21).

T1-diabetes generally occurs in adolescents or young adults and must be controlled by regular blood glucose monitoring and insulin delivery. Better education, control of the disease, and treatment of life-threatening complications have helped T1-diabetes patients to live longer. Although patients may be considered to have blood glucose under control, no insulin delivery method is as precise as the pancreas, therefore fluctuations in blood glucose levels continue, which puts patients at risk for additional complications.

T2-diabetes is associated with resistance to insulin signaling in the tissues (pancreas, liver, muscle and brain) and increased insulin production by the pancreas. Long-term high demand for insulin results in eventual pancreatic β-cell death, after which patients are T1-diabetic and dependent on insulin injections for glucose control. Risk factors for T2-diabetes include obesity (either genetic, or as a result of poor diet and inactivity) and fetal malnutrition or over nutrition (2). Gestational diabetes is a form of insulin resistance that occurs during pregnancy and it usually reverses itself after birth.

1.3.3. Complications of diabetes mellitus

Osteoporosis from T1-diabetes is the main focus of this dissertation and will be discussed at length in Section 1.4. Other complications from diabetes include retinopathy, nephropathy, peripheral neuropathy and impaired wound healing. Hyperglycemia induces elevated reactive oxygen species (ROS) and advanced glycation end products (AGE), which can cause cell death and are thought to perpetrate many diabetic complications. These complications also arise in part from changes in microvasculature. Macrovascular changes from both T1- diabetes and T2-diabetes leave patients at higher risk for cardiovascular disease than non-diabetics (2). Risk for each complication increases with increasing glycated hemoglobin (Hb A_{1C}, a measure of glucose control) (2, 22), therefore tight control of blood glucose is important. However, no treatment for

diabetes can control glucose as well as a functional pancreas, so complications from diabetes cannot simply be treated with insulin.

1.3.4. Animal models of T1-diabetes and T2-diabetes

Animal models of diabetes are important for studying not only the disease itself, but also its many complications, including osteoporosis. Most rodent models of type 1 diabetes are either pharmacologic or spontaneous (23), while type 2 diabetes can be modeled pharmacologically, with spontaneous genetic rodents, and with administration of a high-fat diet. Pharmacologic agents used to model type 1 diabetes include streptozotocin, alloxan, dithizone, vacor and 8-hydroxyquinolone (23). Widely used to study diabetic complications, streptozotocin (STZ) is a glucose mimetic that diffuses into insulin secreting pancreatic β-cells through the non-insulin responsive glucose transporter GLUT2 (24). The effects of STZ include DNA damage and subsequent β-cell death (24). In mice, five daily low dose intraperitoneal injections (40 mg/kg body weight) induce significantly detectable non-fasting hyperglycemia within three days of the first injection (See Chapter 2) (25) and a full type 1 diabetic phenotype of hyperglycemia and hypoinsulinemia after twelve days (26). A single large dose (50-60 mg/kg) of STZ is effective at inducing type 1 diabetes in rats (24). Injecting 100 mg/kg STZ soon after the birth of rats induces mild hyperglycemia and impaired glucose tolerance by 8-10 weeks of age and is, therefore, a pharmacologic method of studying type 2 diabetes in rodents. Pharmacologic

induction of diabetes can be performed in any age of rodent and in animals (primarily mice) with genetic manipulations, making it a convenient and easily controlled model. However, to confirm results from STZ and other pharmacologic models, investigators often turn to spontaneous models of diabetes mellitus.

Spontaneous mouse models of type 1 diabetes include the non-obese diabetic (NOD) model and the $Ins2^{+/-Akita}$ mouse. The NOD mouse generally develops diabetes sometime between 12 and 30 weeks of age (23, 27), making it difficult to study complications that are affected by age, such as osteoporosis. Additionally, only 60% of male mice actually develop a diabetic phenotype (23), which increases the number of animals necessary for a complete study. The $Ins2^{+/-Akita}$ mouse is heterozygous for the insulin gene. Demand on the pancreas for insulin production from only one allele leads to β-cell death within 4-6 weeks of life (28). Because it occurs early and consistently, diabetes induction is much easier to predict and better for examining diabetic complications at early time points. Additionally, these mice can be used to understand complications in young mice that are still growing, which is when type 1 diabetes generally develops in humans. Spontaneously diabetic BioBreeding (BB) rats develop type 1 diabetes around 12 weeks of age, which is during puberty, making the time of induction representative of human disease (23). Pathogenesis in BB rats is a result of autoimmune attack of the pancreas, similar to humans (23). Unfortunately, BB rats develop severe diabetes and ketoacidosis and survival is dependent on insulin treatment (23), which is similar to the human situation, but adds complexity to data interpretation.

Non-pharmacologic models of T2-diabetes include the leptin deficient ob/ob and leptin receptor deficient db/db mice. The absence of leptin or leptin signaling (respectively) induces increased food consumption to the point of developing obesity, impaired glucose tolerance, increased insulin production, and eventual pancreatic beta cell death due to high demand on the pancreas (29). The Zucker (fa/fa) rat is also a model of leptin resistance, similar to db/db mice (23, 30). Several other spontaneous rodent models exist that each have slight variations in diabetes induction, severity, and phenotype of complications, making them useful for studying the human condition, which is in itself heterogeneous (23). T2-diabetes can also be induced by administering research animals with a high fat diet (31).

1.4. BONE PHENOTYPE IN DIABETES MELLITUS

1.4.1. Type 2 diabetic bone phenotype

In human studies, T2-diabetes has been associated with increased risk of nonvertebral fracture, despite increased cortical thickness and increased trabecular bone mineral density (BMD) (1). Additionally, some fractures in type 2 (and type 1) diabetic patients are thought to be due to increased falls as a result of neuropathy and poor vision, but this does not completely explain the increased fracture risk phenotype (32). Adjusting for body mass index (BMI) reduces the correlation between bone density and diabetes, however it does not completely

eliminate statistical significance (1). Hyperinsulinemia associated with insulin resistance has been thought to perpetrate increased bone density that cannot be correlated to body mass (33). Medications, age and progression of T2-diabetes (all of which can have bone effects) have complicated interpretations of human studies. It is likely that more rapid bone loss occurs in T2-diabetic patients over with aging, especially if pancreatic β-cell function ceases, and insulin secretion stops (32).

The bone phenotype of mouse models of T2-diabetes is variable depending on the model examined. Leptin/leptin receptor-deficient mice have high bone mass early in life, then because of the deficiency in the leptin pathway, become obese, insulin resistant, and eventually lose β-cell function (34, 35). When diabetic, these mice have reduced bone formation and increased marrow adiposity in the long bones, but do not have bone loss or increased marrow adiposity in the vertebrae (36-39). This is not a perfect model of T2-diabetes, since leptin is known to have direct effects on the skeleton. Leptin deficient mice will be discussed in further detail in Sections 1.4.3.2.1. Alternately, in high fat diet induced obesity and diabetes more closely mimics the human etiology, but in these mice, bone loss is primarily due to increased resorption, whereas it remains unclear how resorption is altered in T2-diabetic patients (32, 40, 41).

1.4.2. Type 1 diabetic osteoporosis

Osteoporosis is a serious complication of T1-diabetes, leaving patients at risk for bone loss, fracture and impaired fracture healing (42-44). Young patients diagnosed with T1-diabetes have reduced growth, which correlates with the level of glycemic control (1, 45, 46). Serum osteocalcin is significantly reduced in diabetic patients of all ages, suggesting reduced bone formation (47). In the same study, serum procollagen carboxy-terminal extension peptide (PICP), a marker of bone resorption, was unchanged.

Rodent models of T1-diabetes have a bone phenotype similar to that of humans. In both STZ-mice and rats, T1-diabetes causes bone loss and impaired bone healing (48-54). Non-obese diabetic (NOD) mice are susceptible to development of autoimmune T1-diabetes and display a similar bone phenotype to that of STZ-diabetic mice (55). Spontaneously diabetic BioBreeding (BB) rats also have bone loss due to decreased bone turnover and impaired intestinal calcium absorption (56, 57).

1.4.3. Mechanisms of type 1 diabetic bone loss

Understanding the mechanism(s) of reduced bone formation in type 1 diabetes is essential for determining what treatments will be most effective at improving bone density, strength and healing in patients (26). We do not believe that hypoinsulinemia directly contributes to reduced osteoblast activity because euglycemic insulin receptor knockout (IRKO) -L1 mice that do not express insulin receptor (and therefore have no insulin signaling) in osteoblasts do not have

reduced bone density or reduced bone remodeling normally seen in T1-diabetes (58). Other potential mechanisms of reduced bone formation include bone inflammation, altered lineage selection of MSCs, hyperglycemia/hyperosmolarity and reactive oxygen species (ROS). It is important to keep in mind that reduced osteoblast activity could be a result of not only impaired differentiation, but also increased apoptosis. We are currently examining the extent to which increased apoptosis contributes to diabetic bone loss, and it will be briefly discussed in relation to PTH treatment in Chapter 6.

1.4.3.1. Characterization of early bone metabolism and bone inflammation

While our lab has demonstrated bone loss and reduced osteoblast markers 5 days after confirmation of diabetes (equivalent to 17 days after the first STZ injection (days post injection, dpi)) (48, 59), understanding temporal changes in bone during diabetes induction may help elucidate the mechanism of diabetic osteoporosis. Hyperglycemia has been associated with increased inflammatory markers (C-reactive protein (CRP), TNFα, and adiponectin), which can increase osteoblast apoptosis, ROS and impair maturation (60-63). If inflammation was in part responsible for impaired bone formation, it is presumable that we would be able to detect it either systemically or locally in bone at some point before bone changes are apparent. Therefore, in Chapter 2 we examined the bone metabolism of control and STZ mice at several time points between 1 and 17 days after the first STZ injection (days post injection,

dpi). Here we also characterized proinflammatory cytokine markers in bone and serum, and tested whether deficiency of one of the altered cytokines, interferon gamma (IFN-γ) could ameliorate diabetic bone loss.

1.4.3.2. Is diabetes-induced marrow fat bad for bone?

In addition to reduced bone formation and unchanged or reduced resorption in type 1 diabetic bone, STZ and NOD mice have an obvious increase in bone marrow adipocyte number (26, 48, 55, 59, 64-66). STZ mice have increased expression of peroxisome proliferator-activated receptor gamma (PPARγ) 2 in bone, a transcription factor important for adipocyte maturation (48). Because adipocytes are derived from the same stem cells that give rise to osteoblasts, the increased marrow adiposity suggests that differentiation of MSCs may be shunted away from the osteoblast lineage and toward the adipocyte lineage under diabetic conditions (48). It is also possible that adipocytes secrete factors (i.e. tumor necrosis factor alpha (TNFα)) into the marrow microenvironment that reduce osteoblast differentiation or increase osteoblast apoptosis. High marrow fat has also been implicated in bone loss models of aging (67, 68) and unloading (69).

1.4.3.2.1. Leptin

Interestingly, increased adiposity is not observed in male or female vertebrae, although it is present in tibia, femur and calvaria (66). In this respect the T1-diabetic bone phenotype resembles that of leptin-deficient mice (39) and T1-diabetic mice also have suppressed leptin (66). Leptin is a small protein (16 kDa) secreted by adipocytes and involved in bone mass regulation. The effects of leptin on bone are complex; it can stimulate or inhibit bone formation depending upon bone location and whether leptin is functioning directly on osteoblasts (through receptors (70, 71)) or indirectly through the hypothalamus (34, 36, 37, 71, 72). In children and during adolescence, decreases in serum leptin levels, associated with reduced food intake and some disease conditions, are thought to contribute to reduced bone formation and growth (36, 73). Absence of leptin in mice also results in bone loss as well as increased bone marrow adiposity (39, 74). Similarly, increased leptin levels, as observed in obesity (75), are correlated with increased bone mass (76). Several studies have tested the potential therapeutic benefits of leptin treatment on bone loss and marrow adipocyte accumulation. In vitro studies demonstrate that leptin promotes bone marrow stromal cells to exhibit an osteoblast rather than adipocyte phenotype (70, 71, 77). Consistent with this finding, subcutaneous infusion of leptin with osmotic mini-pumps reduces marrow adiposity and increases bone mass in ob/ob mice (38). Similarly, leptin treatment reduces bone loss from ovariectomy (78) and tail suspension (79). In sum, these studies suggest the efficacy of leptin treatment to restore bone density under conditions of bone loss. Therefore, we tested the ability of leptin to treat diabetic bone loss in Chapter 3.

1.4.3.2.2. C/EBPβ and MSC lineage selection

In order to test altered MSC lineage selection as a mechanism of diabetic bone loss, we previously inhibited PPARγ2 with bisphenol-A-diglycidyl ether (BADGE) in control and diabetic mice (59). BADGE was effective at reducing diabetic hyperlipidemia and bone marrow adipocyte accumulation. However, BADGE did not prevent reduced bone formation (osteocalcin and Runx2 expression) or reduced bone density from T1-diabetes. These results suggest that marrow adipocyte differentiation is not linked to reduced osteoblast bone formation. However, PPARγ2 expression occurs later than C/EBPβ and C/EBPδ in adipocyte differentiation (Figure 3), therefore we could not exclude that MSCs differentiated into preadipocytes but could not fully mature in BADGE treated diabetic mice. In order to address this issue, we examined diabetic bone loss in mice deficient in C/EBPβ, an early adipocyte transcription factor, in Chapter 4.

CCAAT enhancer binding proteins (C/EBPs) are members of the basic region-leucine zipper (bZIP) class of transcription factors. A key regulator of adipocyte lineage selection C/EBPβ, it is transiently expressed during early adipocyte differentiation with C/EBPδ, and then followed by expression of PPARγ2 and C/EBPα (8-10). C/EBPβ exists in three isoforms: transcriptionally active LAP-1 and LAP-2 and generally inactive LIP (10). Overexpression of C/EBPβ alone induces adipocyte differentiation in NIH-3T3 fibroblasts, while LIP overexpression can prevent it (80, 81). Total deficiency of C/EBPβ protects mice

from obesity and reduces body fat mass (82-84). Combined knockout of C/EBPβ and C/EBPδ leads to an even greater block to the adipocyte phenotype and adiposity (85).

C/EBPβ has been shown to affect osteoblast differentiation and bone density. These effects are dependent on when (early vs. late differentiation), where (local vs. systemic), and which (LAP vs. LIP, or both) C/EBPβ is expressed. C/EBPβ is normally expressed during early and late stages of osteoblast differentiation, with decreased expression during middle stages (86). Complete knockout of C/EBPβ in mice results in decreased total body mass and total bone mineral density (BMD) (83). Similarly, targeted expression of the C/EBPβ inactive form, LIP, to preosteoblasts and osteoblasts results in osteopenia in transgenic mice due to decreased bone formation (87).

1.4.3.2.3. Wnt/β-catenin signaling

Wnt/β-catenin signaling through TCF/LEF-induced transcription is a potent regulator of bone formation and adipocyte differentiation (88, 89). Wnts are secreted ligands that bind low density lipoprotein receptor-related protein 5/6 (LRP5/6) and frizzled (Fzd) membrane receptors (Figure 5). Dimerization of the LRP and Fzd receptors in response to wnts initializes a signaling cascade that inhibits glycogen synthase kinase 3 beta (GSK3β). Without the wnt signal (or in the presence of endogenous pathway inhibitors such as dickkopf (Dkk) proteins), GSK3β actively phosphorylates cytoplasmic β-catenin, targeting it for

degradation. When GSK3β is inactive (as in the presence of a wnt ligand), transcriptionally active β-catenin (dephosphorylated on serine (Ser) 37 or threonine (Thr) 41) accumulates in the cytoplasm and translocates to the nucleus where it initiates transcription of genes with TCF/LEF binding sites, such as Runx2 (90, 91).

Mice null for LRP5 have low bone density and blindness, consistent with the rare recessive disorder, osteoporosis-pseudoglioma syndrome (OPPG), while gain of function of LRP5 results in high bone mass due to increased osteoblast activity (92-97). Although complete loss of function of LRP6 is fatal, loss of one allele causes more bone loss in mice deficient in LRP5 by exacerbating reduced bone formation (98). Similarly, modulation of Wnt10b affects only bone formation, not resorption (99). Wnt10b knockout (-KO) mice have low bone density while mice overexpressing Wnt10b (Wnt10b-Tg) have high bone density and low marrow adiposity (99). These mice have attenuated bone loss from aging and ovariectomy (99). In vitro activation and inhibition of wnt signaling results in inhibition and activation of adipogenesis, respectively (100, 101), through regulation of expression of PPARγ and C/EBPα (102, 103). Wnt1, 5a and 7b have also been shown to promote osteoblast and/or suppress adipocyte differentiation (98).

Endogenous agonists and antagonists can further regulate wnt signaling. Dally protein enhances the interaction between wnts and Fzds, while Dkks and secreted frizzled-related proteins (sFRP) antagonize it. Additionally, sclerostin, prevents the Fzd-LRP interaction. Targeted inhibition of Wnt agonists and

antagonists is a relatively new and promising area of interest for treatment of osteosclerotic and osteoporotic diseases (89). We therefore examined Wnt pathway family member changes in diabetic bone, and examined the ability of overexpression of Wnt10b to counteract osteoporosis in STZ mice in Chapter 5.

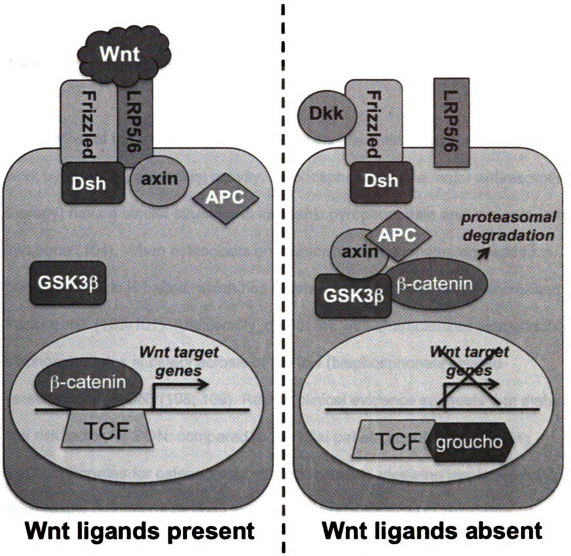

Figure 5. **β-catenin signaling in the presence and absence of wnt ligands.** In the presence of wnt ligands (*left*), β-catenin accumulates in the cytoplasm and translocates to the nucleus, where it can activate TCF/LEF responsive gene transcription. In the absence of wnt ligands or when Dkk binds frizzled (*right*), β-catenin is targeted for degradation by GSK3β.

1.4.4. Treatment of T1-diabetic bone loss

1.4.4.1. Antiresorptive treatments

Most of the treatments for osteoporosis are antiresorptive, meaning they work by inhibiting osteoclast activity. Bisphosphonates (the major antiresorptive therapy) have a similar structure to inorganic pyrophosphate and is incorporated into bone (104). When osteoclasts encounter bisphosphonates embedded in bone, resorption is halted, which has recently been associated with increased fracture risk (105-107). Additionally, one of the well-characterized side effects of bisphosphonates is osteonecrosis of the jaw (bisphosphonate-related osteonecrosis, BON) (108, 109). Recent clinical evidence suggests that diabetes is a risk factor for BON: compared to the total patient population receiving bisphosphonates for osteoporosis, diabetic patients receiving bisphosphonates were nearly 5 times more likely to be diagnosed with BON (110). Other antiresorptive treatments for osteoporosis include hormone replacement therapy and selective estrogen receptor modulators (SERMs), and calcitonin. However, because bone loss from T1-diabetes is due to reduced osteoblast bone formation, and not increased resorption, therapies that target bone formation directly may be most appropriate.

1.4.4.2. Anabolic intermittent PTH

Anabolic treatments for osteoporosis are those that promote bone formation, rather than inhibit resorption. Currently, the only anabolic treatment in use is a truncated form of endogenous PTH. Also called teriparatide, PTH(1-34) is administered intermittently by daily subcutaneous injections and can cause a net increase in bone formation and reduction of fracture risk (111-113). In humans, PTH(1-34) is used to treat only severe osteoporosis because of elevated risk of osteosarcoma in rats treated with higher than approved human doses (114, 115). However, use of PTH(1-34) in a broader patient group may prove to be appropriate, especially when osteoporosis is caused by bone formation defects, as in T1-diabetes.

There are no reports examining the efficacy of PTH(1-34) treatment for T1-diabetic bone loss in humans. In laboratory animals, intermittent PTH(1-34) treatment has proven to be anabolic (111), and is effective at increasing bone formation in models of unloading, ovariectomy, and alcohol consumption (113, 116-120). Additionally, 4-week intermittent PTH(1-34) treatment of STZ-diabetic rats improves bone density parameters 4, 6 and 8 weeks after diabetes induction (121). However, the effects of PTH(1-34) therapy on mouse models of diabetes-induced bone loss have not been determined. In Chapter 6, we tested whether intermittent PTH(1-34) treatment could be beneficial for T1-diabetic patients, by examining the ability of PTH(1-34) to prevent and reverse diabetes-induced bone loss in STZ mice.

1.5. SUMMARY

Understanding the mechanism of any disease or disease complication is imperative for proper treatment. Using mouse and cell culture models, our past studies have demonstrated that hyperglycemia and T1-diabetes reduce osteoblast differentiation and increase adipocyte differentiation in the marrow. The following chapters characterize the time course of bone phenotype changes in diabetes, with regard to osteoblast/adipocyte differentiation and inflammation in bone. Additionally, I examined the effects of two commercially available treatments (leptin and intermittent PTH) and two genetic manipulations (C/EBPβ knockout and overexpression of Wnt10b) on diabetic bone changes. My experiments have provided us with new insight into the mechanisms of diabetic bone loss (which are most likely multi-faceted) and suggested how best to treat it with the therapies available today. Finally, these chapters provide a launching pad for additional investigation into bone changes from diabetes, which will likely provide new insights into our understanding of bone itself.

1.6. REFERENCES

1. **Bilezikian JP, Raisz LG, Rodan GA** 2002 Principles of bone biology. 2nd ed. San Diego, Calif., USA: Academic Press

2. **Kronenberg H, Williams RH** 2008 Williams textbook of endocrinology. Ed. 11 / ed. Philadelphia, PA: Saunders/Elsevier

3. **Karsenty G** 2001 Minireview: transcriptional control of osteoblast differentiation. Endocrinology 142:2731-2733

4. **Hartmann C** 2009 Transcriptional networks controlling skeletal development. Curr Opin Genet Dev 19:437-443

5. **McCabe LR, Banerjee C, Kundu R, Harrison RJ, Dobner PR, Stein JL, Lian JB, Stein GS** 1996 Developmental expression and activities of specific fos and jun proteins are functionally related to osteoblast maturation: role of Fra-2 and Jun D during differentiation. Endocrinology 137:4398-4408

6. **Hassan MQ, Javed A, Morasso MI, Karlin J, Montecino M, van Wijnen AJ, Stein GS, Stein JL, Lian JB** 2004 Dlx3 transcriptional regulation of osteoblast differentiation: temporal recruitment of Msx2, Dlx3, and Dlx5 homeodomain proteins to chromatin of the osteocalcin gene. Mol Cell Biol 24:9248-9261

7. **Acampora D, Merlo GR, Paleari L, Zerega B, Postiglione MP, Mantero S, Bober E, Barbieri O, Simeone A, Levi G** 1999 Craniofacial, vestibular and bone defects in mice lacking the Distal-less-related gene Dlx5. Development 126:3795-3809

8. **Darlington GJ, Ross SE, MacDougald OA** 1998 The role of C/EBP genes in adipocyte differentiation. J Biol Chem 273:30057-30060

9. **Cao Z, Umek RM, McKnight SL** 1991 Regulated expression of three C/EBP isoforms during adipose conversion of 3T3-L1 cells. Genes Dev 5:1538-1552

10. **Ramji DP, Foka P** 2002 CCAAT/enhancer-binding proteins: structure, function and regulation. Biochem J 365:561-575

11. **Sul HS** 2009 Minireview: Pref-1: role in adipogenesis and mesenchymal cell fate. Mol Endocrinol 23:1717-1725

12. **Rosen ED, Spiegelman BM** 2000 Molecular regulation of adipogenesis. Annu Rev Cell Dev Biol 16:145-171

13. **Hoenderop JG, Nilius B, Bindels RJ** 2005 Calcium absorption across epithelia. Physiol Rev 85:373-422

14. **Bellido T, Ali AA, Plotkin LI, Fu Q, Gubrij I, Roberson PK, Weinstein RS, O'Brien CA, Manolagas SC, Jilka RL** 2003 Proteasomal degradation of Runx2 shortens parathyroid hormone-induced anti-apoptotic signaling in osteoblasts. A putative explanation for why intermittent administration is needed for bone anabolism. J Biol Chem 278:50259-50272

15. **Kulkarni NH, Halladay DL, Miles RR, Gilbert LM, Frolik CA, Galvin RJ, Martin TJ, Gillespie MT, Onyia JE** 2005 Effects of parathyroid hormone on Wnt signaling pathway in bone. J Cell Biochem 95:1178-1190

16. **Terauchi M, Li JY, Bedi B, Baek KH, Tawfeek H, Galley S, Gilbert L, Nanes MS, Zayzafoon M, Guldberg R, Lamar DL, Singer MA, Lane TF, Kronenberg HM, Weitzmann MN, Pacifici R** 2009 T lymphocytes amplify the anabolic activity of parathyroid hormone through Wnt10b signaling. Cell Metab 10:229-240

17. **Keller H, Kneissel M** 2005 SOST is a target gene for PTH in bone. Bone 37:148-158

18. **Rosen CJ** 2005 Clinical practice. Postmenopausal osteoporosis. N Engl J Med 353:595-603

19. **Gabriel SE, Tosteson AN, Leibson CL, Crowson CS, Pond GR, Hammond CS, Melton LJ, 3rd** 2002 Direct medical costs attributable to osteoporotic fractures. Osteoporos Int 13:323-330

20. **Concannon P, Rich SS, Nepom GT** 2009 Genetics of type 1A diabetes. N Engl J Med 360:1646-1654

21. **Robles DT, Eisenbarth GS** 2001 Type 1A diabetes induced by infection and immunization. J Autoimmun 16:355-362

22. **Skyler JS** 1996 Diabetic complications. The importance of glucose control. Endocrinol Metab Clin North Am 25:243-254

23. **Rees DA, Alcolado JC** 2005 Animal models of diabetes mellitus. Diabet Med 22:359-370

24. **Szkudelski T** 2001 The mechanism of alloxan and streptozotocin action in B cells of the rat pancreas. Physiol Res 50:537-546

25. **Motyl KJ, Botolin S, Irwin R, Appledorn DM, Kadakia T, Amalfitano A, Schwartz RC, McCabe LR** 2009 Bone inflammation and altered gene expression with type I diabetes early onset. J Cell Physiol 218:575-583

26. **McCabe LR** 2007 Understanding the pathology and mechanisms of type I diabetic bone loss. J Cell Biochem 102:1343-1357

27. **Atkinson MA, Leiter EH** 1999 The NOD mouse model of type 1 diabetes: as good as it gets? Nat Med 5:601-604

28. **Yoshioka M, Kayo T, Ikeda T, Koizumi A** 1997 A novel locus, Mody4, distal to D7Mit189 on chromosome 7 determines early-onset NIDDM in nonobese C57BL/6 (Akita) mutant mice. Diabetes 46:887-894

29. **Hamann A, Matthaei S** 1996 Regulation of energy balance by leptin. Exp Clin Endocrinol Diabetes 104:293-300

30. **Kasiske BL, O'Donnell MP, Keane WF** 1992 The Zucker rat model of obesity, insulin resistance, hyperlipidemia, and renal injury. Hypertension 19:I110-115

31. **Winzell MS, Ahren B** 2004 The high-fat diet-fed mouse: a model for studying mechanisms and treatment of impaired glucose tolerance and type 2 diabetes. Diabetes 53 Suppl 3:S215-219

32. **Schwartz AV, Sellmeyer DE** 2007 Diabetes, fracture, and bone fragility. Curr Osteoporos Rep 5:105-111

33. **Schwartz AV** 2003 Diabetes Mellitus: Does it Affect Bone? Calcif Tissue Int 73:515-519

34. **Ducy P, Amling M, Takeda S, Priemel M, Schilling AF, Beil FT, Shen J, Vinson C, Rueger JM, Karsenty G** 2000 Leptin inhibits bone formation through a hypothalamic relay: a central control of bone mass. Cell 100:197-207

35. **Takeda S, Elefteriou F, Levasseur R, Liu X, Zhao L, Parker KL, Armstrong D, Ducy P, Karsenty G** 2002 Leptin regulates bone formation via the sympathetic nervous system. Cell 111:305-317

36. **Hamrick MW** 2004 Leptin, bone mass, and the thrifty phenotype. J Bone Miner Res 19:1607-1611

37. **Hamrick MW, Della Fera MA, Choi YH, Hartzell D, Pennington C, Baile CA** 2007 Injections of leptin into rat ventromedial hypothalamus increase adipocyte apoptosis in peripheral fat and in bone marrow. Cell Tissue Res 327:133-141

38. **Hamrick MW, Della-Fera MA, Choi YH, Pennington C, Hartzell D, Baile CA** 2005 Leptin treatment induces loss of bone marrow adipocytes and increases bone formation in leptin-deficient ob/ob mice. J Bone Miner Res 20:994-1001

39. **Hamrick MW, Pennington C, Newton D, Xie D, Isales C** 2004 Leptin deficiency produces contrasting phenotypes in bones of the limb and spine. Bone 34:376-383

40. **Patsch JM, Kiefer FW, Varga P, Pail P, Rauner M, Stupphann D, Resch H, Moser D, Zysset PK, Stulnig TM, Pietschmann P** Increased bone resorption and impaired bone microarchitecture in short-term and extended high-fat diet-induced obesity. Metabolism

41. **Halade GV, Rahman MM, Williams PJ, Fernandes G** High fat diet-induced animal model of age-associated obesity and osteoporosis. J Nutr Biochem

42. **Levin ME, Boisseau VC, Avioli LV** 1976 Effects of diabetes mellitus on bone mass in juvenile and adult-onset diabetes. N Engl J Med 294:241-245

43. **Auwerx J, Dequeker J, Bouillon R, Geusens P, Nijs J** 1988 Mineral metabolism and bone mass at peripheral and axial skeleton in diabetes mellitus. Diabetes 37:8-12

44. **Kemink SA, Hermus AR, Swinkels LM, Lutterman JA, Smals AG** 2000 Osteopenia in insulin-dependent diabetes mellitus; prevalence and aspects of pathophysiology. J Endocrinol Invest 23:295-303

45. **Danne T, Kordonouri O, Enders I, Weber B** 1997 Factors influencing height and weight development in children with diabetes. Results of the Berlin Retinopathy Study. Diabetes Care 20:281-285

46. **Holl RW, Grabert M, Heinze E, Sorgo W, Debatin KM** 1998 Age at onset and long-term metabolic control affect height in type-1 diabetes mellitus. Eur J Pediatr 157:972-977

47. **Bouillon R, Bex M, Van Herck E, Laureys J, Dooms L, Lesaffre E, Ravussin E** 1995 Influence of age, sex, and insulin on osteoblast function: osteoblast dysfunction in diabetes mellitus. J Clin Endocrinol Metab 80:1194-1202

48. **Botolin S, Faugere MC, Malluche H, Orth M, Meyer R, McCabe LR** 2005 Increased bone adiposity and peroxisomal proliferator-activated receptor-gamma2 expression in type I diabetic mice. Endocrinology 146:3622-3631

49. **Hamada Y, Kitazawa S, Kitazawa R, Fujii H, Kasuga M, Fukagawa M** 2007 Histomorphometric analysis of diabetic osteopenia in streptozotocin-induced diabetic mice: a possible role of oxidative stress. Bone 40:1408-1414

50. **Shires R, Teitelbaum SL, Bergfeld MA, Fallon MD, Slatopolsky E, Avioli LV** 1981 The effect of streptozotocin-induced chronic diabetes mellitus on bone and mineral homeostasis in the rat. J Lab Clin Med 97:231-240

51. **Krakauer JC, McKenna MJ, Buderer NF, Rao DS, Whitehouse FW, Parfitt AM** 1995 Bone loss and bone turnover in diabetes. Diabetes 44:775-782

52. **McCracken M, Lemons JE, Rahemtulla F, Prince CW, Feldman D** 2000 Bone response to titanium alloy implants placed in diabetic rats. Int J Oral Maxillofac Implants 15:345-354

53. **Shyng YC, Devlin H, Sloan P** 2001 The effect of streptozotocin-induced experimental diabetes mellitus on calvarial defect healing and bone turnover in the rat. Int J Oral Maxillofac Surg 30:70-74

54. **Fowlkes JL, Bunn RC, Liu L, Wahl EC, Coleman HN, Cockrell GE, Perrien DS, Lumpkin CK, Jr., Thrailkill KM** 2008 Runt-related transcription factor 2 (RUNX2) and RUNX2-related osteogenic genes are down-regulated throughout osteogenesis in type 1 diabetes mellitus. Endocrinology 149:1697-1704

55. **Botolin S, McCabe LR** 2007 Bone loss and increased bone adiposity in spontaneous and pharmacologically induced diabetic mice. Endocrinology 148:198-205

56. **Nyomba BL, Verhaeghe J, Thomasset M, Lissens W, Bouillon R** 1989 Bone mineral homeostasis in spontaneously diabetic BB rats. I. Abnormal vitamin D metabolism and impaired active intestinal calcium absorption. Endocrinology 124:565-572

57. **Verhaeghe J, Suiker AM, Nyomba BL, Visser WJ, Einhorn TA, Dequeker J, Bouillon R** 1989 Bone mineral homeostasis in spontaneously diabetic BB rats. II. Impaired bone turnover and decreased osteocalcin synthesis. Endocrinology 124:573-582

58. **Irwin R, Lin HV, Motyl KJ, McCabe LR** 2006 Normal bone density obtained in the absence of insulin receptor expression in bone. Endocrinology 147:5760-5767

59. **Botolin S, McCabe LR** 2006 Inhibition of PPARgamma prevents type I diabetic bone marrow adiposity but not bone loss. J Cell Physiol 209:967-976

60. **Goldberg RB** 2009 Cytokine and cytokine-like inflammation markers, endothelial dysfunction, and imbalanced coagulation in development of diabetes and its complications. J Clin Endocrinol Metab 94:3171-3182

61. **Li YP, Stashenko P** 1992 Proinflammatory cytokines tumor necrosis factor-alpha and IL-6, but not IL-1, down-regulate the osteocalcin gene promoter. J Immunol 148:788-794

62. **Yang XD, Tisch R, Singer SM, Cao ZA, Liblau RS, Schreiber RD, McDevitt HO** 1994 Effect of tumor necrosis factor alpha on insulin-dependent diabetes mellitus in NOD mice. I. The early development of autoimmunity and the diabetogenic process. J Exp Med 180:995-1004

63. **Togari A, Arai M, Mogi M, Kondo A, Nagatsu T** 1998 Coexpression of GTP cyclohydrolase I and inducible nitric oxide synthase mRNAs in mouse osteoblastic cells activated by proinflammatory cytokines. FEBS Lett 428:212-216

64. **Motyl K, McCabe LR** 2009 Streptozotocin, Type I Diabetes Severity and Bone. Biol Proced Online

65. **Motyl KJ, McCabe LR** 2009 Leptin treatment prevents type I diabetic marrow adiposity but not bone loss in mice. J Cell Physiol 218:376-384

66. **Martin LM, McCabe LR** 2007 Type I diabetic bone phenotype is location but not gender dependent. Histochem Cell Biol 128:125-133

67. **Nuttall ME, Patton AJ, Olivera DL, Nadeau DP, Gowen M** 1998 Human trabecular bone cells are able to express both osteoblastic and adipocytic phenotype: implications for osteopenic disorders. J Bone Miner Res 13:371-382

68. **Verma S, Rajaratnam JH, Denton J, Hoyland JA, Byers RJ** 2002 Adipocytic proportion of bone marrow is inversely related to bone formation in osteoporosis. J Clin Pathol 55:693-698

69. **Ahdjoudj S, Lasmoles F, Holy X, Zerath E, Marie PJ** 2002 Transforming growth factor beta2 inhibits adipocyte differentiation induced by skeletal unloading in rat bone marrow stroma. J Bone Miner Res 17:668-677

70. **Reseland JE, Syversen U, Bakke I, Qvigstad G, Eide LG, Hjertner O, Gordeladze JO, Drevon CA** 2001 Leptin is expressed in and secreted from primary cultures of human osteoblasts and promotes bone mineralization. J Bone Miner Res 16:1426-1433

71. **Cornish J, Callon KE, Bava U, Lin C, Naot D, Hill BL, Grey AB, Broom N, Myers DE, Nicholson GC, Reid IR** 2002 Leptin directly regulates bone cell function in vitro and reduces bone fragility in vivo. J Endocrinol 175:405-415

72. **Karsenty G** 2001 Leptin controls bone formation through a hypothalamic relay. Recent Prog Horm Res 56:401-415

73. **Chan JL, Mantzoros CS** 2005 Role of leptin in energy-deprivation states: normal human physiology and clinical implications for hypothalamic amenorrhoea and anorexia nervosa. Lancet 366:74-85

74. **Steppan CM, Crawford DT, Chidsey-Frink KL, Ke H, Swick AG** 2000 Leptin is a potent stimulator of bone growth in ob/ob mice. Regul Pept 92:73-78

75. **Considine RV, Sinha MK, Heiman ML, Kriauciunas A, Stephens TW, Nyce MR, Ohannesian JP, Marco CC, McKee LJ, Bauer TL, et al.** 1996 Serum immunoreactive-leptin concentrations in normal-weight and obese humans. N Engl J Med 334:292-295

76. **Goulding A, Taylor RW** 1998 Plasma leptin values in relation to bone mass and density and to dynamic biochemical markers of bone resorption and formation in postmenopausal women. Calcif Tissue Int 63:456-458

77. **Thomas T, Gori F, Khosla S, Jensen MD, Burguera B, Riggs BL** 1999 Leptin acts on human marrow stromal cells to enhance differentiation to osteoblasts and to inhibit differentiation to adipocytes. Endocrinology 140:1630-1638

78. **Martin A, de Vittoris R, David V, Moraes R, Begeot M, Lafage-Proust MH, Alexandre C, Vico L, Thomas T** 2005 Leptin modulates both resorption and formation while preventing disuse-induced bone loss in tail-suspended female rats. Endocrinology 146:3652-3659

79. **Burguera B, Hofbauer LC, Thomas T, Gori F, Evans GL, Khosla S, Riggs BL, Turner RT** 2001 Leptin reduces ovariectomy-induced bone loss in rats. Endocrinology 142:3546-3553

80. **Yeh WC, Cao Z, Classon M, McKnight SL** 1995 Cascade regulation of terminal adipocyte differentiation by three members of the C/EBP family of leucine zipper proteins. Genes Dev 9:168-181

81. **Wu Z, Xie Y, Bucher NL, Farmer SR** 1995 Conditional ectopic expression of C/EBP beta in NIH-3T3 cells induces PPAR gamma and stimulates adipogenesis. Genes Dev 9:2350-2363

82. **Millward CA, Heaney JD, Sinasac DS, Chu EC, Bederman IR, Gilge DA, Previs SF, Croniger CM** 2007 Mice with a deletion in the gene for CCAAT/enhancer-binding protein beta are protected against diet-induced obesity. Diabetes 56:161-167

83. **Staiger J, Lueben MJ, Berrigan D, Malik R, Perkins SN, Hursting SD, Johnson PF** 2009 C/EBPbeta regulates body composition, energy balance-related hormones and tumor growth. Carcinogenesis 30:832-840

84. **Schroeder-Gloeckler JM, Rahman SM, Janssen RC, Qiao L, Shao J, Roper M, Fischer SJ, Lowe E, Orlicky DJ, McManaman JL, Palmer C, Gitomer WL, Huang W, O'Doherty RM, Becker TC, Klemm DJ, Jensen DR, Pulawa LK, Eckel RH, Friedman JE** 2007 CCAAT/enhancer-binding protein beta deletion reduces adiposity, hepatic steatosis, and diabetes in Lepr(db/db) mice. J Biol Chem 282:15717-15729

85. **Tanaka T, Yoshida N, Kishimoto T, Akira S** 1997 Defective adipocyte differentiation in mice lacking the C/EBPbeta and/or C/EBPdelta gene. EMBO J 16:7432-7443

86. **Gutierrez S, Javed A, Tennant DK, van Rees M, Montecino M, Stein GS, Stein JL, Lian JB** 2002 CCAAT/enhancer-binding proteins (C/EBP) beta and delta activate osteocalcin gene transcription and synergize with

Runx2 at the C/EBP element to regulate bone-specific expression. J Biol Chem 277:1316-1323

87. **Harrison JR, Huang YF, Wilson KA, Kelly PL, Adams DJ, Gronowicz GA, Clark SH** 2005 Col1a1 promoter-targeted expression of p20 CCAAT enhancer-binding protein beta (C/EBPbeta), a truncated C/EBPbeta isoform, causes osteopenia in transgenic mice. J Biol Chem 280:8117-8124

88. **Moon RT** 2005 Wnt/beta-catenin pathway. Sci STKE 2005:cm1

89. **Baron R, Rawadi G** 2007 Targeting the Wnt/beta-catenin pathway to regulate bone formation in the adult skeleton. Endocrinology 148:2635-2643

90. **Clevers H** 2006 Wnt/beta-catenin signaling in development and disease. Cell 127:469-480

91. **Dong YF, Soung do Y, Schwarz EM, O'Keefe RJ, Drissi H** 2006 Wnt induction of chondrocyte hypertrophy through the Runx2 transcription factor. J Cell Physiol 208:77-86

92. **Gong Y, Slee RB, Fukai N, Rawadi G, Roman-Roman S, Reginato AM, Wang H, Cundy T, Glorieux FH, Lev D, Zacharin M, Oexle K, Marcelino J, Suwairi W, Heeger S, Sabatakos G, Apte S, Adkins WN, Allgrove J, Arslan-Kirchner M, Batch JA, Beighton P, Black GC, Boles RG, Boon LM, Borrone C, Brunner HG, Carle GF, Dallapiccola B, De Paepe A, Floege B, Halfhide ML, Hall B, Hennekam RC, Hirose T, Jans A, Juppner H, Kim CA, Keppler-Noreuil K, Kohlschuetter A, LaCombe D, Lambert M, Lemyre E, Letteboer T, Peltonen L, Ramesar RS, Romanengo M, Somer H, Steichen-Gersdorf E, Steinmann B, Sullivan B, Superti-Furga A, Swoboda W, van den Boogaard MJ, Van Hul W, Vikkula M, Votruba M, Zabel B, Garcia T, Baron R, Olsen BR, Warman ML** 2001 LDL receptor-related protein 5 (LRP5) affects bone accrual and eye development. Cell 107:513-523

93. **Boyden LM, Mao J, Belsky J, Mitzner L, Farhi A, Mitnick MA, Wu D, Insogna K, Lifton RP** 2002 High bone density due to a mutation in LDL-receptor-related protein 5. N Engl J Med 346:1513-1521

94. **Little RD, Carulli JP, Del Mastro RG, Dupuis J, Osborne M, Folz C, Manning SP, Swain PM, Zhao SC, Eustace B, Lappe MM, Spitzer L, Zweier S, Braunschweiger K, Benchekroun Y, Hu X, Adair R, Chee L, FitzGerald MG, Tulig C, Caruso A, Tzellas N, Bawa A, Franklin B, McGuire S, Nogues X, Gong G, Allen KM, Anisowicz A, Morales AJ, Lomedico PT, Recker SM, Van Eerdewegh P, Recker RR, Johnson ML** 2002 A mutation in the LDL receptor-related protein 5 gene results in the autosomal dominant high-bone-mass trait. Am J Hum Genet 70:11-19

95. **Kato M, Patel MS, Levasseur R, Lobov I, Chang BH, Glass DA, 2nd, Hartmann C, Li L, Hwang TH, Brayton CF, Lang RA, Karsenty G, Chan L** 2002 Cbfa1-independent decrease in osteoblast proliferation, osteopenia, and persistent embryonic eye vascularization in mice deficient in Lrp5, a Wnt coreceptor. J Cell Biol 157:303-314

96. **Babij P, Zhao W, Small C, Kharode Y, Yaworsky PJ, Bouxsein ML, Reddy PS, Bodine PV, Robinson JA, Bhat B, Marzolf J, Moran RA, Bex F** 2003 High bone mass in mice expressing a mutant LRP5 gene. J Bone Miner Res 18:960-974

97. **Holmen SL, Giambernardi TA, Zylstra CR, Buckner-Berghuis BD, Resau JH, Hess JF, Glatt V, Bouxsein ML, Ai M, Warman ML, Williams BO** 2004 Decreased BMD and limb deformities in mice carrying mutations in both Lrp5 and Lrp6. J Bone Miner Res 19:2033-2040

98. **Kubota T, Michigami T, Ozono K** 2009 Wnt signaling in bone metabolism. J Bone Miner Metab 27:265-271

99. **Bennett CN, Longo KA, Wright WS, Suva LJ, Lane TF, Hankenson KD, MacDougald OA** 2005 Regulation of osteoblastogenesis and bone mass by Wnt10b. Proc Natl Acad Sci U S A 102:3324-3329

100. **Bennett CN, Ross SE, Longo KA, Bajnok L, Hemati N, Johnson KW, Harrison SD, MacDougald OA** 2002 Regulation of Wnt signaling during adipogenesis. J Biol Chem 277:30998-31004

101. **Ross SE, Hemati N, Longo KA, Bennett CN, Lucas PC, Erickson RL, MacDougald OA** 2000 Inhibition of adipogenesis by Wnt signaling. Science 289:950-953

102. **Ross SE, Erickson RL, Gerin I, DeRose PM, Bajnok L, Longo KA, Misek DE, Kuick R, Hanash SM, Atkins KB, Andresen SM, Nebb HI, Madsen L, Kristiansen K, MacDougald OA** 2002 Microarray analyses during adipogenesis: understanding the effects of Wnt signaling on adipogenesis and the roles of liver X receptor alpha in adipocyte metabolism. Mol Cell Biol 22:5989-5999

103. **Kang S, Bennett CN, Gerin I, Rapp LA, Hankenson KD, Macdougald OA** 2007 Wnt signaling stimulates osteoblastogenesis of mesenchymal precursors by suppressing CCAAT/enhancer-binding protein alpha and peroxisome proliferator-activated receptor gamma. J Biol Chem 282:14515-14524

104. **Tashjian AH, Jr., Gagel RF** 2006 Teriparatide [human PTH(1-34)]: 2.5 years of experience on the use and safety of the drug for the treatment of osteoporosis. J Bone Miner Res 21:354-365

105. **Abrahamsen B, Eiken P, Eastell R** 2009 Subtrochanteric and diaphyseal femur fractures in patients treated with alendronate: a register-based national cohort study. J Bone Miner Res 24:1095-1102

106. **Goh SK, Yang KY, Koh JS, Wong MK, Chua SY, Chua DT, Howe TS** 2007 Subtrochanteric insufficiency fractures in patients on alendronate therapy: a caution. J Bone Joint Surg Br 89:349-353

107. **Kwek EB, Goh SK, Koh JS, Png MA, Howe TS** 2008 An emerging pattern of subtrochanteric stress fractures: a long-term complication of alendronate therapy? Injury 39:224-231

108. **Migliorati CA, Schubert MM, Peterson DE** 2009 Bisphosphonate osteonecrosis (BON): unanswered questions and research possibilities. Rev Recent Clin Trials 4:99-109

109. **Mariotti A** 2008 Bisphosphonates and osteonecrosis of the jaws. J Dent Educ 72:919-929

110. **Khamaisi M, Regev E, Yarom N, Avni B, Leitersdorf E, Raz I, Elad S** 2007 Possible association between diabetes and bisphosphonate-related jaw osteonecrosis. J Clin Endocrinol Metab 92:1172-1175

111. **Dempster DW, Cosman F, Parisien M, Shen V, Lindsay R** 1993 Anabolic actions of parathyroid hormone on bone. Endocr Rev 14:690-709

112. **Neer RM, Arnaud CD, Zanchetta JR, Prince R, Gaich GA, Reginster JY, Hodsman AB, Eriksen EF, Ish-Shalom S, Genant HK, Wang O, Mitlak BH** 2001 Effect of parathyroid hormone (1-34) on fractures and bone mineral density in postmenopausal women with osteoporosis. N Engl J Med 344:1434-1441

113. **Burr DB, Hirano T, Turner CH, Hotchkiss C, Brommage R, Hock JM** 2001 Intermittently administered human parathyroid hormone(1-34) treatment increases intracortical bone turnover and porosity without reducing bone strength in the humerus of ovariectomized cynomolgus monkeys. J Bone Miner Res 16:157-165

114. **Vahle JL, Long GG, Sandusky G, Westmore M, Ma YL, Sato M** 2004 Bone neoplasms in F344 rats given teriparatide [rhPTH(1-34)] are dependent on duration of treatment and dose. Toxicol Pathol 32:426-438

115. **Vahle JL, Sato M, Long GG, Young JK, Francis PC, Engelhardt JA, Westmore MS, Linda Y, Nold JB** 2002 Skeletal changes in rats given daily subcutaneous injections of recombinant human parathyroid hormone (1-34) for 2 years and relevance to human safety. Toxicol Pathol 30:312-321

116. **Tanaka S, Sakai A, Tanaka M, Otomo H, Okimoto N, Sakata T, Nakamura T** 2004 Skeletal unloading alleviates the anabolic action of intermittent PTH(1-34) in mouse tibia in association with inhibition of PTH-induced increase in c-fos mRNA in bone marrow cells. J Bone Miner Res 19:1813-1820

117. **Liu CC, Kalu DN** 1990 Human parathyroid hormone-(1-34) prevents bone loss and augments bone formation in sexually mature ovariectomized rats. J Bone Miner Res 5:973-982

118. **Liu CC, Kalu DN, Salerno E, Echon R, Hollis BW, Ray M** 1991 Preexisting bone loss associated with ovariectomy in rats is reversed by parathyroid hormone. J Bone Miner Res 6:1071-1080

119. **Turner RT, Evans GL, Cavolina JM, Halloran B, Morey-Holton E** 1998 Programmed administration of parathyroid hormone increases bone

formation and reduces bone loss in hindlimb-unloaded ovariectomized rats. Endocrinology 139:4086-4091

120. **Sibonga JD, Iwaniec UT, Shogren KL, Rosen CJ, Turner RT** 2007 Effects of parathyroid hormone (1-34) on tibia in an adult rat model for chronic alcohol abuse. Bone 40:1013-1020

121. **Tsuchida T, Sato K, Miyakoshi N, Abe T, Kudo T, Tamura Y, Kasukawa Y, Suzuki K** 2000 Histomorphometric evaluation of the recovering effect of human parathyroid hormone (1-34) on bone structure and turnover in streptozotocin-induced diabetic rats. Calcif Tissue Int 66:229-233

CHAPTER 2

Motyl KJ*, Botolin S*, Irwin R*, Appledorn DM, Kadakia T, Amalfitano A, Schwartz RC, McCabe LR 2009 Bone inflammation and altered gene expression with type I diabetes early onset. J Cell Physiol 218:575-583

*authors contributed equally.

CHAPTER 2

2. BONE INFLAMMATION AND ALTERED GENE EXPRESSION WITH TYPE I DIABETES EARLY ONSET

2.1. ABSTRACT

Type I diabetes is associated with bone loss and marrow adiposity. To identify early events involved in the etiology of diabetic bone loss, diabetes was induced in mice by multiple low dose streptozotocin injections. Serum markers of bone metabolism and inflammation as well as tibial gene expression were examined between 1 and 17 days post injection (dpi). At 3 dpi, when blood glucose levels were significantly elevated, body, fat pad and muscle mass were decreased. Serum markers of bone resorption and formation significantly decreased at 5 dpi in diabetic mice and remained suppressed throughout the time course. An osteoclast gene, TRAP5 mRNA, was suppressed at early and late time points. Suppression of osteogenic genes (runx2 and osteocalcin) and induction of adipogenic genes (PPARγ2 and aP2) were evident as early as 5 dpi. These changes were associated with an elevation of serum cytokines, but more importantly we observed an increase in the expression of cytokines in bone, supporting the idea that bone, itself, exhibits an inflammatory response during diabetes induction. This inflammation could in turn contribute to diabetic bone pathology. Mice deficient in IFN-γ (one of the key cytokines elevated in bone and

known to be involved in bone regulation) did not prevent diabetic bone pathology. Taken together, our findings indicate that bone becomes inflamed with the onset of T1-diabetes and during this time bone phenotype markers become altered. However, inhibition of one cytokine, IFN-γ was not sufficient to prevent the rapid bone phenotype changes.

2.2. INTRODUCTION

Type I diabetes is a complex disorder associated with multiple long term complications. It evolves with progression to nearly complete beta cell destruction and establishment of a hyperglycemic state. Unfortunately, at the time clinical symptoms present, pancreatic β-cells are irreversibly and almost completely damaged. This makes it difficult to monitor and understand the early events in the etiology of diabetic complications. Data on the progression of early changes is scarce and comes from experimental models of induced diabetes such as streptozotocin injected diabetic mice. In this model, animals are injected daily with streptozotocin, for 5 consecutive days. Streptozotocin is a nitrosourea derived drug from *Streptomyces achromogenes* which causes pancreatic β-islet infiltration of T cells and macrophages in rodents, similar to the histology of human type I pancreatic biopsies (1, 2). Monitoring of the glycemic profile in fasting rats following streptozotocin (80 mg/kg by intraperitoneal injection) treatment demonstrates a rapid response with evidence of hyperglycemia and reduced plasma insulin levels within two hours (3). This response is followed by

a drop in blood glucose levels and high plasma insulin levels at 6 hours, but ultimately a progressive state of chronic hyperglycemia ensues (3).

It is known that one of the complications of type I diabetes is bone loss and ongoing population studies continue to support these observations in humans (4-13). Similarly, rodent type I diabetes models also exhibit significant bone loss (14-22). Examination of bone metabolism markers in humans and rodent models suggest that diabetic bone loss is primarily due to a defect in bone formation rather than resorption (17, 18, 23-25). In fact, analyses of serum markers of bone resorption indicate that, if anything, resorption is actually decreased in parallel with the decrease in osteoblast activity (18, 25, 26). However, it remains unknown if osteoclast activation occurs early in the disease progression and contributes to the significant bone loss seen at later time points.

The above findings support the notion that type I diabetes promotes a true suppression of bone formation most likely through a reduction of osteoblast numbers and/or maturation. Previously, we demonstrated that streptozotocin-induced diabetes in BALB/c male mice is associated with bone loss and suppression of serum osteocalcin and osteocalcin mRNA levels in bone (18). In addition, visible changes in bone histology marked by increased marrow adiposity were observed and further confirmed by increased mRNA levels of markers of adipocyte maturation, PPARγ2 and aP2 (18). The elevated expression of adipogenic markers and decreased expression of osteogenic markers was apparent as early as 17 and 19 days after the first injection of streptozotocin (18, 27). Considering the present literature on the timing of early

changes in streptozotocin induced diabetes, and our previous data, we hypothesize that the commitment to a suppressed osteoblast phenotype and increased bone marrow adiposity in diabetes occurs early during the onset of diabetes. Here we demonstrate that osteoclast activity is not increased during the progression of diabetes as and is actually significantly reduced by 5 dpi, as determined by serum PYD and TRAP5 mRNA, although we did observe an early decrease and an rapid increase at 3 dpi in RANKL expression. We also found a reduction in serum osteocalcin and mRNA levels of osteogenic markers and an increase in adipocyte markers within 5 to 7 days dpi (18, 27). Systemic and local cytokine expression increased during this time, indicating that bone is a site of inflammation during disease onset. These findings indicate that diabetes-induced changes in bone phenotype and inflammation occur rapidly and in parallel with changes in metabolic status. Of the cytokines elevated in bone RNA samples, IFN-γ (known to contribute to the regulation of bone remodeling (28-37)) was found to be consistently elevated early and during bone phenotype adaptation to diabetes. However, IFN-γ deficiency was not sufficient to prevent diabetic bone loss, suggesting that other cytokines, factors or combinations of factors may need to be targeted to prevent this diabetes complication.

2.3. MATERIALS AND METHODS

2.3.1. Streptozotocin mouse injections

Adult (15 week old) male wild type or IFN-$\gamma^{-/-}$ mice (BALB/c strain; Jackson Laboratories, Bar Harbor, ME) were intraperitoneally injected daily with streptozotocin (40 μg/g body weight in 0.1 citrate buffer) for 5 days (38, 39). Controls were injected with citrate buffer alone. Twenty-four hours after the first injection, animals were considered as 1 day post injection. Wild type mice were harvested 1, 3, 5, 7, 9, 11, 17 or 32 days post the first injection (dpi). IFN-$\gamma^{-/-}$ mice were harvested 32 dpi, after bone loss was visible with mCT. All mice were kept on a light/dark (12h/12h) cycle at 23°C, and received food (standard lab chow) and water ad libitum. Mice were euthanized and tibiae were immediately removed, freed from soft tissue, snap-frozen in liquid nitrogen, and stored at -80°C (for RNA analyses). Animal studies were conducted in accordance with the Michigan State University Institutional Animal Care and Use Committee.

2.3.2. Genotyping

Knockout of IFN-γ was confirmed by RT-PCR as described below with primers specific for the wild type and knockout gene locus, according to the protocol provided by The Jackson Laboratory. Wild type primers were 5'-AGA AGT AAG TGG AAG GGC CCA GAA G-3' and 5'-AGG GAA ACT GGG AGA

GGA GAA ATA T-3'. Knockout primers were 5'-TCA GCG CAG GGG CGC CCG GTT CTT T-3' and 5'-ATC GAC AAG ACC GGC TTC CAT CCG-3'. PCR amplicons were separated on a 2% agarose DNA gel with a 100 bp DNA ladder (Invitrogen, Calsbad, CA).

2.3.3. Plasma measurements

Blood was obtained from mice at the time of euthanasia and blood serum prepared from each sample by centrifugation for 5 min at 3000 rpm. Serum was stored frozen at –20°C. Glucose concentration in serum samples was determined using a Glucose Assay Kit (Sigma, Saint Louis, MO). Serum osteocalcin levels were measured using Mouse Osteocalcin EIA Kit (Biomedical Technologies Inc. Stoughton, MA, USA) according to manufacturer instructions. Serum PYD was measured using Metra® PYD kit (Quidel Corporation, San Diego, CA, USA) according to manufacturer instructions. Quantitative determination of non-esterified (free) fatty acids in mouse serum was performed according to manufacturer instructions using Wako NEFA C test kit (Wako Chemicals USA, Inc. Richmond, VA, USA). Serum cytokines were measured using the Bio-Plex multiplex mouse cytokine 23-plex bead-based assay according to manufacture protocol (Bio-Rad, Hercules, CA). Standard curves were run for each cytokine and serum concentrations were calculated.

2.3.4. RNA Analysis

Whole tibias were crushed under liquid nitrogen conditions using a Bessman Tissue Pulverizer and RNA extracted using the method of Chomczynski and Sacchi as previously described (40, 41). RNA integrity was verified by formaldehyde-agarose gel electrophoresis. Synthesis of cDNA was performed by reverse transcription with 2 μg of total RNA using the Superscript II kit with oligo $dT_{(12-18)}$ primers as described by the manufacturer (Invitrogen, Carlsbad, CA). cDNA (1 μl) was amplified by PCR in a final volume of 25 μl using the iQ SYBR Green Supermix (Bio-Rad, Hercules, CA) with 10 pmol of each primer (Integrated DNA Technologies, Coralville, IA). Osteocalcin was amplified using 5'-ACG GTA TCA CTA TTT AGG ACC TGT G-3' and 5'-ACT TTA TTT TGG AGC TGC TGT GAC-3' (42). Runx2 was amplified using 5'- GAC AGA AGC TTG ATG ACT CTA AAC C-3' and 5'- TCT GTA ATC TGA CTC TGT CCT TGT G-3' (43). PPARγ2 was amplified using 5'-TGA AAC TCT GGG AGA TTC TCC TG-3' and 5'-CCA TGG TAA TTT CTT GTG AAG TGC-3' (44). Adipocyte fatty acid-binding protein 4 (aP2) was amplified using 5'-GCG TGG AAT TCG ATG AAA TCA-3' and 5'-CCC GCC ATC TAG GGT TAT GA-3' (45). TRAP5 was amplified using 5'-AAT GCC TCG ACC TGG GA-3' and 5'-CGT AGT CCT CCT TGG CTG CT-3' (46). RANKL was amplified using 5'-TTT GCA GGA CTC GAC TCT GGA G-3' and 5'-TCC CTC CTT TCA TCA GGT TAT GAG-3' according to Zhao et al. (47). OPG was amplified using 5'-GAA GAA GAT CAT

CCA AGA CAT TGA C-3' and 5'-TCC ATA AAC TGA GTA GCT TCA GGA G-3'. IL-6 was amplified using 5'-ATC CAG TTG CCT TCT TGG GAC TGA-3' and 5' TAA GCC TCC GAC TTG TGA AGT GGT-3'. The following cytokine primers and their PCR protocols are previously described: IL-1Ra (48), LT-β (49), IL-1α (50), IFN-γ (51), MCP-1 (52), KC (52), MIP-1β (53) and TNF-α (54). Cyclophilin, which was not modulated under diabetic conditions, was used as a control for RNA levels; it was amplified using 5'-ATT CAT GTG CCA GGG TGG TGA C-3' and 5'-CCG TTT GTG TTT GGT CCA GCA-3' (55, 56) and exhibited similar kinetics of amplification compared to other genes examined. In some cases HPRT was also used as a non-modulated control gene and was amplified using 5'-AAG CCT AAG ATG AGC GCA AG-3' and 5'-TTA CTA GGC AGA TGG CCA CA-3' (57). Real time PCR was carried out for 40 cycles using the iCycler (Bio-Rad, Hercules, CA) and data were evaluated using the iCycler software. Each cycle consisted of 95°C for 15 seconds, 60°C for 30 seconds (except for runx2 and osteocalcin, which had an annealing temperature of 65°C) and 72°C for 30 seconds. RNA-free samples, a negative control, did not produce amplicons. Melting curve and gel analyses (sizing, isolation and sequencing) were used to verify single products of the appropriate base pair size.

Cytokine expression was also examined by ribonuclease protection assay (RPA) using the multi template probe sets mCK-2b and mCK-3b according to the manufacturer instructions (BD Biosciences, California BD RiboQuant™ assay). Briefly, RNA (5 μg) was hybridized to 1 X 10^6 cpm of the probe in 10 μl of hybridization buffer. Samples were denatured at 95°C, incubated at 56°C for 16

hours, treated with RNase (19.2 ng/100 μl) for 45 minutes at 30°C, and incubated with proteinase K (27 mg/18ul) for 15 minutes at 37°C. Precipitated RNA was resuspended in 5 μl of gel loading buffer and resolved on a ~8 M urea, 4.75% polyacrylamide gel. Radiolabeled probe (alone) was used as a marker for each cytokine band. Controls include samples without RNA and a) with RNase to demonstrate efficient RNA degradation and b) without RNase to detect general degradation of probe.

2.3.5. Micro-computed tomography (μCT) analysis

Tibias were scanned using a GE Explore Locus μCT system at a voxel resolution of 20 μm obtained from 720 views. Each run included control and diabetic, wild type and IFN-$\gamma^{-/-}$ bones, and a calibration phantom to standardize grayscale values and maintain consistency. Based on auto threshold and isosurface analyses of multiple bone samples, a fixed threshold (1400) was used to separate bone from bone marrow. Trabecular bone analyses were done in a region of trabecular bone defined at 0.17 mm (approximately 1% of the total length) immediately distal to the growth plate of the proximal tibia extending 2 mm toward the diaphysis, and excluding the outer cortical shell. Trabecular bone volume fraction (BVF) was computed by GE Healthcare MicroView software or visualization and analysis of volumetric image data.

2.3.6. Statistical analysis

All statistical analyses were performed using Microsoft Excel data analysis program for t-test analysis. Values are expressed as a mean ± SE.

2.4. RESULTS

Previously, we demonstrated that multiple low dose streptozotocin-induced diabetes caused changes in body weight, serum parameters and bone histology, as well as gene expression resulting in bone loss (18). We also reported that these changes were evident five days after confirmation of diabetes (58). Based on the protocol for diabetes induction (daily injections of streptozotocin for 5 days followed by a 7 day period prior to confirmation of diabetes), the day 5 time point in our past studies was actually 17 days after the animals received their first injection of streptozotocin (17 dpi). The marked changes that we observed at this time suggested that the events involved in the changes in bone and serum parameters must occur earlier. To identify the progression of these events, we injected mice with streptozotocin and examined serum, muscle and bone parameters at 1, 3, 5, 7, 9, 11, and 17 dpi of streptozotocin or citrate buffer (vehicle control).

The STZ-injected mice exhibited weight loss at 3 dpi which plateaus by 5 dpi (Figure 6). Blood glucose levels were significantly increased at 3 dpi and continued to rise over the course of diabetes induction (Figure 6). The immediate change in body mass was not associated with elevated serum free fatty acids (Figure 6), but was directly associated with the loss of femoral fat pad weight and size, which were significantly reduced at 3 dpi and reached maximum reduction in size at 5 dpi (Figure 6). The mass of the tibialis anterior muscle was

also significantly reduced with the onset of diabetes (Figure 6), indicating a reduction in mass of several mesenchymal derived tissues.

Figure 6. **Time course of general body parameters during the onset of type I diabetes in BALB/c mice.** Diabetes was induced by 5 daily streptozotocin injections beginning on day 0. Body, muscle (tibialis), and fat pad (femoral) mass and serum parameters (glucose and free fatty acids (FFA)) were measured at 1, 3, 5, 7, 9, 11, and 17 days post injection (dpi) of streptozotocin (triangles) or citrate buffer (vehicle control, squares). Values represent averages obtained from 5-6 mice per condition per time point +/- SE. *p<05.

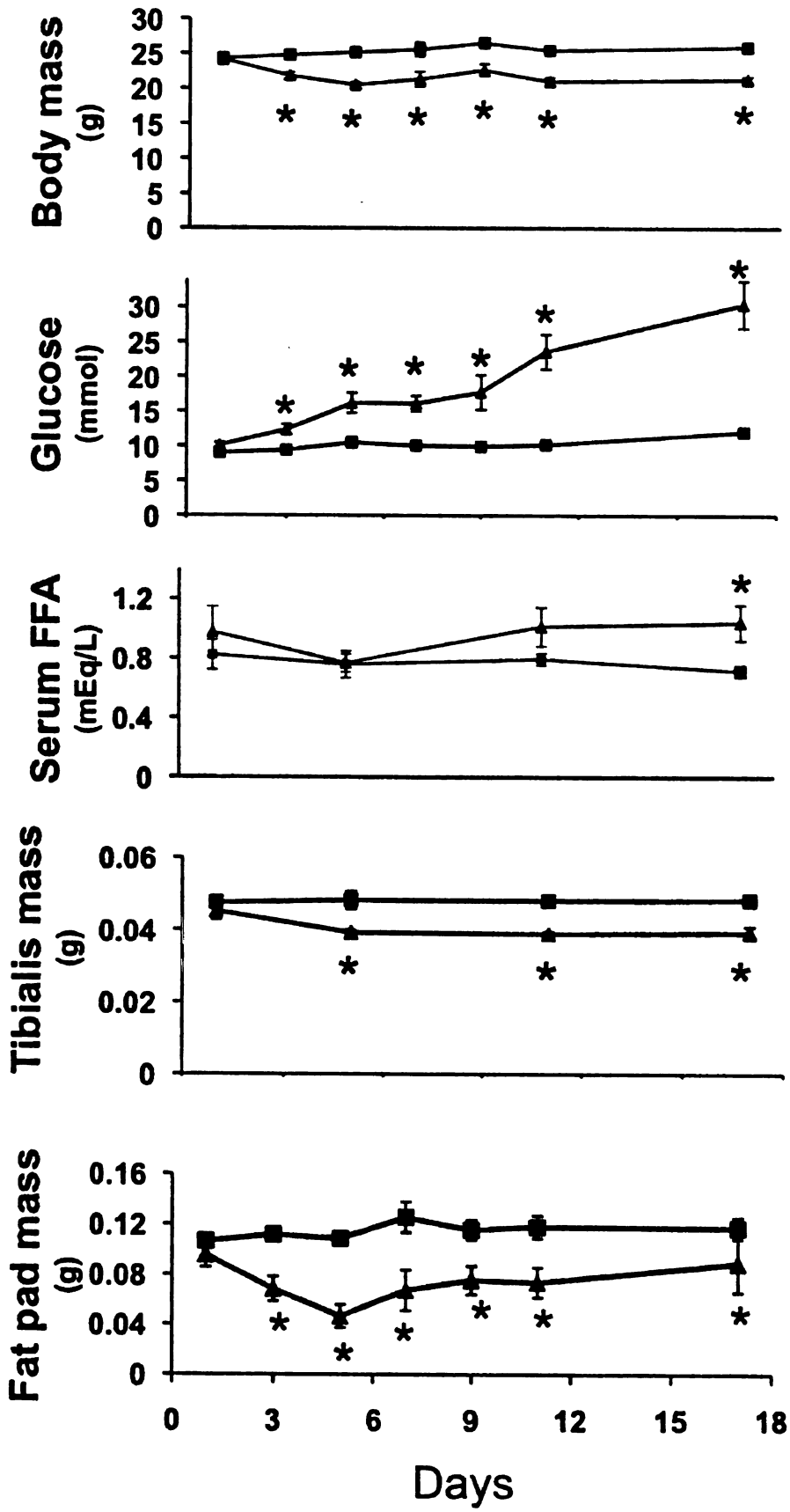
Body mass
(g)
30
25
20
15
10
5
0
Glucose
(mmol)
30
25
20
15
10
5
0
Serum FFA
(mEq/L)
1.2
0.8
0.4
0
Tibialis mass
(g)
0.06
0.04
0.02
0
Fat pad mass
(g)
0.16
0.12
0.08
0.04
0
0
3
6
9
12
15
18
Days

Previously, we demonstrated that at 17 dpi, diabetic mice exhibited decreased serum levels of osteocalcin (bone formation marker), decreased expression of mature osteoblast markers and increased expression of adipocyte markers in bone. To determine when the onset of these changes first occurred, we collected serum and isolated tibia RNA from 8-11 mice per condition at 1, 3, 5, 7, 9, 11, and 17 dpi of streptozotocin or citrate buffer (vehicle control). At 5 dpi, the onset of diabetes significantly decreased serum osteocalcin levels indicating that bone formation was suppressed immediately (Figure 7A). Consistent with the suppression of serum bone formation markers, osteocalcin mRNA levels were significantly reduced in diabetic tibias at 5 dpi. Osteocalcin mRNA levels also trended to decrease within 24 hours of the first streptozotocin-injection. Similar changes were seen with runx2 mRNA levels. Specifically, runx2 expression was significantly suppressed at 1 and 5 dpi and beyond. Interestingly, we found that adipocyte markers were equally responsive and that induction of diabetes upregulates aP2 and PPARγ2 mRNA levels as early as 5 and 7 dpi, respectively (Figure 7B). This correlates with the elevation of blood glucose and other early events of diabetes that we observed.

Figure 7. **Significant bone phenotype changes are evident at 5 dpi.** ***A.*** Serum osteocalcin (OC) levels were determined in mice injected with citrate buffer (controls, squares) or streptozotocin (triangles) at 1, 3, 5, 7, 9, 11, and 17 dpi. Values are averages +/- SE obtained from 8-11 mice per condition. *$p<0.05$. ***B.*** Total RNA was extracted from tibia isolated from citrate buffer (vehicle control, squares) and streptozotocin (triangles) injected mice at 1, 3, 5, 7, 9, 11, and 17 dpi. Levels of osteocalcin (OC), runx2, PPARγ2 and aP2 mRNAs were determined by real time RT-PCR and are expressed relative to cyclophilin (housekeeping gene). Values are averages +/- SE obtained from 5-6 mice per condition per time point. *$p<0.05$.

A.

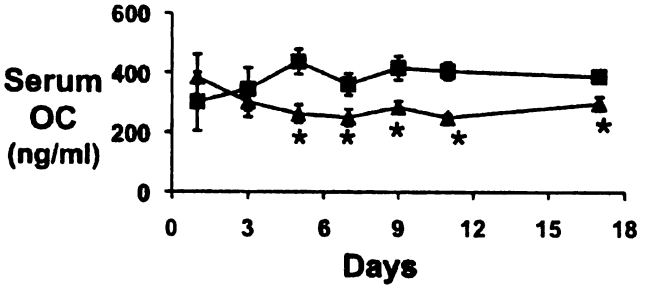
Serum OC (ng/ml)
600
400
200
0
0 3 6 9 12 15 18
Days

B.

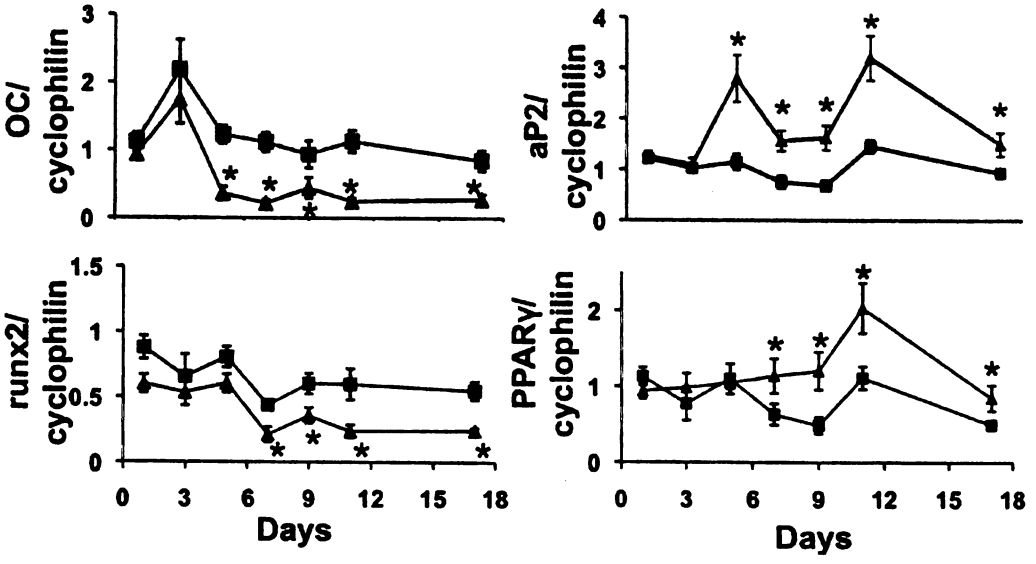
OC/ cyclophilin
aP2/ cyclophilin
runx2/ cyclophilin
PPARγ/ cyclophilin
Days
Days

Our past studies have indicated that serum and RNA markers of osteoclast maturation and activity are decreased in T1-diabetic mice. To determine if these changes are apparent early in T1-diabetes onset we measured several osteoclast parameters. Figure 8 demonstrates that expression of osteoclast regulators, osteoprotegrin (OPG) and RANKL, in bone during the time course was variable. At 1 dpi RANKL was suppressed but was then levels significantly increased at day 3 and then returned and remained at normal levels after 5 dpi. OPG levels did not change early on, but were reduced at later time points. The ratio of the two parameters (not shown) was highly variable in both control and T1-diabetic mice. Therefore we examined a serum marker of resorption, PYD levels, and found a significant decrease at all time points studied (Figure 8). Serum was examined because T1-diabetic mice exhibit polyurea and potentially nephropathy, both of which could have a major impact on urine measurements. As a further assessment of osteoclast activity we measured TRAP5 mRNA levels in bone (Figure 8) and found that they were decreased at early time points (1 and 3 dpi) and at 17 dpi, consistent with our previous reports.

Figure 8. **Analyses of osteoclast regulators, markers and activity.** Total RNA was extracted from tibia isolated from citrate buffer (vehicle control, squares) and streptozotocin (triangles) injected mice at 1, 3, 5, 7, 9, 11, and 17 dpi. Levels of osteoprotegrin (OPG), RANKL, and TRAP5 mRNAs were determined by real time RT-PCR and are expressed relative to HPRT (housekeeping gene). Values are averages +/- SE obtained from 5-6 mice per condition per time point. *$p<0.05$. Serum isolated at time points 1, 5, 11 and 17 was analyzed for pyridinoline crosslink PYD levels. Values are averages +/- SE obtained from 8-11 mice per condition. *$p<0.05$.

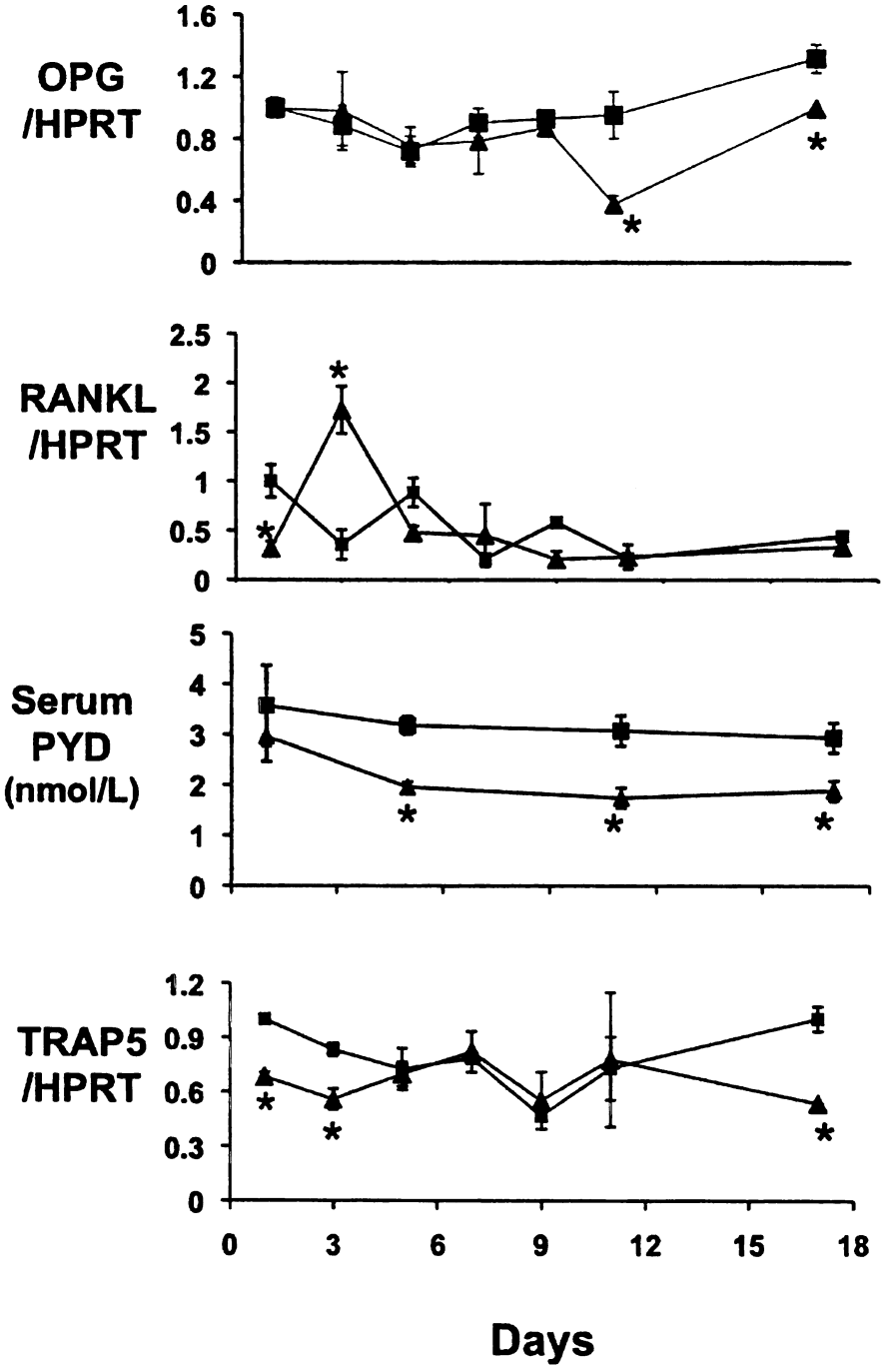
OPG /HPRT
1.6
1.2
0.8
0.4
0
RANKL /HPRT
2.5
2
1.5
1
0.5
0
Serum PYD (nmol/L)
5
4
3
2
1
0
TRAP5 /HPRT
1.2
0.9
0.6
0.3
0
0
3
6
9
12
15
18
Days

We hypothesized that T1-diabetes associated immunologic responses resulting from early pancreatic beta cell destruction could contribute to changes observed in bone phenotype. Therefore, we examined the levels of 23 different cytokines in the serum of control and diabetic mice. The serum profiles during the onset of type I diabetes varied for each cytokine with some showing no modulation (IL-2, -3, -5, and IL-12 (p70)), some trending toward an increase at early time points ($p < 0.10$; IL-1β, IL-9, IL-10, IFN-γ and KC), some showing significant increases at 3 dpi ($p<0.05$; IL-1α, IL-6, IL-12 (p70), IL-13, IL-17, MCP-1, MIP-1β, and TNF-α) and some showing a significant elevation at later time points (at 5, 7 and/or 9dpi; IL-17, MCP-1, MIP-1α, MIP-1β, Rantes, and TNF-α) compared to vehicle treated mice. Figure 9 shows only the serum cytokines that were significantly elevated by greater than 2-fold at any time point during the onset of type I diabetes. Cytokines whose levels are statistically higher than vehicle treated mice prior to and/or during changes in gene expression in bone (ie, IL-1α, IL-6, IFN-γ, TNF-α) could be potential contributors to this process.

Figure 9. **Serum cytokine levels increase during the early onset of diabetes.** Serum cytokine levels were determined using the Bio-Plex multiplex mouse cytokine 23 plex bead-based assay (Bio-Rad). Of the 23 cytokines the 7 cytokines shown exhibited the greatest induction at any one time point. Values are averages +/- SE obtained from 3-6 mice per condition per time point. *$p<0.05$.

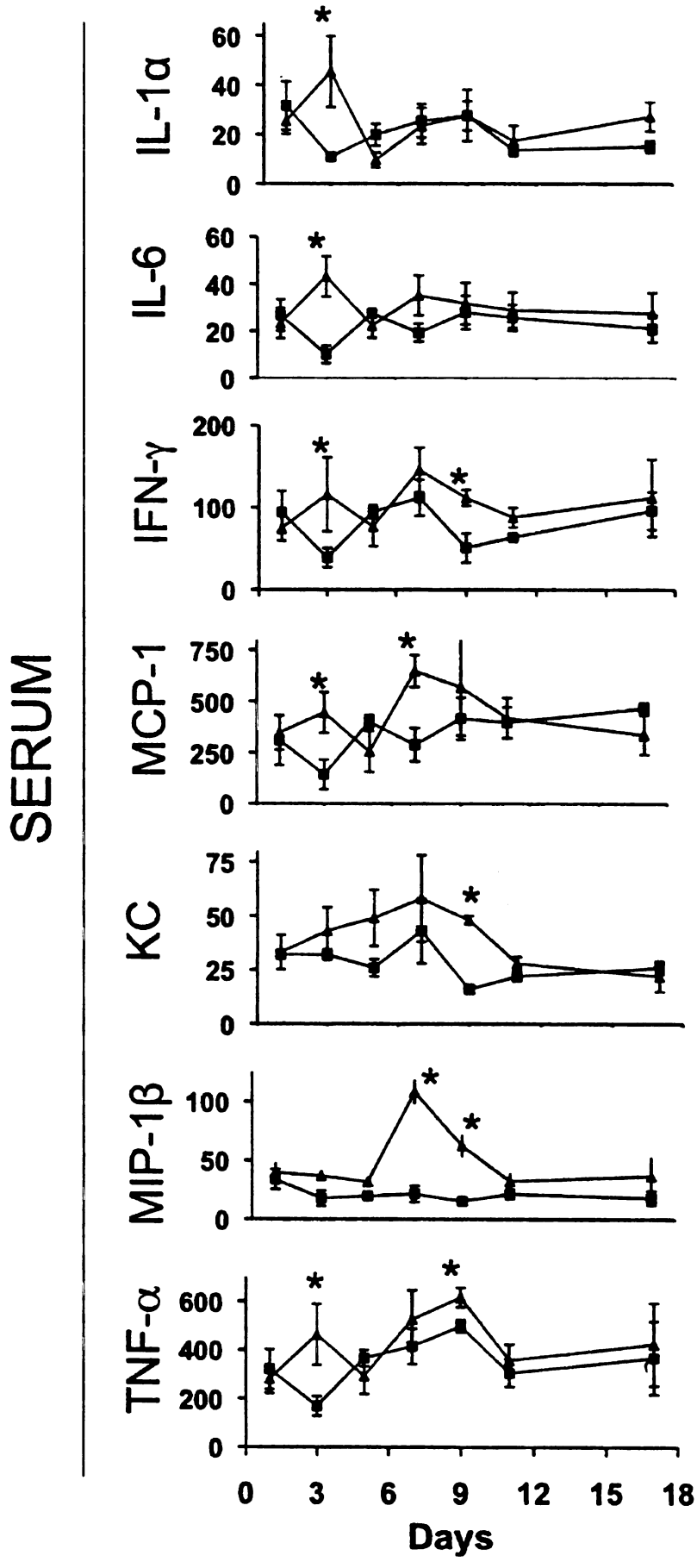
SERUM
IL-1α
60
40
20
0
IL-6
60
40
20
0
IFN-γ
200
100
0
MCP-1
750
500
250
0
KC
75
50
25
0
MIP-1β
100
50
0
TNF-α
600
400
200
0
0
3
6
9
12
15
18
Days

Locally elevated cytokine gene expression in bone could have an even greater impact on bone remodeling, since theoretically cytokine concentrations would be highest at sites of secretion. Therefore, to determine if cytokine expression is modulated in diabetic bone, we measured mRNA levels of multiple cytokines using RNase protection assays on RNA isolated from mouse tibias at 5 dpi, the time point at which the earliest suppression of osteoblast gene expression was seen. Figure 10 demonstrates clear increases in TNF-α, IFN-γ, IL-1Rα and LT-β mRNA levels. Real time RT-PCR confirmed the induction of these cytokines at 5 dpi (Figure 11). Cytokine RNA levels were not elevated prior to this point (data not shown). Examination of additional cytokines revealed that IL-6 expression was also elevated at 5 dpi while IL-1α was the only cytokine elevated at 17 dpi. MIP-1β, KC and MCP-1 mRNAs were unchanged or decreased in diabetic bone. The induction of IL-6, TNF-α, IL-1Ra and LT-β in diabetic mouse bone was transient and returned to control levels by 7 dpi and. Only the elevation of IFN-γ expression was found to be sustained over a period of several days, but by day 9 levels were back to control values (not shown) and by day 17 levels were lower than controls (similar to the LT-β profile). Treatment of osteoblasts (MC3T3-E1 cells) or isolated calvaria *in vitro* with STZ at concentrations up to 0.5 mg/ml did not cause an increase in cytokine expression (data not shown) supporting a role for diabetes onset (not STZ) in bone inflammation.

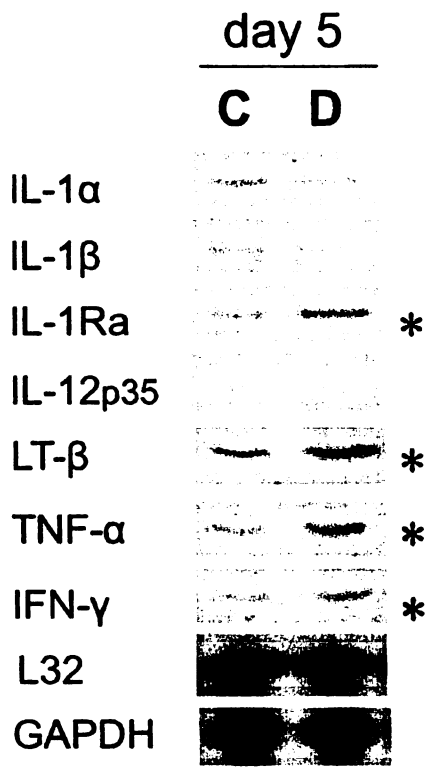

Figure 10. **IL-1Ra, LT-β, TNF-α and IFN-γ mRNA levels are increased in diabetic bone.** Representative autoradiograph of an RNase protection assay using RNA isolated from control (C) and diabetic (D) mouse whole tibias at 5 dpi. *represents signals significantly increased as determined by densitometry. *$p<0.05$.

Figure 1
early sta
ces from
pacietes
nt expre
m 3-6

Figure 11. **Cytokine mRNA levels are increased predominantly during the early stage (5 dpi) of the onset of diabetes.** Total RNA extracted from whole tibias from control (square) and diabetic (triangle) mice during the progression of diabetes onset. Cytokine mRNA levels were determined by real time RT-PCR and expressed relative to HPRT levels. Values are averages +/- SE obtained from 3-6 mice per condition per time point. *$p<0.05$.

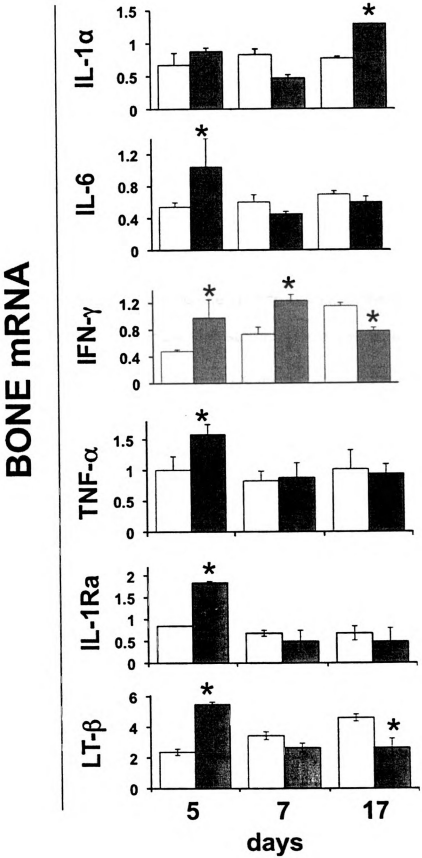
BONE mRNA
IL-1α
IL-6
IFN-γ
TNF-α
IL-1Ra
LT-β
1.5
1
0.5
0
1.2
0.8
0.4
2
1.5
6
4
2
*
5
7
17
days

Given that 1) IFN-γ induction was the most sustained of the cytokines we examined and 2) IFN-γ has been demonstrated to contribute to bone pathologies, we examined the role of IFN-γ in diabetic bone loss. To do this, diabetes was induced in mice that lack expression of IFN-γ (IFN-$\gamma^{-/-}$). The absence of IFN-γ was confirmed by genotyping wild type and IFN-$\gamma^{-/-}$ mice using primers specific for the wild type or knockout cassette sequences. Specifically, a 320 base pairs (bp) amplicon is indicative of the defective gene insert with a premature stop codon while a 260 bp amplicon represents amplification of the wild type gene (Figure 12A). As shown in Figure 11B, streptozotocin was capable of inducing diabetes in both wild type and IFN-$\gamma^{-/-}$ mice as evidenced by an elevation in blood glucose levels above 300 mg/dL (Figure 12B). Bones were examined 32 days after the first streptozotocin injection so that bone loss, if it occurred, would be great enough to be detected by micro-computed tomography analysis. As shown in Figure 12C, IFN-γ deficiency was unable to prevent diabetes-induced loss of bone volume fraction (which was not significantly different from wild type mice). Correspondingly, osteocalcin mRNA levels were suppressed and aP2 levels were increased in diabetic IFN-$\gamma^{-/-}$ mice similar to wild type mice (Figure 12C) and early lineage markers were similarly altered (decreased runx2 and increase PPARγ2, not shown).

Figure 12. **IFN-γ deficiency does not prevent diabetic bone loss**. Diabetes was induced in wild type and IFN-$\gamma^{-/-}$ (IFN-γ deficient) mice by 5 daily streptozotocin injections. Bones were analyzed at 32 dpi. ***A.*** DNA amplicons from a PCR reaction with primers specific to wild type or IFN-$\gamma^{-/-}$ mice were separated on a 2% agarose gel. Wild type and IFN-$\gamma^{-/-}$ amplicons ran at the expected molecular weight of 260 bp and 320 bp, respectively. ***B.*** Diabetes was induced in WT and IFN-$\gamma^{-/-}$ mice as indicated by blood glucose levels greater than 300 mg/dL. Values represent mean ± SE; n > 9 mice per condition. *$p<0.05$ compared to genotype-matched non-diabetic controls. ***C.*** Osteocalcin (OC) and aP2 gene mRNA levels (obtained by real time RT-PCR analysis of tibial RNA and quantitated relative to HPRT levels) and tibial bone volume fraction (BVF) were determined and expressed as % change in diabetic compared to control values for each genotype, wild type (WT, white bars) and IFN-$\gamma^{-/-}$ (gray bars). Values represent mean ± SE; n > 9 mice per condition.

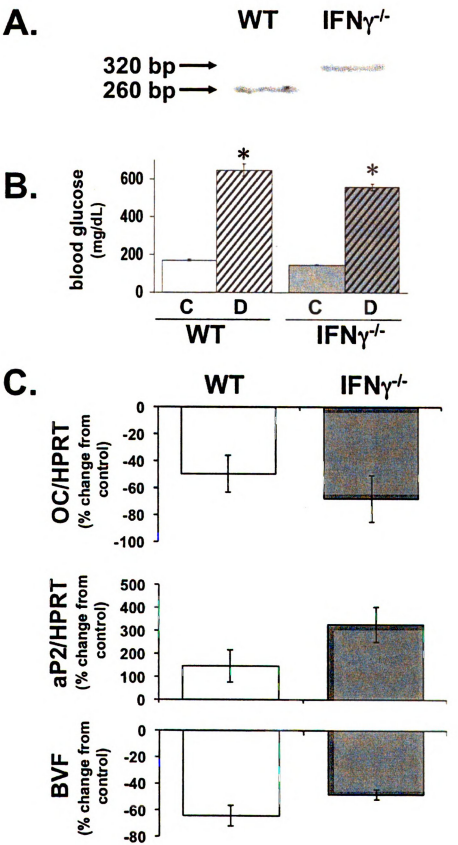
A.
WT
IFNγ-/-
320 bp
260 bp
B.
blood glucose (mg/dL)
600
400
200
0
*
*
C
D
C
D
WT
IFNγ-/-
C.
WT
IFNγ-/-
OC/HPRT (% change from control)
0
-20
-40
-60
-80
-100
aP2/HPRT (% change from control)
500
400
300
200
100
0
BVF (% change from control)
0
-20
-40
-60
-80

2.5. DISCUSSION

Type I diabetes is associated with significant bone loss (8, 18, 22), increased bone marrow adiposity (18) and increased fracture risk (9, 59). Changes in bone phenotype are reported at 2 or 4 weeks post-confirmation of diabetes. In our previous studies, we looked as early as 5-7 days after the confirmation of diabetes, which amounts to 17 days after the first injection of streptozotocin (18, 27). Here we utilized the suppression of pancreatic β-cell function by multiple low dose streptozotocin injection to analyze rapid changes in bone that occur at the onset of diabetes prior to the mice attaining maximal hyperglycemia.

Our findings demonstrated that changes in body mass, blood glucose levels, fat and muscle mass, as well as bone phenotype occurred before or by 5 days after the first injection of streptozotocin. Pighin et al. (60) also reported reduced fat pad mass in mice 6 days after injection of streptozotocin. The adipose tissue lipolysis that we observed suggests that free fatty acids were being mobilized as an energy source during the onset of insulin deficiency (60, 61). However, we were unable to detect an increase in serum free fatty acids at early time points as reported by others (60), but increases were observed at later time points 17, 19, 26, 33, and 40 dpi (corresponding with days 5, 7, 14, 21 and 28 days after diabetes confirmation) consistent with previous reports (18, 27). Possibly, at early time points there was a rapid uptake of mobilized fats by

tissues in our mouse model. Also, we observed a 3 mM, 6 mM, and then 16 mM increase in blood glucose levels within 3, 5 and 11 days of streptozotocin injection, respectively. This is in contrast to Pighin et al. (60) who found that blood glucose levels were not significantly elevated until day 12. The metabolic differences between these studies (glucose and lipid levels in the blood) could stem from differences between mouse strains (C57BL/6J versus BALB/c) and/or differences in streptozotocin effectiveness in early pancreatic β-cell destruction.

Only a handful of studies have examined the early effects of streptozotocin-induced diabetes on gene expression. Wang et al. (62) reported some of the earliest changes: a significant reduction of both GLUT2 protein and mRNA expression in pancreatic islets isolated from streptozotocin-injected mice 4 days after the first streptozotocin injection. In our studies, we saw decreased runx2 and osteocalcin mRNA levels and increased PPARγ2 and aP2 at 5 dpi that were maintained out to day 17 and are consistent with differences we see at later stages (ie: day 40 dpi) (18, 27). This suggests that the immediate changes in mouse blood glucose levels and overall metabolic state may in turn dramatically, immediately, and chronically influence osteoblast and adipocyte maturation.

In our studies, streptozotocin was used to induce diabetes and allow identification of the early onset of T1-diabetes-associated changes in bone phenotype, something that cannot be done in models of spontaneous T1-diabetes occurrence. One cannot exclude that secondary effects of streptozotocin could contribute to our findings. However, STZ alone was unable to induce a cytokine response in bone *in vitro.* In addition, studies in other

models of diabetes including non-obese T1-diabetic mice (NOD) (22) and in virally induced diabetic animals (23) demonstrate similar bone pathologies to the STZ-induced T1-diabetic mouse model. For example, NOD mice exhibit decreased bone formation and increased marrow adiposity similar to the multiple low dose streptozotocin model (63). While spontaneously diabetic mouse models allow analyses without pharmacologic treatments, our studies demonstrate the utility of the streptozotocin model in the examination of changes occurring at the onset of diabetes prior to maximum states of hyperglycemia. This time period would be difficult to study in spontaneously diabetic mice.

While our past studies did not find an enhancement of osteoclast number and/or activity in T1-diabetic mice at 17, 19, 26, 33, and 40 dpi (18, 27), the question remained: "does bone resorption/osteoclast activation occur during the early onset of diabetes prior to these time points?" To answer this question we monitored the expression of osteoclast markers, activity, and regulators. We did observe and increase in RANKL at 3 dpi which could be related to early increases in cytokines that perhaps are not detectable in whole bone RNA analyses, however, TRAP5 levels were significantly decreased at this time point and by 5 dpi levels of both parameters were not different from controls. Serum PYD levels, on the other hand, were significantly decreased in diabetic animals 5 days after the first streptozotocin injection and remained reduced through day 17. Systemic levels of PYD represent the amount of bone resorption going on in all bones, which may explain why they are more consistent throughout the time course. While some studies examine urinary markers of resorption, results can

be confounded by secondary effects of T1-diabetes on kidney function and urinary volume, which is why we focused on serum parameters. However, our past studies have demonstrated reduced or not modified osteoclast activity by both serum and urinary parameter measures at later time points (18). Our findings of reduced or no change in osteoclast activity are consistent with the majority of reports demonstrating reduced or no change in resorption parameters in T1-diabetic mouse or rat bones (16-18, 21, 58, 64-69). In addition, *in vitro* studies show that high glucose and advanced glycosylation end products can suppress osteoclast activation and bone resorption (70, 71) and, in T1-diabetic patients, serum bone resorption markers are unaltered (11, 72, 73) or decreased (74, 75) compared to controls. However, there are a few contrasting reports suggesting that advanced glycosylation end products and STZ induced diabetes can enhance osteoclast activity (76, 77). Differences between studies could result from the severity of diabetes, different cell lines, mouse versus rat effects, and potentially gender differences.

Induction of T1-diabetes in spontaneous models and in streptozotocin-induced models is associated with pancreatic inflammation. Consistent with this, our diabetic mice exhibited significant increases in serum cytokine levels including IL-1α, IFN-γ and TNF-α at early time points (3 dpi) and for several cytokines at later time points (9 dpi). Studies in rats demonstrate increases in serum IL-1β and TNF-α within 5 days of the first injection of streptozotocin (78). Similarly, mononuclear/macrophage cells isolated from diabetic mice and humans exhibit increased IFN-γ, TNF-α, IL-1β, and IL-6 secretion and/or gene

expression compared to controls (79-81). The cytokine profiles are thought to represent a major T helper (Th)1 cellular immune response that outweighs the Th2 response (81, 82). Studies examining the influence of Th1 cells on osteoblast activity indicate that osteoblasts cultured with Th1 cytokine-conditioned medium exhibit suppression of alkaline phosphatase activity (a marker of osteoblast maturation) whereas Th2 cytokine-conditioned medium did not affect alkaline phosphatase activity (30).

Indicative of local bone inflammation, the mRNA levels of several cytokines were elevated in bone, including LT-β, IL-6, IFN-γ and TNF-α. However, not all of the cytokines elevated in diabetic mouse serum (MCP-1, KC, MIP-1β) were elevated in bone. This could be the result of a subpopulation of immune cells residing in the bone marrow and/or interactions between immune and bone cells that leads to a unique cytokine profile and/or secondary cytokine inductions at distal sites. Cytokines such as TNF-α, IL-1 and IFN-γ are known to increase osteoblast nitric oxide production and induce apoptosis, and to decrease growth and maturation *in vitro* (83-94). *In vitro* studies also demonstrate that hyperglycemia is capable of increasing macrophage expression of IL-1, IL-6 and TNF-α and could therefore contribute to the elevations that we observe (80). A related induction of the inflammatory response is seen in hyperglycemic type II diabetic mice in response to *P. gingivalis* challenge or fracture conditions; specifically, local diabetic mouse bone exhibits greater expression of MCP-1, MIP, and TNF-α mRNA compared to control mice (95).

Because of the increased cytokine expression during early bone phenotype changes, we hypothesize that inflammation and cytokine production are necessary for induction of diabetic bone loss. Under conditions of increased cytokine production, such as rheumatoid arthritis (without corticosteroid treatment), bone formation and resorption rates are decreased similarly to T1-diabetic bones (18, 63, 96, 97). Of the cytokine fingerprint seen in diabetic mice, we were particularly interested in IFN-γ since it is the only cytokine found to be significantly induced in bone within 24 hours of diabetes induction, is also elevated at 5 and 7 dpi, is shown to suppress osteoblast growth, maturation and increase apoptosis *in vitro* (98, 99), and is demonstrated to regulate bone density in vivo. Of particular interest is the finding that the ability of Th1 cytokine-conditioned medium to suppress osteoblast maturation is lost when given in combination with IFN-γ neutralizing antibody (30).

To test whether IFN-γ is a key mediator of diabetic bone loss, we induced diabetes with streptozotocin in IFN-γ knockout mice. Based on cell culture models and the finding that IFN-γ treatment increases resorption in patients with osteopetrosis (33), as well as the observation that IFN-γR$^{-/-}$ mice are protected from OVX-induced bone loss (100), we hypothesized that IFN-γ-deficiency would reduce the severity of the diabetic bone phenotype. However, we found that osteocalcin and aP2 gene expression patterns were similar in both genotypes, and that the magnitude of diabetic bone loss (% change in bone volume fraction) in the knockout was similar to that of the wild type mice. From these findings we conclude that IFN-γ is not solely responsible for streptozotocin-induced diabetic

osteoporosis. This is consistent with reports demonstrating negative (not protective) skeletal effects in IFNγR1-null (IFN-$\gamma R^{-/-}$) mice, including increased resorption and susceptibility to arthritic bone loss (32, 101, 102). Bone loss could result from the loss of IFN-γ inhibition of IL-1-induced osteoclast activity (103, 104).

In summary, the streptozotocin-induced diabetes mouse model of bone loss, marked by decreased bone formation, is well suited to studying early changes in bone phenotype/gene expression. Our studies demonstrate that changes (suppression of osteogenic genes and induction of adipogenic genes) are evident within 5 days of the first injection of streptozotocin, a time prior to observable hyperlipidemia and maximum hyperglycemia. During this period, there is systemic as well as local bone inflammation, suggesting a potential role for inflammation in the observed pathological bone changes. Our studies indicate that IFN-γ exhibits early and prolonged elevation during this period, but deficiency of this single cytokine was not sufficient to prevent bone loss in diabetic mice. Identifying and understanding the role of factors present at the early stages of diabetes onset will provide a foundation to identify the cause of diabetic bone loss and effective preventative treatments.

2.6. ACKNOWLEDGEMENTS

We would like to thank Lindsay Martin for her insightful comments and Alison Bauer for her help with the IFN-γ mice. This work was funded by grants

from the National Institutes of Health (RO1DK061184) and the American Diabetes Association (7-07-RA-105) to LRM. A.A. was supported by the National Institutes of Health grants RO1DK069884 and P01CA078673, as well the Osteopathic Heritage Foundation. The authors have no financial conflicts.

2.7. REFERENCES

1. **Maksimovic-Ivanic D, Trajkovic V, Miljkovic DJ, Mostarica Stojkovic M, Stosic-Grujicic S** 2002 Down-regulation of multiple low dose streptozotocin-induced diabetes by mycophenolate mofetil. Clin Exp Immunol 129:214-223

2. **Drachenberg CB, Klassen DK, Weir MR, Wiland A, Fink JC, Bartlett ST, Cangro CB, Blahut S, Papadimitriou JC** 1999 Islet cell damage associated with tacrolimus and cyclosporine: morphological features in pancreas allograft biopsies and clinical correlation. Transplantation 68:396-402

3. **West E, Simon OR, Morrison EY** 1996 Streptozotocin alters pancreatic beta-cell responsiveness to glucose within six hours of injection into rats. West Indian Med J 45:60-62

4. **Tuominen JT, Impivaara O, Puukka P, Ronnemaa T** 1999 Bone mineral density in patients with type 1 and type 2 diabetes. Diabetes Care 22:1196-1200.

5. **Hui SL, Epstein S, Johnston CC, Jr.** 1985 A prospective study of bone mass in patients with type I diabetes. J Clin Endocrinol Metab 60:74-80

6. **Bouillon R** 1991 Diabetic bone disease [editorial]. Calcif Tissue Int 49:155-160

7. **Krakauer JC, McKenna MJ, Buderer NF, Rao DS, Whitehouse FW, Parfitt AM** 1995 Bone loss and bone turnover in diabetes. Diabetes 44:775-782

8. **Inzerillo AM, Epstein S** 2004 Osteoporosis and diabetes mellitus. Rev Endocr Metab Disord 5:261-268

9. **Schwartz AV, Sellmeyer DE, Ensrud KE, Cauley JA, Tabor HK, Schreiner PJ, Jamal SA, Black DM, Cummings SR** 2001 Older women with diabetes have an increased risk of fracture: a prospective study. J Clin Endocrinol Metab 86:32-38.

10. **Leidig-Bruckner G, Ziegler R** 2001 Diabetes mellitus a risk for osteoporosis? Exp Clin Endocrinol Diabetes 109:S493-514.

11. **Kemink SA, Hermus AR, Swinkels LM, Lutterman JA, Smals AG** 2000 Osteopenia in insulin-dependent diabetes mellitus; prevalence and aspects of pathophysiology. J Endocrinol Invest 23:295-303

12. **Forsen L, Meyer HE, Midthjell K, Edna TH** 1999 Diabetes mellitus and the incidence of hip fracture: results from the Nord-Trondelag Health Survey. Diabetologia 42:920-925.

13. **Auwerx J, Dequeker J, Bouillon R, Geusens P, Nijs J** 1988 Mineral metabolism and bone mass at peripheral and axial skeleton in diabetes mellitus. Diabetes 37:8-12

14. **Hough S, Avioli LV, Bergfeld MA, Fallon MD, Slatopolsky E, Teitelbaum SL** 1981 Correction of abnormal bone and mineral metabolism in chronic streptozotocin-induced diabetes mellitus in the rat by insulin therapy. Endocrinology 108:2228-2234

15. **Goodman WG, Hori MT** 1984 Diminished bone formation in experimental diabetes. Relationship to osteoid maturation and mineralization. Diabetes 33:825-831.

16. **Verhaeghe J, Suiker AM, Nyomba BL, Visser WJ, Einhorn TA, Dequeker J, Bouillon R** 1989 Bone mineral homeostasis in spontaneously diabetic BB rats. II. Impaired bone turnover and decreased osteocalcin synthesis. Endocrinology 124:573-582

17. **Verhaeghe J, van Herck E, Visser WJ, Suiker AM, Thomasset M, Einhorn TA, Faierman E, Bouillon R** 1990 Bone and mineral metabolism in BB rats with long-term diabetes. Decreased bone turnover and osteoporosis. Diabetes 39:477-482

18. **Botolin S, Faugere MC, Malluche H, Orth M, Meyer R, McCabe LR** 2005 Increased bone adiposity and peroxisomal proliferator-activated receptor-gamma2 expression in type I diabetic mice. Endocrinology 146:3622-3631

19. **Waud CE, Marks SC, Jr., Lew R, Baran DT** 1994 Bone mineral density in the femur and lumbar vertebrae decreases after twelve weeks of diabetes in spontaneously diabetic-prone BB/Worcester rats. Calcif Tissue Int 54:237-240

20. **Verhaeghe J, Oloumi G, van Herck E, van Bree R, Dequeker J, Einhorn TA, Bouillon R** 1997 Effects of long-term diabetes and/or high-dose 17 beta-estradiol on bone formation, bone mineral density, and strength in ovariectomized rats. Bone 20:421-428

21. **Herrero S, Calvo OM, Garcia-Moreno C, Martin E, San Roman JI, Martin M, Garcia-Talavera JR, Calvo JJ, del Pino-Montes J** 1998 Low bone density with normal bone turnover in ovariectomized and streptozotocin-induced diabetic rats. Calcif Tissue Int 62:260-265.

22. **Thrailkill KM, Liu L, Wahl EC, Bunn RC, Perrien DS, Cockrell GE, Skinner RA, Hogue WR, Carver AA, Fowlkes JL, Aronson J, Lumpkin CK, Jr.** 2005 Bone formation is impaired in a model of type 1 diabetes. Diabetes 54:2875-2881

23. **Yoon JW, Reddi AH** 1984 Decreased bone formation and mineralization in virus-induced diabetes mellitus. Am J Physiol 246:C177-179

24. **Takeshita N, Ishida H, Yamamoto T, Koh G, Kurose T, Tsuji K, Okamoto Y, Ikeda H, Seino Y** 1993 Circulating levels and bone contents of bone gamma-carboxyglutamic acid-containing protein in rat models of non-insulin-dependent diabetes mellitus. Acta Endocrinol (Copenh) 128:69-73

25. **Cakatay U, Telci A, Kayali R, Akcay T, Sivas A, Aral F** 1998 Changes in bone turnover on deoxypyridinoline levels in diabetic patients. Diabetes Res Clin Pract 40:75-79

26. **Horcajada-Molteni MN, Chanteranne B, Lebecque P, Davicco MJ, Coxam V, Young A, Barlet JP** 2001 Amylin and bone metabolism in streptozotocin-induced diabetic rats. J Bone Miner Res 16:958-965

27. **Botolin S, McCabe L** in revision Inhibition of PPAR-? prevents type I diabetic bone marrow adiposity but not bone loss. Journal of Bone and Mineral Research

28. **Gao Y, Grassi F, Ryan MR, Terauchi M, Page K, Yang X, Weitzmann MN, Pacifici R** 2007 IFN-gamma stimulates osteoclast formation and bone loss in vivo via antigen-driven T cell activation. J Clin Invest 117:122-132

29. **Kasama T, Isozaki T, Odai T, Matsunawa M, Wakabayashi K, Takeuchi HT, Matsukura S, Adachi M, Tezuka M, Kobayashi K** 2007 Expression of angiopoietin-1 in osteoblasts and its inhibition by tumor necrosis factor-alpha and interferon-gamma. Transl Res 149:265-273

30. **Young N, Mikhalkevich N, Yan Y, Chen D, Zheng WP** 2005 Differential regulation of osteoblast activity by Th cell subsets mediated by parathyroid hormone and IFN-gamma. J Immunol 175:8287-8295

31. **Fox SW, Chambers TJ** 2000 Interferon-gamma directly inhibits TRANCE-induced osteoclastogenesis. Biochem Biophys Res Commun 276:868-872

32. **Takayanagi H, Ogasawara K, Hida S, Chiba T, Murata S, Sato K, Takaoka A, Yokochi T, Oda H, Tanaka K, Nakamura K, Taniguchi T** 2000 T-cell-mediated regulation of osteoclastogenesis by signalling cross-talk between RANKL and IFN-gamma. Nature 408:600-605

33. **Key LL, Jr., Rodriguiz RM, Willi SM, Wright NM, Hatcher HC, Eyre DR, Cure JK, Griffin PP, Ries WL** 1995 Long-term treatment of osteopetrosis with recombinant human interferon gamma. N Engl J Med 332:1594-1599

34. **Rodriguiz RM, Key LL, Jr., Ries WL** 1993 Combination macrophage-colony stimulating factor and interferon-gamma administration ameliorates the osteopetrotic condition in microphthalmic (mi/mi) mice. Pediatr Res 33:384-389

35. **Mann GN, Jacobs TW, Buchinsky FJ, Armstrong EC, Li M, Ke HZ, Ma YF, Jee WS, Epstein S** 1994 Interferon-gamma causes loss of bone volume in vivo and fails to ameliorate cyclosporin A-induced osteopenia. Endocrinology 135:1077-1083

36. **Baker PJ, Dixon M, Evans RT, Dufour L, Johnson E, Roopenian DC** 1999 CD4(+) T cells and the proinflammatory cytokines gamma interferon and interleukin-6 contribute to alveolar bone loss in mice. Infect Immun 67:2804-2809

37. **Moriyama H, Ukai T, Hara Y** 2002 Interferon-gamma production changes in parallel with bacterial lipopolysaccharide induced bone resorption in mice: an immunohistometrical study. Calcif Tissue Int 71:53-58

38. **Pechhold K, Patterson NB, Blum C, Fleischacker CL, Boehm BO, Harlan DM** 2001 Low dose streptozotocin-induced diabetes in rat insulin promoter-mCD80-transgenic mice is T cell autoantigen-specific and CD28 dependent. J Immunol 166:2531-2539

39. **Szkudelski T** 2001 The mechanism of alloxan and streptozotocin action in B cells of the rat pancreas. Physiol Res 50:537-546

40. **McCabe LR, Kockx M, Lian J, Stein J, Stein G** 1995 Selective expression of fos- and jun-related genes during osteoblast proliferation and differentiation. Exp Cell Res 218:255-262

41. **Chomczynski P, Sacchi N** 1987 Single-step method of RNA isolation by acid guanidinium thiocyanate-phenol-chloroform extraction. Anal Biochem 162:156-159

42. **Ontiveros C, McCabe LR** 2003 Simulated microgravity suppresses osteoblast phenotype, Runx2 levels and AP-1 transactivation. J Cell Biochem 88:427-437

43. **Ontiveros C, Irwin R, Wiseman RW, McCabe LR** 2004 Hypoxia suppresses runx2 independent of modeled microgravity. J Cell Physiol 200:169-176

44. **Kast-Woelbern HR, Dana SL, Cesario RM, Sun L, de Grandpre LY, Brooks ME, Osburn DL, Reifel-Miller A, Klausing K, Leibowitz MD** 2004 Rosiglitazone induction of Insig-1 in white adipose tissue reveals a novel interplay of peroxisome proliferator-activated receptor gamma and sterol regulatory element-binding protein in the regulation of adipogenesis. J Biol Chem 279:23908-23915

45. **Li J, Takaishi K, Cook W, McCorkle SK, Unger RH** 2003 Insig-1 "brakes" lipogenesis in adipocytes and inhibits differentiation of preadipocytes. Proc Natl Acad Sci U S A 100:9476-9481

46. **Wiren KM, Zhang XW, Toombs AR, Kasparcova V, Gentile MA, Harada S, Jepsen KJ** 2004 Targeted overexpression of androgen receptor in osteoblasts: unexpected complex bone phenotype in growing animals. Endocrinology 145:3507-3522

47. **Zhao S, Zhang YK, Harris S, Ahuja SS, Bonewald LF** 2002 MLO-Y4 osteocyte-like cells support osteoclast formation and activation. J Bone Miner Res 17:2068-2079

48. **Lindberg MK, Moverare S, Eriksson AL, Skrtic S, Gao H, Dahlman-Wright K, Gustafsson JA, Ohlsson C** 2002 Identification of estrogen-regulated genes of potential importance for the regulation of trabecular bone mineral density. J Bone Miner Res 17:2183-2195

49. **Weih DS, Yilmaz ZB, Weih F** 2001 Essential role of RelB in germinal center and marginal zone formation and proper expression of homing chemokines. J Immunol 167:1909-1919

50. **Schwab AM, Granholm S, Persson E, Wilkes B, Lerner UH, Conaway HH** 2005 Stimulation of resorption in cultured mouse calvarial bones by thiazolidinediones. Endocrinology 146:4349-4361

51. **Mohanty SK, Shivakumar P, Sabla G, Bezerra JA** 2006 Loss of interleukin-12 modifies the pro-inflammatory response but does not prevent duct obstruction in experimental biliary atresia. BMC Gastroenterol 6:14

52. **Ikejima S, Sasaki S, Sashinami H, Mori F, Ogawa Y, Nakamura T, Abe Y, Wakabayashi K, Suda T, Nakane A** 2005 Impairment of host resistance to Listeria monocytogenes infection in liver of db/db and ob/ob mice. Diabetes 54:182-189

53. **Lacroix-Lamande S, Mancassola R, Naciri M, Laurent F** 2002 Role of gamma interferon in chemokine expression in the ileum of mice and in a murine intestinal epithelial cell line after Cryptosporidium parvum infection. Infect Immun 70:2090-2099

54. **Weghofer M, Karlic H, Haslberger A** 2001 Quantitative analysis of immune-mediated stimulation of tumor necrosis factor-alpha in macrophages measured at the level of mRNA and protein synthesis. Ann Hematol 80:733-736

55. **Lewis ML, Hughes-Fulford M** 2000 Regulation of heat shock protein message in Jurkat cells cultured under serum-starved and gravity-altered conditions. J Cell Biochem 77:127-134

56. **Trogan E, Choudhury RP, Dansky HM, Rong JX, Breslow JL, Fisher EA** 2002 Laser capture microdissection analysis of gene expression in macrophages from atherosclerotic lesions of apolipoprotein E-deficient mice. Proc Natl Acad Sci U S A 99:2234-2239

57. **Vengellur A, LaPres JJ** 2004 The role of hypoxia inducible factor 1alpha in cobalt chloride induced cell death in mouse embryonic fibroblasts. Toxicol Sci 82:638-646

58. **Botolin S, McCabe LR** 2006 Inhibition of PPARgamma prevents type I diabetic bone marrow adiposity but not bone loss. J Cell Physiol 209:967-976

59. **Miao J, Brismar K, Nyren O, Ugarph-Morawski A, Ye W** 2005 Elevated hip fracture risk in type 1 diabetic patients: a population-based cohort study in Sweden. Diabetes Care 28:2850-2855

60. **Pighin D, Karabatas L, Pastorale C, Dascal E, Carbone C, Chicco A, Lombardo YB, Basabe JC** 2005 Role of lipids in the early developmental stages of experimental immune diabetes induced by multiple low-dose streptozotocin. J Appl Physiol 98:1064-1069

61. **Solomon SS, Heckemeyer CM, Barker JA, Duckworth WC** 1985 Hormonal control of lipolysis in perifused adipocytes from diabetic rats. Endocrinology 117:1350-1354

62. **Wang Z, Gleichmann H** 1998 GLUT2 in pancreatic islets: crucial target molecule in diabetes induced with multiple low doses of streptozotocin in mice. Diabetes 47:50-56

63. **Botolin S, McCabe LR** 2007 Bone loss and increased bone adiposity in spontaneous and pharmacologically induced diabetic mice. Endocrinology 148:198-205

64. **Mishima N, Sahara N, Shirakawa M, Ozawa H** 2002 Effect of streptozotocin-induced diabetes mellitus on alveolar bone deposition in the rat. Arch Oral Biol 47:843-849

65. **He H, Liu R, Desta T, Leone C, Gerstenfeld LC, Graves DT** 2004 Diabetes causes decreased osteoclastogenesis, reduced bone formation, and enhanced apoptosis of osteoblastic cells in bacteria stimulated bone loss. Endocrinology 145:447-452

66. **Locatto ME, Abranzon H, Caferra D, Fernandez MC, Alloatti R, Puche RC** 1993 Growth and development of bone mass in untreated alloxan diabetic rats. Effects of collagen glycosylation and parathyroid activity on bone turnover. Bone Miner 23:129-144

67. **Verhaeghe J, Thomsen JS, van Bree R, van Herck E, Bouillon R, Mosekilde L** 2000 Effects of exercise and disuse on bone remodeling, bone mass, and biomechanical competence in spontaneously diabetic female rats. Bone 27:249-256.

68. **Halleen JM, Alatalo SL, Suominen H, Cheng S, Janckila AJ, Vaananen HK** 2000 Tartrate-resistant acid phosphatase 5b: a novel serum marker of bone resorption. J Bone Miner Res 15:1337-1345

69. **Halleen JM, Ylipahkala H, Alatalo SL, Janckila AJ, Heikkinen JE, Suominen H, Cheng S, Vaananen HK** 2002 Serum tartrate-resistant acid phosphatase 5b, but not 5a, correlates with other markers of bone turnover and bone mineral density. Calcif Tissue Int 71:20-25

70. **Wittrant Y, Gorin Y, Woodruff K, Horn D, Abboud HE, Mohan S, Abboud-Werner SL** 2008 High d(+)glucose concentration inhibits RANKL-induced osteoclastogenesis. Bone

71. **Valcourt U, Merle B, Gineyts E, Viguet-Carrin S, Delmas PD, Garnero P** 2007 Non-enzymatic glycation of bone collagen modifies osteoclastic activity and differentiation. J Biol Chem 282:5691-5703

72. **Bonfanti R, Mora S, Prinster C, Bognetti E, Meschi F, Puzzovio M, Proverbio MC, Chiumello G** 1997 Bone modeling indexes at onset and during the first year of follow-Up in insulin-dependent diabetic children. Calcif Tissue Int 60:397-400

73. **Valerio G, del Puente A, Esposito-del Puente A, Buono P, Mozzillo E, Franzese A** 2002 The lumbar bone mineral density is affected by long-term poor metabolic control in adolescents with type 1 diabetes mellitus. Horm Res 58:266-272

74. **Gunczler P, Lanes R, Paz-Martinez V, Martins R, Esaa S, Colmenares V, Weisinger JR** 1998 Decreased lumbar spine bone mass and low bone turnover in children and adolescents with insulin dependent diabetes mellitus followed longitudinally. J Pediatr Endocrinol Metab 11:413-419

75. **Cloos C, Wahl P, Hasslacher C, Traber L, Kistner M, Jurkuhn K, Schmidt-Gayk H** 1998 Urinary glycosylated, free and total pyridinoline and free and total deoxypyridinoline in diabetes mellitus. Clin Endocrinol (Oxf) 48:317-323

76. **Ding KH, Wang ZZ, Hamrick MW, Deng ZB, Zhou L, Kang B, Yan SL, She JX, Stern DM, Isales CM, Mi QS** 2006 Disordered osteoclast formation in RAGE-deficient mouse establishes an essential role for RAGE in diabetes related bone loss. Biochem Biophys Res Commun 340:1091-1097

77. **Hie M, Shimono M, Fujii K, Tsukamoto I** 2007 Increased cathepsin K and tartrate-resistant acid phosphatase expression in bone of streptozotocin-induced diabetic rats. Bone 41:1045-1050

78. **El-Mahmoudy A, Shimizu Y, Shiina T, Matsuyama H, Nikami H, Takewaki T** 2005 Macrophage-derived cytokine and nitric oxide profiles in type I and type II diabetes mellitus: effect of thymoquinone. Acta Diabetol 42:23-30

79. **Cvetkovic I, Al-Abed Y, Miljkovic D, Maksimovic-Ivanic D, Roth J, Bacher M, Lan HY, Nicoletti F, Stosic-Grujicic S** 2005 Critical role of macrophage migration inhibitory factor activity in experimental autoimmune diabetes. Endocrinology 146:2942-2951

80. **Wen Y, Gu J, Li SL, Reddy MA, Natarajan R, Nadler JL** 2006 Elevated glucose and diabetes promote interleukin-12 cytokine gene expression in mouse macrophages. Endocrinology 147:2518-2525

81. **Rachmiel M, Bloch O, Bistritzer T, Weintrob N, Ofan R, Koren-Morag N, Rapoport MJ** 2006 TH1/TH2 cytokine balance in patients with both type 1 diabetes mellitus and asthma. Cytokine 34:170-176

82. **Rabinovitch A, Suarez-Pinzon WL** 1998 Cytokines and their roles in pancreatic islet beta-cell destruction and insulin-dependent diabetes mellitus. Biochem Pharmacol 55:1139-1149

83. **Mogi M, Kinpara K, Kondo A, Togari A** 1999 Involvement of nitric oxide and biopterin in proinflammatory cytokine-induced apoptotic cell death in mouse osteoblastic cell line MC3T3-E1. Biochem Pharmacol 58:649-654

84. **Mogi M, Kondo A, Kinpara K, Togari A** 2000 Anti-apoptotic action of nerve growth factor in mouse osteoblastic cell line. Life Sci 67:1197-1206

85. **Togari A, Arai M, Mogi M, Kondo A, Nagatsu T** 1998 Coexpression of GTP cyclohydrolase I and inducible nitric oxide synthase mRNAs in mouse osteoblastic cells activated by proinflammatory cytokines. FEBS Lett 428:212-216

86. **Ozeki N, Mogi M, Nakamura H, Togari A** 2002 Differential expression of the Fas-Fas ligand system on cytokine-induced apoptotic cell death in mouse osteoblastic cells. Arch Oral Biol 47:511-517

87. **Liu R, Bal HS, Desta T, Behl Y, Graves DT** 2006 Tumor necrosis factor-alpha mediates diabetes-enhanced apoptosis of matrix-producing cells and impairs diabetic healing. Am J Pathol 168:757-764

88. **Yang XD, Tisch R, Singer SM, Cao ZA, Liblau RS, Schreiber RD, McDevitt HO** 1994 Effect of tumor necrosis factor alpha on insulin-dependent diabetes mellitus in NOD mice. I. The early development of autoimmunity and the diabetogenic process. J Exp Med 180:995-1004

89. **Lee LF, Xu B, Michie SA, Beilhack GF, Warganich T, Turley S, McDevitt HO** 2005 The role of TNF-alpha in the pathogenesis of type 1 diabetes in the nonobese diabetic mouse: analysis of dendritic cell maturation. Proc Natl Acad Sci U S A 102:15995-16000

90. **Hayward MD, Jones BK, Saparov A, Hain HS, Trillat AC, Bunzel MM, Corona A, Li-Wang B, Strenkowski B, Giordano C, Shen H, Arcamone**

E, Weidlick J, Vilensky M, Tugusheva M, Felkner RH, Campbell W, Rao Y, Grass DS, Buiakova O 2007 An extensive phenotypic characterization of the hTNFalpha transgenic mice. BMC Physiol 7:13

91. **Gilbert L, He X, Farmer P, Rubin J, Drissi H, van Wijnen AJ, Lian JB, Stein GS, Nanes MS** 2002 Expression of the osteoblast differentiation factor RUNX2 (Cbfa1/AML3/Pebp2alpha A) is inhibited by tumor necrosis factor-alpha. J Biol Chem 277:2695-2701

92. **Li YP, Stashenko P** 1992 Proinflammatory cytokines tumor necrosis factor-alpha and IL-6, but not IL-1, down-regulate the osteocalcin gene promoter. J Immunol 148:788-794

93. **Nanes MS** 2003 Tumor necrosis factor-alpha: molecular and cellular mechanisms in skeletal pathology. Gene 321:1-15

94. **Zhou FH, Foster BK, Zhou XF, Cowin AJ, Xian CJ** 2006 TNF-alpha mediates p38 MAP kinase activation and negatively regulates bone formation at the injured growth plate in rats. J Bone Miner Res 21:1075-1088

95. **Graves DT, Kayal RA** 2008 Diabetic complications and dysregulated innate immunity. Front Biosci 13:1227-1239

96. **Compston JE, Vedi S, Croucher PI, Garrahan NJ, O'Sullivan MM** 1994 Bone turnover in non-steroid treated rheumatoid arthritis. Ann Rheum Dis 53:163-166

97. **McCabe LR** 2007 Understanding the pathology and mechanisms of type I diabetic bone loss. J Cell Biochem 102:1343-1357

98. **Smith DD, Gowen M, Mundy GR** 1987 Effects of interferon-gamma and other cytokines on collagen synthesis in fetal rat bone cultures. Endocrinology 120:2494-2499

99. **Chen RM, Chen TL, Chiu WT, Chang CC** 2005 Molecular mechanism of nitric oxide-induced osteoblast apoptosis. J Orthop Res 23:462-468

100. **Cenci S, Toraldo G, Weitzmann MN, Roggia C, Gao Y, Qian WP, Sierra O, Pacifici R** 2003 Estrogen deficiency induces bone loss by increasing T cell proliferation and lifespan through IFN-gamma-induced class II transactivator. Proc Natl Acad Sci U S A 100:10405-10410

101. **Takayanagi H, Sato K, Takaoka A, Taniguchi T** 2005 Interplay between interferon and other cytokine systems in bone metabolism. Immunol Rev 208:181-193

102. **Manoury-Schwartz B, Chiocchia G, Bessis N, Abehsira-Amar O, Batteux F, Muller S, Huang S, Boissier MC, Fournier C** 1997 High susceptibility to collagen-induced arthritis in mice lacking IFN-gamma receptors. J Immunol 158:5501-5506

103. **Gowen M, Mundy GR** 1986 Actions of recombinant interleukin 1, interleukin 2, and interferon-gamma on bone resorption in vitro. J Immunol 136:2478-2482

104. **Takayanagi H** 2005 Mechanistic insight into osteoclast differentiation in osteoimmunology. J Mol Med 83:170-179

CHAPTER 3

Motyl KJ, McCabe LR 2009 Leptin treatment prevents type I diabetic marrow adiposity but not bone loss in mice. J Cell Physiol 218:376-384

CHAPTER 3

3. LEPTIN TREATMENT PREVENTS TYPE I DIABETIC MARROW ADIPOSITY BUT NOT BONE LOSS IN MICE

3.1. ABSTRACT

Leptin is a hormone secreted by adipocytes that is implicated in the regulation of bone density. Serum leptin levels are decreased in rodent models of type 1 (T1-) diabetes and in diabetic patients. Whether leptin mediates diabetic bone changes is unclear. Therefore, we treated control and T1-diabetic mice with chronic (28 day) subcutaneous infusion of leptin or saline to elucidate the therapeutic potential of leptin for diabetic osteoporosis. Leptin prevented the increase of marrow adipocytes and the increased aP2 expression that we observed in vehicle-treated diabetic mice. However, leptin did not prevent T1-diabetic decreases in trabecular bone volume fraction or bone mineral density in tibia or vertebrae. Consistent with this finding, markers of bone formation (osteocalcin RNA and serum levels) in diabetic mice were not restored to normal levels with leptin treatment. Interestingly, markers of bone resorption (TRAP5 RNA and serum levels) were decreased in diabetic mice by leptin treatment. In summary, we have demonstrated a link between low leptin levels in T1-diabetes and marrow adiposity. However, leptin treatment alone was not successful in preventing bone loss.

3.2. INTRODUCTION

Leptin is a small protein (16 kDa) secreted by adipocytes and involved in bone mass regulation. The effects of leptin on bone are complex; it can stimulate or inhibit bone formation depending upon bone location and whether leptin is functioning directly on osteoblasts (through receptors (1, 2)) or indirectly through the hypothalamus (2-6). In children and during adolescence, decreases in serum leptin levels, associated with reduced food intake and some disease conditions, are thought to contribute to reduced bone formation and growth (3, 7). Absence of leptin in mice also results in bone loss as well as increased bone marrow adiposity (8, 9). Similarly, increased leptin levels, as observed in obesity (10), are correlated with increased bone mass (11). Several studies have tested the potential therapeutic benefits of leptin treatment on bone loss and marrow adipocyte accumulation. *In vitro* studies demonstrate that leptin promotes bone marrow stromal cells to exhibit an osteoblast rather than adipocyte phenotype (1, 2, 12). Consistent with this finding, subcutaneous infusion of leptin with osmotic mini-pumps reduces marrow adiposity and increases bone mass in *ob/ob* mice (13). Similarly, leptin treatment reduces bone loss from ovariectomy (14) and tail suspension (15). In sum, these studies suggest the efficacy of leptin treatment to restore bone density under conditions of bone loss.

Diabetes mellitus (types 1, 2 and gestational forms) is a metabolic disease marked by hyperglycemia due to defective insulin action (lack of insulin or tissue insulin resistance), which results in impaired glucose uptake by insulin

responsive cells. Type 1 (T1) diabetes is generally first diagnosed in adolescents or young adults and affects nearly one million children and adults in the United States. In T1-diabetes, insulin-secreting pancreatic β-cells are destroyed as a result of autoimmunity. This causes severe hyperglycemia that must be controlled by insulin delivery in humans. In addition to hyperglycemia, weight loss can occur in patients that do not have an adequate insulin therapy. T2-diabetes, generally diagnosed in adults, also results in hyperglycemia but insulin levels, body weight, and serum lipids are increased. Whereas effects of T2-diabetes on bone remain controversial due to increased fracture risk and increased bone mineral density in these patients (16), it is recognized that osteoporosis is a serious complication of T1-diabetes, leaving child and adult patients at risk for bone loss, fracture and impaired fracture healing (17-20).

Previously we demonstrated that streptozotocin-induced T1-diabetic mice exhibit weight loss, decreased body fat mass and bone loss (21). Bone formation by osteoblasts is decreased while resorption is unchanged or decreased in diabetic humans and rodents (21-23). Interestingly, both STZ-induced and spontaneous mouse models of T1-diabetes exhibit an increase in bone marrow adiposity despite the loss of peripheral fat depots (21, 24, 25). A reciprocal relationship between bone volume/density and marrow adipocyte number (consistent with altered mesenchymal stem cell lineage selection) has been implicated as a mechanism for diabetic (21, 24, 26, 27), age-related (28, 29), and unloading-induced (30) bone loss. However, while an increase in adiposity was observed in tibia, femur and calvaria in T1-diabetic mice, vertebrae

did not exhibit an increase in adiposity (26). In this respect, the T1-diabetic bone phenotype resembles that of leptin-deficient mice, which have increased marrow adiposity and bone loss in the femur but no change in marrow adiposity in the vertebrae (8). Because of this finding, we measured fed serum leptin and found that it was decreased in both male and female T1-diabetic mice (26), consistent with reports in STZ-diabetic rats (31).

These findings led us to hypothesize that decreased serum leptin levels contribute to T1-diabetic bone loss and altered mesenchymal lineage selection. Therefore we treated control and diabetic mice with leptin and examined bone parameters. Consistent with our hypothesis, we observed reduced bone marrow adiposity in leptin-treated diabetic mice; however, bone loss was not prevented.

3.3. MATERIALS AND METHODS

3.3.1. Animals

Forty 9-week old BALB/c mice were obtained from Harlan Sprague Dawley (Indianapolis, IN). Mice were maintained on standard lab chow and had food and water *ad libitum*. At 14 weeks, mice were divided into four treatment groups: control + vehicle, control + leptin, diabetic + vehicle and diabetic + leptin. Mice were anesthetized with isofluorane and implanted subcutaneously with Alzet mini-osmotic pumps (model 2004, Durect Corporation, Cupertino, CA) that contained either 0.9% sterile saline vehicle (n=20) or 1.3 mg/mL leptin (Amylin,

San Diego, CA) (n=20). Osmotic pumps had a mean pumping rate of 0.21 ± 0.01 μL/hour and therefore delivered 6.6 μg leptin per day. Wounds were closed with staples and mice were given a one-time injection of 0.15 mg carprofen (Pfizer, New York, NY). Starting on the day of implantation (day 0), mice were given five consecutive daily intraperitoneal injections of 50 mg/kg streptozotocin (n=24) or 0.1 M citrate buffer pH 4.5 vehicle (n=16). Body mass and food intake were monitored throughout the experiment. Staples were removed on day 9.

On day 28, mice were fasted 2-3 hours prior to being euthanized. Blood glucose was measured at the time of harvest with an AccuChek Compact glucometer (Roche, Nutley, NJ). Blood was collected at the time of harvest, allowed to rest at room temperature for five minutes, then centrifuged at 4000 rpm for ten minutes. Serum was removed and stored at -80°C and pellet discarded. Tibias were removed and either fixed in 10% formalin or frozen in liquid nitrogen and stored at -80°C. Femoral fat pads and tibialis anterior muscles were removed and weighed, fixed and frozen. All animal procedures were approved by the Michigan State University Institutional Animal Care and Use Committee.

3.3.2. Serum measurements

Serum was stored at -80°C and put through no more than one freeze/thaw cycle. Leptin was measured using the Assay Designs Mouse Leptin Titer Zyme kit (Ann Arbor, MI) according to the manufacturer protocol. Insulin was measured

using a Crystal Chem Inc. Ultra Rat Insulin ELISA kit (Downers Grove, IL) according to the manufacturer protocol.

3.3.3. Bone Histology and Histomorphometry

Bones were fixed in 10% formalin and transferred to 70% EtOH after 24 hours. Fixed samples were processed on an automated Thermo Electron Excelsior tissue processor for dehydration, clearing and infiltration using a routine overnight processing schedule. Samples were then embedded in Surgipath embedding paraffin on a Sakura Tissue Tek II embedding center. Paraffin blocks were sectioned at 5 μm on a Reichert Jung 2030 rotary microtome. Slides were stained with hematoxylin and eosin. Visible adipocytes, greater than 30 μm, were counted in the tibia trabecular region ranging from the proximal growth plate to 2 mm away distally.

3.3.4. Micro Computed Tomography (μCT) Analyses

Fixed tibias were scanned using a GE Explore Locus μCT system at a voxel resolution of 20 μm obtained from 720 views. Beam angle of increment was 0.5 and beam strength was set at 80 peak kV and 450 μA. Each run included control and diabetic, saline and leptin-treated bones and a calibration phantom to standardize grayscale values and maintain consistency. Based on autothreshold and isosurface analyses of multiple bone samples, a fixed threshold (1400) was

used to separate bone from bone marrow. Cortical bone analyses were made in a defined 2 x 2 x 2 mm cube in the mid-diaphysis immediately proximal to the distal tibial-fibular junction, with the exception of cortical bone mineral content (BMC) and bone mineral density (BMD), which were made in a 0.1 x 0.1 x 0.1 mm cube. Trabecular bone analyses were done in a region of trabecular bone defined at 0.17 mm (~1% of the total length) distal to the growth plate of the proximal tibia extending 2 mm toward the diaphysis, and excluding the outer cortical shell. Cortical BMC, BMD, moment of inertia (MOI), thickness, perimeter and area, and trabecular BMC, BMD, volume fraction (BVF), and thickness (TbTh) values were computed by a GE Healthcare MicroView software application for visualization and analysis of volumetric image data. Cortical isosurface images were taken from a section immediately proximal to the tibial-fibular junction measuring 0.3 mm thick. Trabecular isosurface images were taken from a cylindrical region in the tibia immediately distal to the proximal growth plate measuring 0.8 mm in length and 0.8 mm in diameter.

3.3.5. RNA Analyses

Immediately after euthanasia, tibias were cleaned of muscle and connective tissue, snap frozen in liquid nitrogen and stored at -80 °C. Frozen tibias were crushed under liquid nitrogen conditions with a Bessman Tissue Pulverizer (Spectrum Laboratories, Inc., Rancho Dominguez, CA). RNA was isolated with Tri Reagent (Molecular Research Center, Inc., Cincinnati, OH) and

integrity was assessed by formaldehyde-agarose gel electrophoresis. cDNA was synthesized by reverse transcription with Superscript II Reverse Transcriptase Kit and oligo $dT_{(12-18)}$ primers (Invitrogen, Carlsbad, CA) and amplified by real time PCR with iQ SYBR Green Supermix (Biorad, Hercules, CA) and gene-specific primers synthesized by Integrated DNA Technologies (Coralville, IA). HPRT mRNA levels do not fluctuate in diabetes or with increased serum leptin and were used as an internal control. HPRT was amplified using 5'-AAG CCT AAG ATG AGC GCA AG-3' and 5'-TTA CTA GGC AGA TGG CCA CA-3' (32). aP2 was amplified using 5'-GCG TGG AAT TCG ATG AAA TCA-3' and 5'-CCC GCC ATC TAG GGT TAT GA-3' (33). Osteocalcin was amplified using 5'-ACG GTA TCA CTA TTT AGG ACC TGT G-3' and 5'-ACT TTA TTT TGG AGC TGC TGT GAC-3' (34). TRAP5 was amplified using 5'-AAT GCC TCG ACC TGG GA-3' and 5'-CGT AGT CCT CCT TGG CTG CT-3' (35).

3.3.6. Statistical Analyses

All measurements are presented as the mean ± standard error of the mean (SEM). Statistical significance was determined with a student's t-test (assuming equal variance) using Microsoft Excel (Microsoft Corporation).

3.4. RESULTS

3.4.1. Serum leptin, glucose and insulin

To determine if correction of T1-diabetic serum leptin levels could prevent diabetic bone loss and marrow adiposity, osmotic pumps containing either leptin (delivering 6.6 μg leptin per day) or saline (vehicle) were implanted subcutaneously in BALB/c mice and T1-diabetes was induced by 5 daily injections of streptozotocin. Leptin treatment was successful in raising fasting serum leptin levels in both control and diabetic mice (Table 1). Similar to our past results, serum leptin levels in vehicle-treated diabetic mice trended to be lower than vehicle-treated controls, however in this case the difference did not reach statistical significance. This result is likely due to the variability in control mouse leptin levels observed in this study and the difference in fasted (this study) versus fed (past study) serum leptin measurements (36). Analysis of blood glucose levels demonstrated that leptin treatment of control mice causes a decrease in blood glucose levels compared to untreated controls, as previously shown by others in rats (37, 38). As expected, fasting blood glucose levels were increased in diabetic compared to control mice in both normal (501 vs 161 mg/dl, respectively) and high leptin conditions (250 vs 94 mg/dl, respectively) (Table 1). Although the blood glucose level in leptin-treated diabetic mice was significantly lower (by 50%) than vehicle-treated diabetic mice, the fold increase in blood glucose levels compared to corresponding treatment controls was similar

(untreated diabetic/untreated control = 3 fold; leptin-treated diabetic/leptin-treated control = 2.7 fold). Differences in blood glucose levels between leptin-treated and untreated mice may result from the reduced food intake seen in both control leptin-treated and diabetic leptin-treated mice. Examination of fasting serum insulin levels demonstrated that diabetic vehicle-treated mice have lower fasting insulin levels compared to control vehicle-treated mice. Leptin-treated diabetic mice exhibited lower serum insulin levels compared to untreated diabetic mice; however, insulin levels were not lower than leptin-treated controls. This is likely due to leptin treatment effectively reducing insulin levels in non-diabetic mice (Table 1), and enhancing insulin sensitivity, thereby reducing glucose-stimulated insulin release from the pancreas, as previously shown (39-41).

Table 1. Serum and tissue mass measurements.

	CONTROL		DIABETIC	
	Vehicle (n=6)	**Leptin (n=7)**	**Vechicle (n=9)**	**Leptin (n=9)**
Leptin (pg/mL)	65 ± 18	317 ± 105[a]	45 ± 7[b]	344 ± 75[a,c]
Glucose (mg/dL)	161 ± 10	94 ± 10[a]	501 ± 22[a,b]	250 ± 29[a,b,c]
Insulin (ng/mL)	487 ± 46	68 ± 14[a]	186 ± 32[a,b]	129 ± 21[a,b]
Fat Pads (mg)	218 ± 15	79 ± 7[a]	114 ± 13[a]	92 ± 8[a]
Tibialis Anterior (mg)	44 ± 3	39 ± 3	36 ± 3[a]	43 ± 3

[a] $p < 0.05$ compared to C + Vehicle, [b] $p < 0.05$ compared to C + Leptin, [c] $p < 0.05$ compared to D + Vehicle.

3.4.2. Food consumption and body mass

Food intake and body mass were monitored throughout the experiment. As expected, leptin treatment decreased food intake in control mice and suppressed T1-diabetic hyperphagia compared to untreated diabetic mice (Figure 13). The decrease in food intake corresponded to a decrease in body mass (Figure 13) in control but not diabetic mice. Differences were apparent throughout the time course beginning at diabetes confirmation (not shown).

To determine if the weight loss was the result of fat and/or muscle mass loss, these parameters were also examined. As expected and consistent with our past studies, diabetic vehicle-treated mice lost 50% of femoral fat pad mass compared to vehicle-treated controls (Table 1). Even more fat pad mass was lost in control leptin versus vehicle-treated mice (64%), consistent with previous reports (13, 42). No differences were seen between leptin-treated diabetic, vehicle-treated diabetic or leptin-treated control mouse fat pad mass. However, after normalizing for body mass changes, diabetic leptin-treated mice had significantly lower fat pad mass than diabetic vehicle-treated mice (3.6 ± 0.3 mg/g versus 4.5 ± 0.4 mg/g, respectively). Normalizing fat pad mass for body mass did not alter the statistical comparisons in any other case. Similar to our previous findings, diabetic mice had decreased tibialis anterior muscle mass (Table 1). Leptin treatment did not affect muscle weight in control mice, but did prevent diabetic muscle mass loss compared to leptin-treated controls. However, when normalized for body weight, no statistical differences were

apparent between groups, indicating that all muscle mass changes were directly proportional to body weight changes.

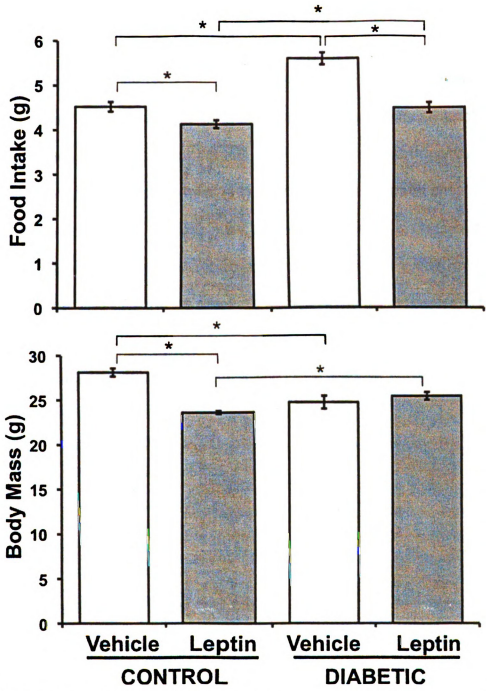

Figure 13. **Leptin treatment prevented diabetic hyperphagia compared to vehicle-treated mice, but did not prevent weight loss.** Food intake and body mass from vehicle-treated (white bars) and leptin-treated (gray bars), control and diabetic mice were monitored throughout the experiment. Shown are average values obtained 28 days after diabetes induction. Values are representative of all time points after diabetes was induced. Bars represent mean ± standard error. $n \geq 6$ per condition. *$p<0.05$ by Student's t-test.

3.4.3. Diabetic marrow adiposity was prevented by leptin treatment

T1-diabetic bone loss is associated with increased marrow adiposity, implicating altered lineage selection of bone marrow stromal cells as a potential mechanism. Because leptin-treatment has been shown to prevent marrow adipocyte accumulation in *ob/ob* mice (13), we hypothesized that it should prevent marrow adiposity in diabetic mice. As expected based on previous reports (21, 24), untreated diabetic tibias exhibited an increase in marrow adipocyte number and aP2 mRNA levels (a marker of mature adipocytes; Figure 14). Consistent with our hypothesis, leptin treatment completely prevented adipocyte accumulation and aP2 mRNA induction in diabetic bone marrow (Figure 14).

Figure 14. **Leptin treatment prevented T1-diabetic marrow adiposity.** (A) Representative hematoxylin and eosin stained sections of decalcificed tibias from vehicle- (white bars) or leptin-treated (gray bars), control and diabetic mice. (B) Marrow adipocyte counts in the proximal tibia, immediately distal to the growth plate. (C) aP2 gene expression was measured by RT-PCR in whole tibia cDNA synthesized from mRNA. aP2 levels were expressed relative to HPRT, an unmodulated housekeeping gene control. Bars represent mean ± standard error. $n \geq 6$ per condition. *$p<0.05$ by Student's t-test.

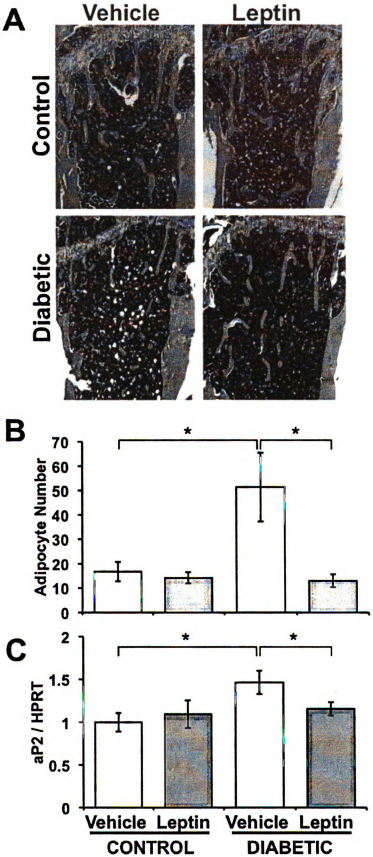
A
Vehicle
Leptin
Control
Diabetic
B
Adipocyte Number
70
60
50
40
30
20
10
0
*
*
C
aP2 / HPRT
2
1.5
1
0.5
0
*
*
Vehicle
Leptin
Vehicle
Leptin
CONTROL
DIABETIC

3.4.4. Leptin did not prevent diabetic bone loss

Given the inverse relationship between bone density and adiposity in diabetes, we examined leptin-treated diabetic bone to see if preventing adiposity would also prevent bone loss. Because leptin can affect long bone and vertebrae differently, we examined both the proximal tibia and L2 vertebrae trabecular bone (Table 2). In control mice, leptin treatment tended to reduce all bone parameters examined in both tibia and vertebrae. Significant reductions (compared to vehicle treatment) were seen in bone volume fraction (BVF) and trabecular thickness in tibia but not vertebrae, consistent with location-dependent leptin effects (5, 8). However, leptin-treated control vertebrae exhibited significant decreases in bone mineral content and density (BMC, BMD). As expected, untreated diabetic mice exhibited a decrease in trabecular bone mineral content and density (BMC, BMD), bone volume fraction (BVF), and trabecular thickness (TbTh) compared to untreated controls at both sites (tibia and vertebrae). These decreases were more prominent than the changes seen in untreated versus leptin-treated controls. In contrast to our original hypothesis, leptin treatment did not prevent the reduction in diabetic trabecular BMC, BMD or BVF in tibia. In vertebrae, leptin treatment did not prevent the diabetes-induced decrease in BMC or BVF. Leptin treatment did significantly increase diabetic vertebral BMD compared to vehicle-treated diabetic mice to the point of not being different from leptin-treated

controls. Because diabetic- and leptin-treated mice lose body weight, we examined changes in BVF relative to total body mass. When corrected for body mass, the leptin-treated control tibia bone volume fraction (BVF/g) was similar to vehicle-treated controls (Figure 15), suggesting the reduction in bone volume is consistent with reduced body size and load. However, bone loss (BVF/g) was still evident in both untreated and leptin-treated diabetic groups (Figure 15).

We further examined cortical bone parameters in the tibia metaphysis (Table 3). Diabetic mice had significantly decreased cortical thickness, which can be attributed to greater inner cortical bone perimeter and increased marrow area. Leptin-treatment (in both control and diabetic mice) also reduced cortical thickness in a similar manner, suggesting the decreased cortical bone could be due to weight changes. When corrected for differences in body mass, cortical thickness was not statistically significant different between groups (Figure 16).

Table 2. Trabecular μCT measurements.

	CONTROL		DIABETIC	
	Vehicle (n=6)	**Leptin (n=7)**	**Vehicle (n=9)**	**Leptin (n=9)**
Tibia				
BMC (mg)	0.82 ± 0.03	0.76 ± 0.02	0.65 ± 0.07[a]	0.66 ± 0.02[b]
BMD (mg/cm^2)	271 ± 10	252 ± 9	213 ± 20[a]	218 ± 5[b]
BVF (%)	16.9 ± 1.1	13.8 ± 1.0[a]	9.6 ± 1.9[a]	10.2 ± 0.6[b]
Tb Th (mm)	0.042 ± 0.001	0.038 ± 0.001[a]	0.035 ± 0.002[a]	0.037 ± 0.001
Vertebrae				
BMC (mg)	0.67 ± 0.03	0.55 ± 0.03[a]	0.48 ± 0.03[a]	0.51 ± 0.02
BMD (mg/cm^2)	273 ± 8	232 ± 12[a]	204 ± 9[a]	220 ± 5[c]
BVF (%)	24.1 ± 2.0	21.0 ± 2.8	11.3 ± 1.6[a]	11.5 ±1.2[b]
Tb Th (mm)	0.044 ± 0.002	0.040 ± 0.003	0.034 ± 0.002[a]	0.032 ± 0.002[b]

[a] $p < 0.05$ compared to C + Vehicle, [b] $p < 0.05$ compared to C + Leptin, [c] $p < 0.05$ compared to D + Vehicle.

Abbreviations: BMC, bone mineral content. BMD, bone mineral density. BVF, bone volume fraction. Tb, trabecular. Th, thickness.

Figure 15. **Leptin did not prevent T1-diabetic bone loss.** Fixed tibias were scanned by μCT and the trabecular area immediately distal to the proximal growth plate was analyzed for bone volume fraction. *Top:* Representative isosurface images of trabecular bone in vehicle- and leptin-treated mice, control and diabetic mice. *Bottom:* Bone volume fraction (BVF) was corrected for body mass. Bars represent mean ± standard error. $n \geq 6$ per condition. *$p<0.05$ by Student's t-test.

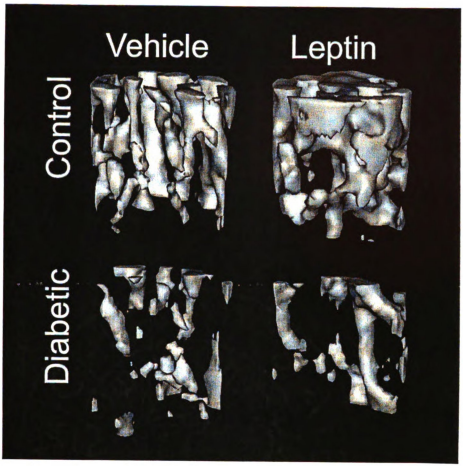
Vehicle
Leptin
Control
Diabetic

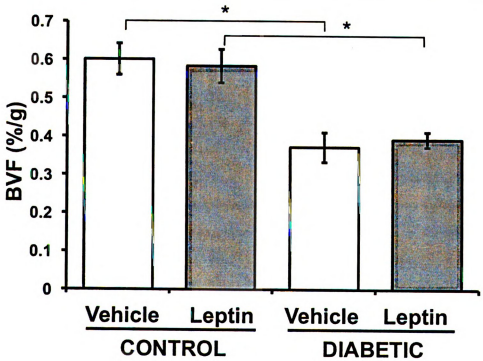
*
*
0.7
0.6
0.5
0.4
0.3
0.2
0.1
0
BVF (%/g)
Vehicle
Leptin
Vehicle
Leptin
CONTROL
DIABETIC

Table 3. Tibia cortical μCT measurements.

	CONTROL		DIABETIC	
	Vehicle (n=6)	**Leptin (n=7)**	**Vehicle (n=9)**	**Leptin (n=9)**
Th (mm)	0.310 ± 0.008	0.285 ± 0.011	0.285 ± 0.007[a]	0.281 ± 0.005
MOI (mm^4)	0.080 ± 0.006	0.070 ± 0.007	0.082 ± 0.009	0.084 ± 0.005
Inner P (mm)	1.48 ± 0.04	1.56 ± 0.05	1.60 ± 0.03[a]	1.64 ± 0.03
Outer P (mm)	3.50 ± 0.03	3.46 ± 0.07	3.48 ± 0.09	3.55 ± 0.06
Marrow A (mm^2)	0.145 ± 0.009	0.162 ± 0.012	0.172 ± 0.006[a]	0.182 ± 0.007
Cortical A (mm^2)	0.718 ± 0.019	0.665 ± 0.029	0.678 ± 0.029	0.681 ± 0.019
BMD (mg/cm^2)	1144 ± 13	1097 ± 26	1070 ± 35	1073 ± 26

[a] $p < 0.05$ compared to C + Vehicle, [b] $p < 0.05$ compared to D + Vehicle, [c] $p < 0.05$ compared to C + Leptin.

Abbreviations: Th, thickness. MOI, moment of inertia. P, perimeter. A, area. BMD, bone mineral density.

Figure 16. **Cortical bone thickness did not differ when corrected for body mass changes.** *Top:* representative isosurface images of cortical bone transverse sections immediately proximal to the tibial-fibular junction. *Bottom:* Cortical thickness expressed per gram body mass. Bars represent mean ± standard error. $n \geq 6$ per condition. *$p<0.05$ by Student's t-test.

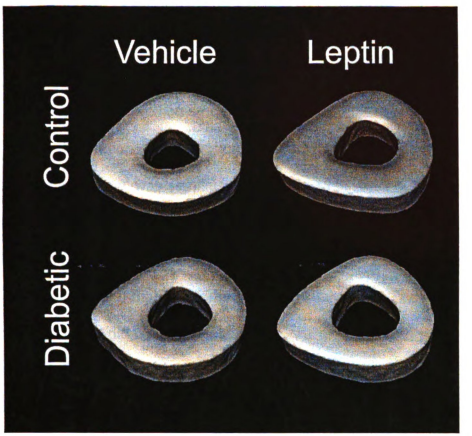
Vehicle
Leptin
Control
Diabetic

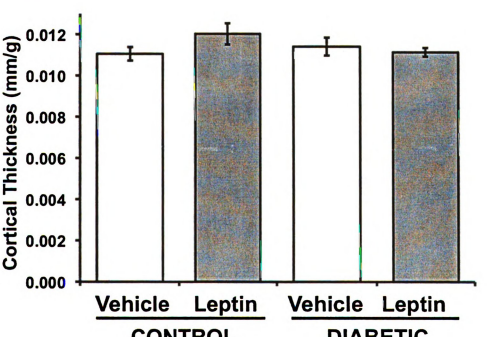
Cortical Thickness (mm/g)
0.012
0.010
0.008
0.006
0.004
0.002
0.000
Vehicle
Leptin
Vehicle
Leptin
CONTROL
DIABETIC

3.4.5. Leptin treatment suppressed bone resorption in diabetes

To understand how the bone changes observed in diabetes and leptin-treatment occurred, we examined whole tibia gene expression and serum for markers of bone formation and resorption (Figure 17). Osteocalcin mRNA, a marker of bone formation, was significantly decreased in vehicle-treated diabetic bone compared to vehicle-treated control. Leptin-treatment had no effect on osteocalcin gene expression in control mice. Interestingly, osteocalcin trended to decrease in leptin-treated diabetic compared to leptin-treated control mice, although this changed did not reach statistical significance. Additionally, the level of osteocalcin mRNA was not different between vehicle-treated diabetic mice and leptin-treated diabetic mice. Both leptin groups tended to have higher serum osteocalcin levels than vehicle-treated controls, although this difference was not statistically significant.

Reports indicated that T1-diabetes generally decreases or does not affect bone resorption. In this study, vehicle-treated diabetic mice had similar levels of bone resorption as vehicle-treated control mice (marked by TRAP5 gene expression and serum TRAP5b levels, Figure 17). We examined serum TRAP5 (versus urine measurements) because diabetic mice develop polyluria and can exhibit nephropathy, both of which can confound urine measurements. Similarly, TRAP5 mRNA and serum TRAP5b were not different in leptin-treated compared to vehicle-treated controls. Diabetes did however decrease serum TRAP5b in leptin-treated mice compared to leptin-treated controls. Interestingly, diabetic

leptin-treated mice had reduced TRAP5 expression and serum TRAP5b compared to vehicle-treated diabetic mice, suggesting that leptin is capable of suppressing resorption in diabetic mice.

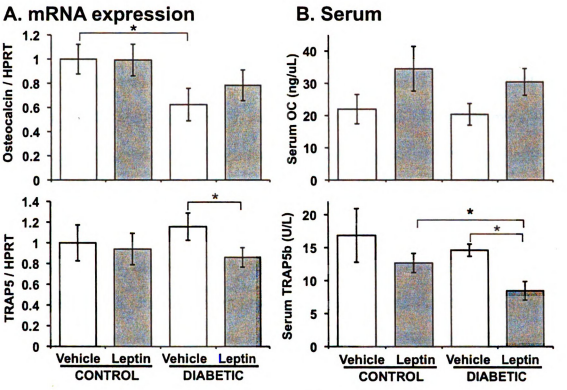

Figure 17. **Leptin treatment suppressed bone resorption diabetes.** (A) Osteocalcin and TRAP5 gene expression was measured by RT-PCR in whole tibia cDNA synthesized from mRNA and were expressed relative to HPRT, an unmodulated housekeeping gene control. (B) Osteocalcin and active TRAP5b were measured in serum collected at 28 days with commercially available ELISA kits. Bars represent mean ± standard error. n≥6 per condition. *p<0.05 by Student's t-test.

3.5. DISCUSSION

We (and others) found serum leptin levels decreased in diabetic rodent models (26, 31, 36, 38). Additionally, we demonstrated that T1-diabetic mice have a location-dependent marrow adiposity phenotype similar to that of leptin-deficient *ob/ob* mice: increased marrow adiposity in long bones with diabetes, but no marrow adipocyte accumulation in the vertebrae (8, 26). Altered mesenchymal stem cell lineage selection is thought to be one mechanism for T1-diabetic bone loss and increased marrow adiposity. We therefore hypothesized that treating diabetic mice with leptin (through an osmotic pump) could prevent bone loss and marrow adipocyte accumulation. We found that although leptin administration completely prevented T1-diabetic marrow adiposity, it did not prevent bone loss in tibia or vertebrae.

As noted previously, serum leptin levels have been demonstrated to be reduced in diabetic rodent models (26, 31, 36, 38) and in diabetic patients (43, 44). In this experiment, we observed a trend toward decreased serum leptin levels in diabetic compared to control mice, but it did not reach significance as we had observed previously (26) (Table 1). In part, we observed increased variability in our control population. In addition, the current study obtained leptin levels from fasted mice, whereas our previous measurements were obtained from fed mice. Akirav, et al. (36) also demonstrate significant decreases in fed serum leptin levels in streptozotocin-induced diabetic compared to control rats, but found no difference between fasting diabetic and control rats. The latter was

the result of reduced leptin levels (to that of diabetic rat levels) in fasted control rats. Although leptin levels are often decreased in T1-diabetic patients (43, 44), fasting serum leptin levels were reported to be unchanged in T1-diabetic children and adolescents aged 6-16 years (45). We expect that if we had isolated serum from fed mice, leptin levels would have been decreased.

To our knowledge, this is the first report demonstrating a role leptin in the accumulation of marrow adipocytes in T1-diabetes. We found that by replacing the leptin that is normally lost by peripheral fat lipolysis in T1-diabetes, we can prevent the increase in adiposity in the marrow that is associated with T1-diabetes. It is possible that subcutaneous leptin administration prevented the increased lipid accumulation and marrow adipocyte differentiation that occurs in diabetes (12) or alternatively acted directly or via sympathetic nervous system (SNS) stimulation on marrow adipocytes to induce apoptosis (46, 47). The latter is supported by a report indicating that central leptin administration to the rat ventromedial hypothalamus causes adipocyte apoptosis in fat pads and in bone marrow (4).

Several reports (21, 29, 48-50) demonstrate increased marrow adiposity with bone loss suggesting that (1) marrow fat accumulation could have negative effects on bone formation, (2) mesenchymal stem cells preferentially choose the adipocyte lineage instead of the osteoblast lineage in disease conditions, and/or (3) trabecular bone volume decreases, therefore fat accumulates, filling in the empty space it has left behind (28, 51-53). However, in this experiment inhibiting marrow adiposity with leptin treatment did not prevent diabetes-induced

decreases in BMC, BMD and BVF in tibia trabecular bone (Table 2, Figure 15). Consistent with this finding, diabetes induced changes in serum bone remodeling markers were not prevented by leptin treatment in rats (54).

Our results also indicated that leptin treatment reduced tibia trabecular bone mass and several vertebral bone parameters (BMC and BMD) in control mice. Other parameters showed trends toward decreases but were not significant. The suppression in bone parameters in control mice was somewhat unexpected since previous reports of chronic leptin treatment in wild type mice suggest that under normal conditions leptin does not affect bone mass (9) and/or may increase bone strength (2). To our knowledge we are the first to examine the influence of leptin treatment on BALB/c mouse bone density, which may account for some of the differences between studies. Leptin treatment has been predominantly examined in the C57BL/6 strain since it is the background for leptin deficient (*ob/ob*) and dysfunctional leptin receptor (*db/db*) genetic mouse models. Although leptin treatment of wild type C57BL/6 mice does not affect most bone parameters, labeled bone forming surface have been reported to be significantly decreased at 2.5 and 10 μg leptin/day doses (13). In that study, the mice were treated for 14 days, so it may be that longer treatments would have resulted in bone loss in control mice as we have seen with a 28 day treatment. It is also important to note that the majority of studies using leptin as bone loss therapeutic (ie: for ovariectomy and disuse (14, 15)) have used rats not mice, suggesting that species differences must also be considered. Regarding gender, key studies demonstrating leptin's bone anabolic potential have used female rats

(unloading and ovariectomy (14, 15)) while both male and female *ob/ob* mouse bones positively respond to leptin treatment (13, 55). Thus, gender is less likely to play a role in our findings.

We hypothesized that leptin treatment of diabetic mice would prevent bone loss based on the finding that subcutaneous infusion of leptin with osmotic mini-pumps reduces marrow adiposity and restores bone mass in leptin deficient *ob/ob* mice (13). Similarly, hypothalamic injection of leptin can also correct skeletal abnormalities in *ob/ob* mice (55). Leptin injection into control (leptin-replete) mice did not affect bone mass (13). This suggests that leptin deficiency could be critical for determining leptin effectiveness. Our diabetic mice exhibit a significant suppression in leptin levels although they are not completely deficient as seen in *ob/ob* mice. It is possible that the low levels of endogenous leptin affect adiposity but not bone loss. An alternative concept is based on the comparative phenotypes between leptin deficient and T1-diabetic mice. While leptin deficient mice lose long bone mass, they have increased vertebral trabecular bone mass (5, 8, 9, 56-58); this is in contrast to T1-diabetic mice, which lose bone at all sites examined to date. Thus, leptin may not be playing a role in regulating bone mass in this disease model. However, the adiposity phenotype, long bone but not vertebral adiposity, is identical to what we observe in T1-diabetic mice and is restored with leptin treatment.

We did observe that leptin treatment increased serum osteocalcin levels (although not statistically significantly) in both control and diabetic mice suggesting a potential positive effect, however at the RNA level, the suppression

in osteocalcin levels by diabetes was not prevented with leptin treatment. Our studies also demonstrate that leptin treatment significantly suppresses osteoclast activity in diabetic mice as indicated by reduced active serum TRAP5b and bone TRAP5 RNA levels. Previous reports suggest that leptin treatment does not influence osteoclast activity (13) or can suppress activity possibly through inducing OPG expression and suppressing RANK ligand (15).

Why was leptin unable to prevent bone loss in diabetes? We do not believe there were any technical problems with leptin administration because of its potent effect on food intake (Figure 13) and marrow adiposity (Figure 14) and because leptin treatment was successful at raising serum leptin levels (Table 1). Concentration could play a role based on recent studies indicating the efficacy of leptin in restoring bone density is concentration dependent. Specifically, Martin et al. (42) demonstrated in the tail-suspended disuse rat model that only low dose leptin treatment (50 μg/kg/day) was effective in preventing femur trabecular bone loss. High dose leptin treatment (500 μg/kg/day) reduced femur bone mass in control rats and did not prevent bone loss in suspended groups. Either treatment dose prevented marrow adiposity. Previous studies in rats have used doses between ~100-350 μg/kg/day with therapeutic success (14, 15). In *ob/ob* mice, successful therapeutic doses have spanned 2.5 - 10 μg/day or ~100-400 μg/kg/day for control mice and ~66-263 μg/kg/day for leptin-deficient mice (13). Our dose was intermediate (6.6 μg/day; ~ 240 μg/kg/day): lower than the high dose in the Martin *et al.* study, but within the range to successfully treat bone loss in *ob/ob* mice (13). While our results exhibited similarities to the high dose leptin

treatment response seen in tail-suspended rats (bone loss in all conditions and adiposity prevention) (42), the high dose (but not the low dose) in that study decreased serum osteocalcin, whereas we observed no significant change in serum osteocalcin levels (Figure 17).

Interestingly, blood glucose levels were significantly reduced by leptin treatment in both control and diabetic mice. This is consistent with a previous report in which STZ-induced, diabetic mice overexpressing leptin became hyperglycemic but were more sensitive to insulin and required lower doses (compared to mice not overexpressing leptin) to maintain euglycemia (59). We do not believe the lower blood glucose in the leptin-treated mice confounded our results because we demonstrated bone loss to the same degree in leptin-treated and vehicle-treated diabetic mice. We also found leptin treatment affected other mouse parameters. For example, leptin-treated control mice exhibited lower body weights than diabetic (vehicle- or leptin-treated) mice. Still, the diabetic mice lost more bone (and more bone/gm body weight), supporting the notion that diabetic weight loss cannot fully account for the bone loss. While leptin treatment caused fat pad loss in control and diabetic mice, it prevented diabetic muscle loss, suggesting that the leptin-treated diabetic mice are leaner compared to the vehicle-treated diabetic mice. Similarly, the leptin-treated control mice were leaner than vehicle-treated control mice. A trend toward reduced fat pad and body mass was seen in wild type mice treated with 10 μg leptin/day although it did not reach significance (13).

Although the reciprocal relationship of fat to bone is often observed in diabetes, it is possible that they are not related to each other and occur through two completely different mechanisms. It is also possible that leptin did inhibit adipocyte differentiation (or only inhibited lipid deposition in adipocytes) and other factors may be necessary to induce osteoblast differentiation. The latter is likely, due to the complex pathology of T1-diabetes, which includes hyperglycemia, hypoinsulinemia, low serum leptin, hyperlipidemia, and inflammation. In a previous study, we demonstrated that inhibition of PPARγ2 with BADGE has a similar effect: prevention of marrow adiposity but not bone loss in diabetes (60). In this case, BADGE prevented hyperlipidemia, suggesting that excess lipids are not requisite for the process of bone loss in T1-diabetics. We have also demonstrated that loss of insulin receptor signaling in bone does not alter bone density, which suggests hypoinsulinemia cannot alone account for bone loss in T1-diabetes (61). It is possible that other factors that have not yet been addressed or a combination of T1-diabetic complications are important for bone loss to occur.

In summary, we have demonstrated a link between low leptin levels in T1-diabetes and marrow adiposity. Although leptin treatment prevented diabetes-induced increased marrow adipocyte number and gene expression, leptin had no effect on bone loss. We conclude, therefore, that it is unlikely that leptin deficiency alone is responsible for diabetic bone loss and that other factors are necessary for the pathogenesis of T1-diabetic osteoporosis.

3.6. ACKNOWLEGEMENTS

The authors thank Amylin for providing the leptin, Regina Irwin for technical assistance and critically reviewing the manuscript and Lindsay Martin, Laura Harris, Dennean Lippner and Erin Nekritz for critically reviewing the manuscript.

3.7. REFERENCES

1. **Reseland JE, Syversen U, Bakke I, Qvigstad G, Eide LG, Hjertner O, Gordeladze JO, Drevon CA** 2001 Leptin is expressed in and secreted from primary cultures of human osteoblasts and promotes bone mineralization. J Bone Miner Res 16:1426-1433

2. **Cornish J, Callon KE, Bava U, Lin C, Naot D, Hill BL, Grey AB, Broom N, Myers DE, Nicholson GC, Reid IR** 2002 Leptin directly regulates bone cell function in vitro and reduces bone fragility in vivo. J Endocrinol 175:405-415

3. **Hamrick MW** 2004 Leptin, bone mass, and the thrifty phenotype. J Bone Miner Res 19:1607-1611

4. **Hamrick MW, Della Fera MA, Choi YH, Hartzell D, Pennington C, Baile CA** 2007 Injections of leptin into rat ventromedial hypothalamus increase adipocyte apoptosis in peripheral fat and in bone marrow. Cell Tissue Res 327:133-141

5. **Ducy P, Amling M, Takeda S, Priemel M, Schilling AF, Beil FT, Shen J, Vinson C, Rueger JM, Karsenty G** 2000 Leptin inhibits bone formation through a hypothalamic relay: a central control of bone mass. Cell 100:197-207

6. **Karsenty G** 2001 Leptin controls bone formation through a hypothalamic relay. Recent Prog Horm Res 56:401-415

7. **Chan JL, Mantzoros CS** 2005 Role of leptin in energy-deprivation states: normal human physiology and clinical implications for hypothalamic amenorrhoea and anorexia nervosa. Lancet 366:74-85

8. **Hamrick MW, Pennington C, Newton D, Xie D, Isales C** 2004 Leptin deficiency produces contrasting phenotypes in bones of the limb and spine. Bone 34:376-383

9. **Steppan CM, Crawford DT, Chidsey-Frink KL, Ke H, Swick AG** 2000 Leptin is a potent stimulator of bone growth in ob/ob mice. Regul Pept 92:73-78

10. **Considine RV, Sinha MK, Heiman ML, Kriauciunas A, Stephens TW, Nyce MR, Ohannesian JP, Marco CC, McKee LJ, Bauer TL, et al.** 1996 Serum immunoreactive-leptin concentrations in normal-weight and obese humans. N Engl J Med 334:292-295

11. **Goulding A, Taylor RW** 1998 Plasma leptin values in relation to bone mass and density and to dynamic biochemical markers of bone resorption and formation in postmenopausal women. Calcif Tissue Int 63:456-458

12. **Thomas T, Gori F, Khosla S, Jensen MD, Burguera B, Riggs BL** 1999 Leptin acts on human marrow stromal cells to enhance differentiation to osteoblasts and to inhibit differentiation to adipocytes. Endocrinology 140:1630-1638

13. **Hamrick MW, Della-Fera MA, Choi YH, Pennington C, Hartzell D, Baile CA** 2005 Leptin treatment induces loss of bone marrow adipocytes and increases bone formation in leptin-deficient ob/ob mice. J Bone Miner Res 20:994-1001

14. **Martin A, de Vittoris R, David V, Moraes R, Begeot M, Lafage-Proust MH, Alexandre C, Vico L, Thomas T** 2005 Leptin modulates both resorption and formation while preventing disuse-induced bone loss in tail-suspended female rats. Endocrinology 146:3652-3659

15. **Burguera B, Hofbauer LC, Thomas T, Gori F, Evans GL, Khosla S, Riggs BL, Turner RT** 2001 Leptin reduces ovariectomy-induced bone loss in rats. Endocrinology 142:3546-3553

16. **Vestergaard P** 2007 Discrepancies in bone mineral density and fracture risk in patients with type 1 and type 2 diabetes--a meta-analysis. Osteoporos Int 18:427-444

17. **Janghorbani M, Van Dam RM, Willett WC, Hu FB** 2007 Systematic review of type 1 and type 2 diabetes mellitus and risk of fracture. Am J Epidemiol 166:495-505

18. **Levin ME, Boisseau VC, Avioli LV** 1976 Effects of diabetes mellitus on bone mass in juvenile and adult-onset diabetes. N Engl J Med 294:241-245

19. **Auwerx J, Dequeker J, Bouillon R, Geusens P, Nijs J** 1988 Mineral metabolism and bone mass at peripheral and axial skeleton in diabetes mellitus. Diabetes 37:8-12

20. **Kemink SA, Hermus AR, Swinkels LM, Lutterman JA, Smals AG** 2000 Osteopenia in insulin-dependent diabetes mellitus; prevalence and aspects of pathophysiology. J Endocrinol Invest 23:295-303

21. **Botolin S, Faugere MC, Malluche H, Orth M, Meyer R, McCabe LR** 2005 Increased bone adiposity and peroxisomal proliferator-activated receptor-gamma2 expression in type I diabetic mice. Endocrinology 146:3622-3631

22. **Bouillon R, Bex M, Van Herck E, Laureys J, Dooms L, Lesaffre E, Ravussin E** 1995 Influence of age, sex, and insulin on osteoblast function: osteoblast dysfunction in diabetes mellitus. J Clin Endocrinol Metab 80:1194-1202

23. **Goodman WG, Hori MT** 1984 Diminished bone formation in experimental diabetes. Relationship to osteoid maturation and mineralization. Diabetes 33:825-831

24. **Botolin S, McCabe LR** 2007 Bone loss and increased bone adiposity in spontaneous and pharmacologically induced diabetic mice. Endocrinology 148:198-205

25. **Fowlkes JL, Bunn RC, Liu L, Wahl EC, Coleman HN, Cockrell GE, Perrien DS, Lumpkin CK, Jr., Thrailkill KM** 2008 Runt-related transcription factor 2 (RUNX2) and RUNX2-related osteogenic genes are down-regulated throughout osteogenesis in type 1 diabetes mellitus. Endocrinology 149:1697-1704

26. **Martin LM, McCabe LR** 2007 Type I diabetic bone phenotype is location but not gender dependent. Histochem Cell Biol 128:125-133

27. **McCabe LR** 2007 Understanding the pathology and mechanisms of type I diabetic bone loss. J Cell Biochem 102:1343-1357

28. **Nuttall ME, Patton AJ, Olivera DL, Nadeau DP, Gowen M** 1998 Human trabecular bone cells are able to express both osteoblastic and adipocytic

phenotype: implications for osteopenic disorders. J Bone Miner Res 13:371-382

29. **Verma S, Rajaratnam JH, Denton J, Hoyland JA, Byers RJ** 2002 Adipocytic proportion of bone marrow is inversely related to bone formation in osteoporosis. J Clin Pathol 55:693-698

30. **Ahdjoudj S, Lasmoles F, Holy X, Zerath E, Marie PJ** 2002 Transforming growth factor beta2 inhibits adipocyte differentiation induced by skeletal unloading in rat bone marrow stroma. J Bone Miner Res 17:668-677

31. **Gulen S, Dincer S** 2007 Effects of leptin on oxidative stress in healthy and Streptozotocin-induced diabetic rats. Mol Cell Biochem 302:59-65

32. **Vengellur A, LaPres JJ** 2004 The role of hypoxia inducible factor 1alpha in cobalt chloride induced cell death in mouse embryonic fibroblasts. Toxicol Sci 82:638-646

33. **Li J, Takaishi K, Cook W, McCorkle SK, Unger RH** 2003 Insig-1 "brakes" lipogenesis in adipocytes and inhibits differentiation of preadipocytes. Proc Natl Acad Sci U S A 100:9476-9481

34. **Ontiveros C, McCabe LR** 2003 Simulated microgravity suppresses osteoblast phenotype, Runx2 levels and AP-1 transactivation. J Cell Biochem 88:427-437

35. **Wiren KM, Zhang XW, Toombs AR, Kasparcova V, Gentile MA, Harada S, Jepsen KJ** 2004 Targeted overexpression of androgen receptor in osteoblasts: unexpected complex bone phenotype in growing animals. Endocrinology 145:3507-3522

36. **Akirav EM, Chan O, Inouye K, Riddell MC, Matthews SG, Vranic M** 2004 Partial leptin restoration increases hypothalamic-pituitary-adrenal activity while diminishing weight loss and hyperphagia in streptozotocin diabetic rats. Metabolism 53:1558-1564

37. **Sindelar DK, Havel PJ, Seeley RJ, Wilkinson CW, Woods SC, Schwartz MW** 1999 Low plasma leptin levels contribute to diabetic hyperphagia in rats. Diabetes 48:1275-1280

38. **Hidaka S, Yoshimatsu H, Kondou S, Tsuruta Y, Oka K, Noguchi H, Okamoto K, Sakino H, Teshima Y, Okeda T, Sakata T** 2002 Chronic central leptin infusion restores hyperglycemia independent of food intake and insulin level in streptozotocin-induced diabetic rats. FASEB J 16:509-518

39. **Barzilai N, Wang J, Massilon D, Vuguin P, Hawkins M, Rossetti L** 1997 Leptin selectively decreases visceral adiposity and enhances insulin action. J Clin Invest 100:3105-3110

40. **Wang JL, Chinookoswong N, Scully S, Qi M, Shi ZQ** 1999 Differential effects of leptin in regulation of tissue glucose utilization in vivo. Endocrinology 140:2117-2124

41. **Sivitz WI, Walsh SA, Morgan DA, Thomas MJ, Haynes WG** 1997 Effects of leptin on insulin sensitivity in normal rats. Endocrinology 138:3395-3401

42. **Martin A, David V, Malaval L, Lafage-Proust MH, Vico L, Thomas T** 2007 Opposite effects of leptin on bone metabolism: a dose-dependent balance related to energy intake and insulin-like growth factor-I pathway. Endocrinology 148:3419-3425

43. **Hanaki K, Becker DJ, Arslanian SA** 1999 Leptin before and after insulin therapy in children with new-onset type 1 diabetes. J Clin Endocrinol Metab 84:1524-1526

44. **Kiess W, Anil M, Blum WF, Englaro P, Juul A, Attanasio A, Dotsch J, Rascher W** 1998 Serum leptin levels in children and adolescents with insulin-dependent diabetes mellitus in relation to metabolic control and body mass index. Eur J Endocrinol 138:501-509

45. **Karaguzel G, Ozdem S, Boz A, Bircan I, Akcurin S** 2006 Leptin levels and body composition in children and adolescents with type 1 diabetes. Clin Biochem 39:788-793

46. **Kim GS, Hong JS, Kim SW, Koh JM, An CS, Choi JY, Cheng SL** 2003 Leptin induces apoptosis via ERK/cPLA2/cytochrome c pathway in human bone marrow stromal cells. J Biol Chem 278:21920-21929

47. **Page KA, Hartzell DL, Li C, Westby AL, Della-Fera MA, Azain MJ, Pringle TD, Baile CA** 2004 beta-Adrenergic receptor agonists increase apoptosis of adipose tissue in mice. Domest Anim Endocrinol 26:23-31

48. **Jilka RL, Weinstein RS, Takahashi K, Parfitt AM, Manolagas SC** 1996 Linkage of decreased bone mass with impaired osteoblastogenesis in a murine model of accelerated senescence. J Clin Invest 97:1732-1740

49. **Kajkenova O, Lecka-Czernik B, Gubrij I, Hauser SP, Takahashi K, Parfitt AM, Jilka RL, Manolagas SC, Lipschitz DA** 1997 Increased adipogenesis and myelopoiesis in the bone marrow of SAMP6, a murine model of defective osteoblastogenesis and low turnover osteopenia. J Bone Miner Res 12:1772-1779

50. **Moerman EJ, Teng K, Lipschitz DA, Lecka-Czernik B** 2004 Aging activates adipogenic and suppresses osteogenic programs in mesenchymal marrow stroma/stem cells: the role of PPAR-gamma2 transcription factor and TGF-beta/BMP signaling pathways. Aging Cell 3:379-389

51. **Duque G** 2008 Bone and fat connection in aging bone. Curr Opin Rheumatol 20:429-434

52. **Gimble JM, Zvonic S, Floyd ZE, Kassem M, Nuttall ME** 2006 Playing with bone and fat. J Cell Biochem 98:251-266

53. **Rosen CJ, Bouxsein ML** 2006 Mechanisms of disease: is osteoporosis the obesity of bone? Nat Clin Pract Rheumatol 2:35-43

54. **Gad HI** 2007 The potential osteogenic effects of systemic leptin and insulin administration in streptozotocin-induced diabetic female rats. Saudi Med J 28:1185-1190

55. **Iwaniec UT, Boghossian S, Lapke PD, Turner RT, Kalra SP** 2007 Central leptin gene therapy corrects skeletal abnormalities in leptin-deficient ob/ob mice. Peptides 28:1012-1019

56. **Takeda S, Elefteriou F, Levasseur R, Liu X, Zhao L, Parker KL, Armstrong D, Ducy P, Karsenty G** 2002 Leptin regulates bone formation via the sympathetic nervous system. Cell 111:305-317

57. **Lorentzon R, Alehagen U, Boquist L** 1986 Osteopenia in mice with genetic diabetes. Diabetes Res Clin Pract 2:157-163

58. **Mathey J, Horcajada-Molteni MN, Chanteranne B, Picherit C, Puel C, Lebecque P, Cubizoles C, Davicco MJ, Coxam V, Barlet JP** 2002 Bone mass in obese diabetic Zucker rats: influence of treadmill running. Calcif Tissue Int 70:305-311

59. **Miyanaga F, Ogawa Y, Ebihara K, Hidaka S, Tanaka T, Hayashi S, Masuzaki H, Nakao K** 2003 Leptin as an adjunct of insulin therapy in insulin-deficient diabetes. Diabetologia 46:1329-1337

60. **Botolin S, McCabe LR** 2006 Inhibition of PPARgamma prevents type I diabetic bone marrow adiposity but not bone loss. J Cell Physiol 209:967-976

61. **Irwin R, Lin HV, Motyl KJ, McCabe LR** 2006 Normal bone density obtained in the absence of insulin receptor expression in bone. Endocrinology 147:5760-5767

CHAPTER 4

4. CCAAT/ENHANCER BINDING PROTEIN BETA-DEFICIENCY ENHANCES TYPE 1 DIABETIC BONE PHENOTYPE BY INCREASING MARROW ADIPOSITY AND BONE RESORPTION

4.1. ABSTRACT

C/EBPβ is an important regulator of adipocyte and osteoblast differentiation from mesenchymal stem cells in bone marrow. Bone loss in type 1 diabetes is accompanied by increased marrow fat, which could directly contribute to reduced osteoblast activity, or could result from altered lineage selection to adipocytes rather than osteoblasts. Increased bone C/EBPβ expression at the onset of diabetes could push progenitors toward the adipocyte lineage. Here, we induced diabetes in *C/EBPβ-null* (knockout, KO) mice to inhibit marrow adiposity and prevent bone loss. Unexpectedly, we determined that C/EBPβ-deficiency actually enhanced the diabetic bone phenotype. While KO mice had reduced peripheral fat depot mass compared to wild type, KO diabetic mice had 5-fold more marrow adipocytes than diabetic wild type mice. Furthermore, tibia trabecular bone volume fraction (BVF) loss was escalated, as diabetic KO mice lost 48% of BVF compared to KO controls while littermate wild type diabetic mice only lost 22% compared to wild type controls. The enhanced marrow adiposity in KO diabetics could be attributed to compensation by C/EBPδ, PPARγ2, and C/EBPα. The osteoblast marker osteocalcin was reduced similarly in diabetic KO

and wild type mice. However, cathepsin K mRNA and osteoclast histomorphometry indicated that resorption was increased in the KO diabetic mice compared to KO controls, which could account for the greater decrease in bone density in C/EBPβ KOs. Taken together, C/EBPβ-deficiency has contrasting effects on diabetes-induced peripheral and bone marrow adipose depot mass, while causing increased bone resorption, contrary to the classical mechanism of type 1 diabetic bone loss.

4.2. INTRODUCTION

CCAAT/ enhancer binding protein beta (C/EBPβ) is a member of the basic region-leucine zipper (bZIP) class of transcription factors. A key regulator of adipocyte lineage selection, it is transiently expressed during early adipocyte differentiation with C/EBPδ, and then followed by expression of peroxisome proliferator-activated receptor gamma (PPARγ) 2 and C/EBPα (1-3). C/EBPβ exists in three isoforms: transcriptionally active LAP-1 and LAP-2 and generally inactive LIP (3). Overexpression of C/EBPβ alone induces adipocyte differentiation in NIH-3T3 fibroblasts, while LIP overexpression can prevent it (4, 5). Total deficiency of C/EBPβ protects mice from obesity and reduces body fat mass (6-8). Combined knockout of C/EBPβ and C/EBPδ leads to an even greater block to the adipocyte phenotype and adiposity (9).

In addition to its role in adipocyte maturation, C/EBPβ has been shown to affect osteoblast differentiation and subsequent bone density. These effects are

dependent on when (early vs. late differentiation), where (local vs. systemic), and which (LAP vs. LIP, or both) C/EBPβ is expressed. C/EBPβ is normally expressed during early and late stages of osteoblast differentiation, with decreased expression during middle stages (10). Complete knockout of C/EBPβ in mice results in decreased total body mass and total bone mineral density (BMD) (7). Similarly, targeted expression of the C/EBPβ inactive form, LIP, to preosteoblasts and osteoblasts results in osteopenia in transgenic mice due to decreased bone formation (11).

Type 1 (T1-) diabetes affects approximately 1 million people in the United States. This subtype of diabetes is characterized by a loss of insulin-secreting pancreatic b-cells and hyperglycemia that must be controlled by insulin delivery in humans. In addition to complications of retinopathy, neuropathy, nephropathy, muscle atrophy and heart disease, T1-diabetes also causes osteoporosis (12-14). Streptozotocin (STZ) is a pharmacologic agent used to induce pancreatic β-cell toxicity and subsequent diabetes in research animals (15). Multiple low doses of STZ (40 mg/kg injections for five consecutive days) induce hyperglycemia in mice by five days after the first injection (DPI). In both STZ-mice and rats, T1-diabetes causes bone loss and impaired bone healing (16-21). Similarly, spontaneously T1-diabetic NOD (non-obese diabetic) mice also lose bone (22). Therefore, the observed bone changes are caused by diabetes and not STZ alone.

Osteoporosis from T1-diabetes is marked by decreased bone formation in both humans and animals (16, 23, 24), while reported effects on osteoclast bone

resorption have been variable. Altered mesenchymal stem cell lineage selection to adipocytes rather than osteoblasts has been implicated as a mechanism for bone loss in diabetes (16, 22, 25), aging (26, 27), and unloading (28). In STZ-diabetic mice, this hypothesis is supported by an increase in expression of adipocyte-specific genes in bone (PPARγ2 and fatty-acid binding protein (FABP) 4) and visible adipocytes in the marrow (16). Marrow adiposity is not a direct result of STZ because NOD mice also have increased adipocyte accumulation accompanying bone loss (22).

Inhibition of marrow adiposity is important for determining whether adiposity causes and could be targeted to treat diabetic osteoporosis. Previously, we demonstrated that treatment with the PPARγ2 inhibitor, bisphenol-A-diglycidyl ether (BADGE), prevents STZ-diabetic marrow adiposity, but does not protect against bone loss (29). One interpretation of this study is that mesenchymal stem cells still differentiate toward the adipocyte lineage, but BADGE forces them to remain in an early-adipocyte stage. Therefore, we hypothesized that inhibition of adipocyte differentiation prior to PPARγ2 induction (at the level of C/EBPβ) could be effective at enhancing or maintaining bone density in T1-diabetes.

In the present study, we demonstrate that C/EBPβ expression is increased in bone with the onset of diabetes. We hypothesize that C/EBPβ may play a role in the diabetic bone pathology by promoting adipocyte lineage selection and increasing marrow adiposity. Therefore, deficiency of C/EBPβ could inhibit T1-diabetic marrow adiposity at the level of lineage selection and subsequently prevent bone loss. To our surprise, we found that C/EBPβ-deficiency does not

prevent the increased marrow adiposity or decreased osteoblast activity classically observed in T1-diabetes. In fact, the absence of C/EBPβ exacerbated diabetic marrow adiposity, despite causing peripheral fat loss. Bone loss was also increased with C/EBPβ-deficiency; however, unlike bone loss in wild type diabetic mice, additional bone loss in KO mice was due to enhanced bone resorption rather than further suppression of osteoblast activity.

4.3. MATERIALS AND METHODS

4.3.1. Animals

BALB/c mice were obtained from Harlan Sprague Dawley (Indianapolis, IN). Heterozygous C/EBPβ (*C/EBPβ*$^{+/-}$) mice were obtained from Peter F. Johnson (NCI, Frederick, MD) (30) and were bred into the BALB/c strain and genotyped at Michigan State University by Jeffrey Leipprandt in the laboratory of Sandra Z. Haslam. All mice were maintained on a 12-hour light, 12-hour dark cycle at 23 °C, were given standard lab chow, and had food and water *ad libitum*. All animal procedures were approved by the Michigan State University Institutional Animal Care and Use Committee. To induce diabetes, 14-week old BALB/c mice, C/EBPβ KO (*C/EBPβ*$^{-/-}$) mice, and wild type littermate controls were injected with either 40 mg/kg STZ (Sigma, St. Louis, MO) or 0.1 M citrate buffer, pH 4.5, vehicle for 5 consecutive days. Diabetes was confirmed 12 days post-first STZ injection (DPI) using a drop of blood from the saphenous vein and

an Accu-Chek Compact glucometer (Roche Diagnostics Corporation, Indianapolis, IN), with blood glucose greater than or equal to 300 mg/dl indicating diabetes. Body mass was monitored during diabetes induction and throughout the experiment. BALB/c mice were euthanized at 5, 19, 28 and 40 DPI. *C/EBPβ* KO mice and wild type littermate controls were euthanized at 40 DPI.

4.3.2. RNA Analyses

Immediately after euthanasia, tibias were cleansed of muscle and connective tissue, snap frozen in liquid nitrogen, and stored at -80 °C. Frozen tibias were crushed under liquid nitrogen conditions with a Bessman Tissue Pulverizer (Spectrum Laboratories, Inc., Rancho Dominguez, CA). RNA was isolated with Tri Reagent (Molecular Research Center, Inc., Cincinnati, OH) and integrity was assessed by formaldehyde-agarose gel electrophoresis. cDNA was synthesized by reverse transcription with Superscript II Reverse Transcriptase Kit and oligo $dT_{(12\text{-}18)}$ primers (Invitrogen, Carlsbad, CA) and amplified by real time PCR with iQ SYBR Green Supermix (Biorad, Hercules, CA) and gene-specific primers synthesized by Integrated DNA Technologies (Coralville, IA). Hypoxanthine guanine phosphoribosyl transferase (HPRT) mRNA levels do not fluctuate in diabetes or deletion of C/EBPβ, and were used as an internal control. HPRT was amplified using 5'-AAG CCT AAG ATG AGC GCA AG-3' and 5'-TTA CTA GGC AGA TGG CCA CA-3' (31). C/EBPβ was amplified using 5'-CAA GCT GAG CGA CGA GTA CA-3' and 5'-CAG CTG CTC CAC CTT CTT CT-3' (32).

FABP4 (aP2) was amplified using 5'-GCG TGG AAT TCG ATG AAA TCA-3' and 5'-CCC GCC ATC TAG GGT TAT GA-3' (33). C/EBPδ was amplified using 5'-CGC AGA CAG TGG TGA GCT TG-3' and 5'-CTT GCG CAC AGC GAT GTT GTT-3' (32). PPARγ2 was amplified using 5'-TGA AAC TCT GGG AGA TTC TCC TG-3' and 5'-CCA TGG TAA TTT CTT GTG AAG TGC-3' (34). C/EBPα was amplified using 5'-GAA CAG CAA CGA GTA CCG GGT -3' and 5'-GCC ATG GCC TTG ACC AAG GAG-3' (32). Osteocalcin was amplified using 5'-ACG GTA TCA CTA TTT AGG ACC TGT G-3' and 5'-ACT TTA TTT TGG AGC TGC TGT GAC-3' (35). Tartrate-resistant acid phosphatase (TRAP5) was amplified using 5'-AAT GCC TCG ACC TGG GA-3' and 5'-CGT AGT CCT CCT TGG CTG CT-3' (36). Cathepsin K was amplified using 5'-GCA GAG GTG TGT ACT ATG-3' and 5'-GCA GGC GTT GTT CTT ATT-3' (37). Amplicons were compared with a 100 bp DNA ladder (Invitrogen, Carlsbad, CA) on a 2% agarose gel in order to verify RT-PCR results and to verify the absence of C/EBPβ in the knockout animals.

4.3.3. Bone histology and histomorphometry

Femurs and tibias were fixed in 10% formalin and transferred to 70% ethanol after 24 hours. Fixed samples were processed on an automated Thermo Electron Excelsior tissue processor for dehydration, clearing, and infiltration using a routine overnight processing schedule. Samples were then embedded in Surgipath embedding paraffin on a Sakura Tissue Tek II embedding center. Paraffin blocks were sectioned at 5 μm on a Reichert Jung 2030 rotary

microtome. Slides were stained for TRAP activity and counter stained with hematoxylin according to manufacturer protocol (387A-1KT, Sigma, St. Louis, MO). Osteoclast surface area was measured and expressed as a percentage of total bone surface in the tibia trabecular region ranging from the proximal growth plate to 2 mm distal. Visible adipocytes, greater than 30 μm, were counted in the same region of the tibia and in the region of the femur immediately proximal to the distal growth plate, extending 2 mm distal.

4.3.4. Micro Computed Tomography (μCT) Analyses

Fixed tibias were scanned using a GE Explore Locus μCT system at a voxel resolution of 20 μm obtained from 720 views. Beam angle of increment was 0.5, and beam strength was set at 80 peak kV and 450 μA. Each run included control and diabetic, WT and C/EBPβ KO bones, and a calibration phantom to standardize grayscale values and maintain consistency. Based on autothreshold and isosurface analyses of multiple bone samples, a fixed threshold (800) was used to separate bone from bone marrow. Trabecular bone analyses were performed in a region of trabecular bone defined at 0.17 mm (~1% of the total length) distal to the growth plate of the proximal tibia extending 2 mm toward the diaphysis, and excluding the outer cortical shell. Trabecular bone mineral content (BMC), bone mineral density (BMD), bone volume fraction (BVF), thickness (TbTh), spacing (TbSp), and number (TbN) values were computed by a GE Healthcare MicroView software application for visualization and analysis of

volumetric image data. Trabecular isosurface images were taken from a cylindrical region in the tibia immediately distal to the proximal growth plate measuring 1.0 mm in length and 1.0 mm in diameter.

4.3.5. Statistical Analyses

All measurements are presented as the mean ± standard error of the mean (SEM). Statistical significance was determined with a student's t-test (assuming equal variance) using Microsoft Excel (Microsoft Corporation, Redmond, WA).

4.4. RESULTS

To determine the temporal pattern of C/EBPβ expression in T1-diabetic bone, we treated mice with STZ or vehicle to induce T1-diabetes and harvested bone at 5, 19, 28 and 40 DPI. At 40 DPI, adipocyte numbers are clearly increased in diabetic bone marrow (Figure 18A), consistent with previous reports from our lab and others (16, 22, 29, 38, 39). However, at 5 DPI, the point at which blood glucose levels become significantly elevated in diabetic mice (190 ± 12 mg/dl versus 152 ± 5 mg/dl in controls), adiposity markers are already beginning to increase at the RNA level (Figure 18B) (40). Therefore, expression of transient transcription factors involved in early adipogenesis should be evident at this early time point. Consistent with adipocyte lineage selection in diabetic

bone, we observed an increase in C/EBPβ mRNA levels at 5 DPI. This increase was concurrent with an increase in aP2, a marker of mature adipocytes. The latter remained elevated throughout the time course (Figure 18B), as we have previously demonstrated (40), while C/EBPβ mRNA levels declined consistent with adipocyte maturation (41).

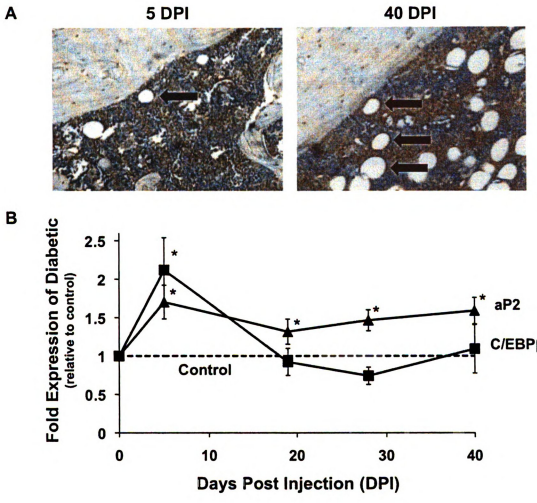

Figure 18. **C/EBPβ expression is increased in diabetic bone in conjunction with aP2 expression and is followed by increased marrow adiposity.** BALB/c mice were injected with streptozotocin (STZ) to induce diabetes. Mice were harvested 5, 19, 28 and 40 days post injection (DPI) with STZ. A: Fixed femurs from diabetic mice at 5 and 40 DPI were stained with hematoxylin. Large white circular features (denoted by arrows) are adipocytes. B: mRNA was extracted from frozen tibias and made into cDNA, which was amplified by RT-PCR with primers specific to C/EBPβ, aP2 and HPRT (a housekeeping gene control). Points represent mean ± standard error of diabetic mRNA levels expressed relative to control values (normalized to one). *p<0.05 by student's t-test.

To determine whether C/EBPβ plays an important role in diabetic bone loss and marrow adiposity, we induced diabetes in C/EBPβ KO mice and wild type littermate controls. Mice were harvested at 40 DPI. Knockout of C/EBPβ was confirmed by RT-PCR in tibia (Figure 19). Consistent with previous studies, the non-diabetic C/EBPβ KO mice had lower glucose levels than non-diabetic wild type mice (42). However, this hypoglycemia was not significant enough to affect diabetes induction in KO mice. Blood glucose levels were increased to greater than 500 mg/dl in both wild type and C/EBPβ KO diabetic mice (Figure 19), and were not significantly different from each other.

General mouse phenotype analyses indicate that *C/EBPβ*$^{-/-}$ mice are smaller than wild type mice: they have lower total body, muscle and fat pad mass, consistent with past studies (7, 42). Consistent with a diabetic phenotype, both wild type and KO diabetic mice lost weight. However the KO diabetic mice lost more weight: -16% versus -7% in diabetic wild type mice (Table 4). Body weights of both control and diabetic KO mice were lower than treatment-matched wild type mice. A portion of the diabetic weight loss can be accounted for by muscle loss (-16% in wild type and -22% in KO mice) and peripheral fat loss (-48%) in both wild type and KO mice (Table 4). Liver mass increased 28% in wild type diabetic compared to control mice, whereas it increased only 10% in KO diabetic compared to control mice (Table 4). Therefore, the greater body mass loss induced by diabetes in the KO animals could be attributed to increased muscle loss and less liver hypertrophy.

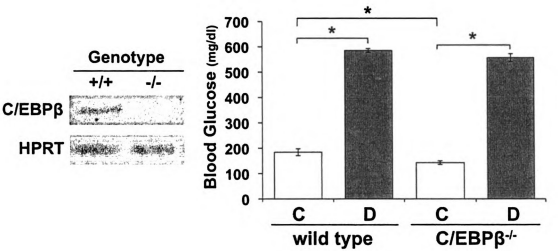

Figure 19. **Diabetes induction did not differ between C/EBPβ knockout and wild type mice.** LEFT: To confirm genotypes, mRNA was extracted from frozen tibias and was made into cDNA with a reverse transcriptase reaction. cDNA was amplified by RT-PCR with primers specific to C/EBPβ and values are expressed relative to HPRT, a housekeeping gene control. Amplicons were separated on 1.5% agarose DNA gel and visualized by ethidium bromide staining. Absence of a C/EBPβ-specific amplicon was indicative of C/EBPβ knockout. RIGHT: Blood glucose was measured in control (C, white bars), diabetic (D, gray bars), wild type (WT) and *C/EBPβ*$^{-/-}$ mice at 40 DPI. Bars represent mean ± standard error. *p<0.05 by student's t-test. N ≥ 5 per condition.

Table 4. Body and tissue masses of 28 day diabetic and untreated wild type and C/EBPβ$^{-/-}$ mice.

	wild type		C/EBPβ$^{-/-}$	
	Control (n=5)	Diabetic (n=9)	Control (n=9)	Diabetic (n=12)
Total Body Mass (g)	27.1 ± 0.5	25.1 ± 0.5*	25.7 ± 0.3^	21.6 ± 0.6*^
Tibialis Anterior (mg)	49 ± 1	41 ± 3*	41 ± 2^	32 ± 2*^
Femoral Fat Pads (mg)	259 ± 11	134 ± 6*	202 ± 14^	105 ± 31*
Liver (g)	1.27 ± 0.06	1.62 ± 0.06*	1.25 ± 0.05	1.37 ± 0.04^

*$p < 0.05$ compared to genotype-matched control.

^$p < 0.05$ compared to treatment-matched wild type.

To determine whether C/EBPβ-deficiency prevented adipocyte accumulation in the diabetic marrow, we quantitated adipocytes in hematoxylin stained tibia sections (Figure 20A and 20B). Marrow adipocyte number did not differ significantly between KO and wild type mice, although KO mice tended to have more adipocytes (Figure 20B). Diabetes increased adipocyte numbers in both wild type and KO mice compared to corresponding controls. Interestingly, marrow adipocyte accumulation was enhanced by the lack of C/EBPβ; KO diabetic mice had over 5-fold more adipocytes than wild type diabetic mice. Similar to adipocyte number, aP2 gene expression increased in wild type diabetic mice compared to wild type control mice (Figure 20C), which is consistent with previous findings (16, 29, 38, 40, 43). C/EBPβ$^{-/-}$ control mice also had significantly lower aP2 expression than wild type control mice. Despite this, diabetes induced aP2 expression in KO mice to levels significantly higher than all other groups.

Figure 20. **Diabetic marrow adiposity was increased by C/EBPβ deficiency.** A: Represenative photomicrographs of tibia sections stained with hematoxylin from control (C) and diabetic (D) wild type and *C/EBPβ*$^{-/-}$ tibias. Photographs were taken 1 mm distal to the proximal growth plate. B: Visible adipocytes were counted in the marrow portion of tibia sections in the area 2 mm distal to the proximal growth plate. C: mRNA was extracted from frozen tibias and was made into cDNA with a reverse transcriptase reaction. cDNA was amplified by RT-PCR with primers specific to aP2, an adipocyte marker, and values were expressed relative to HPRT, a housekeeping gene control. Bars represent mean ± standard error of control (C, white bars), diabetic (D, gray bars), wild type and C/EBPα$^{-/-}$ mice. *$p<0.05$ by student's t-test. $N \geq 5$ per condition.

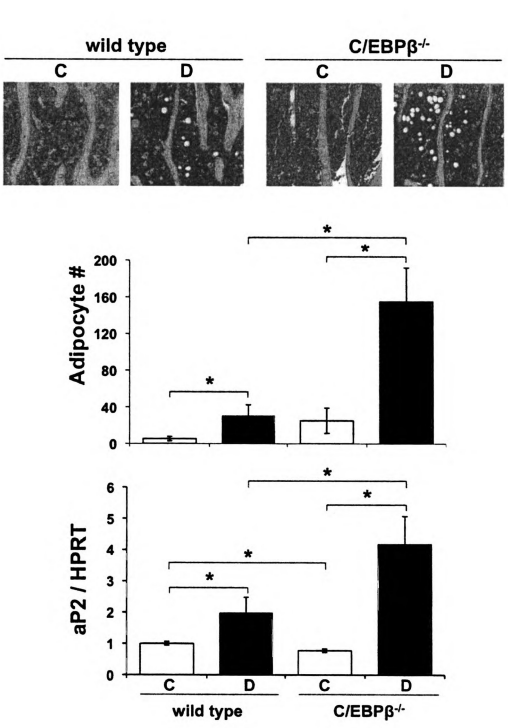
A
wild type
C/EBPβ-/-
C
D
C
D
B
Adipocyte #
200
160
120
80
40
0
*
*
*
C
aP2 / HPRT
6
5
4
3
2
1
0
*
*
*
*
C
D
C
D
wild type
C/EBPβ-/-

In order to understand how deletion of C/EBPβ, a transcription factor important for adipocyte differentiation, could enhance diabetic marrow adiposity, we measured other adipogenic transcription factors in both wild type and KO, control and diabetic mice (Figure 21). C/EBPδ, which is normally expressed with C/EBPβ early in adipocyte differentiation, was significantly decreased (nearly 5-fold) in diabetic wild type compared to diabetic control bone. This decrease was prevented in the *C/EBPβ*$^{-/-}$ mice. PPARγ2 and C/EBPα, both transcription factors present later in adipocyte differentiation, were unchanged in diabetic wild type mice compared to wild type controls, but were significantly elevated in KO diabetic mice compared to KO controls. Heightened adipogenic transcription factor expression in KO diabetic bone (Figure 21) is consistent with the higher marrow adiposity that we observed (Figure 20).

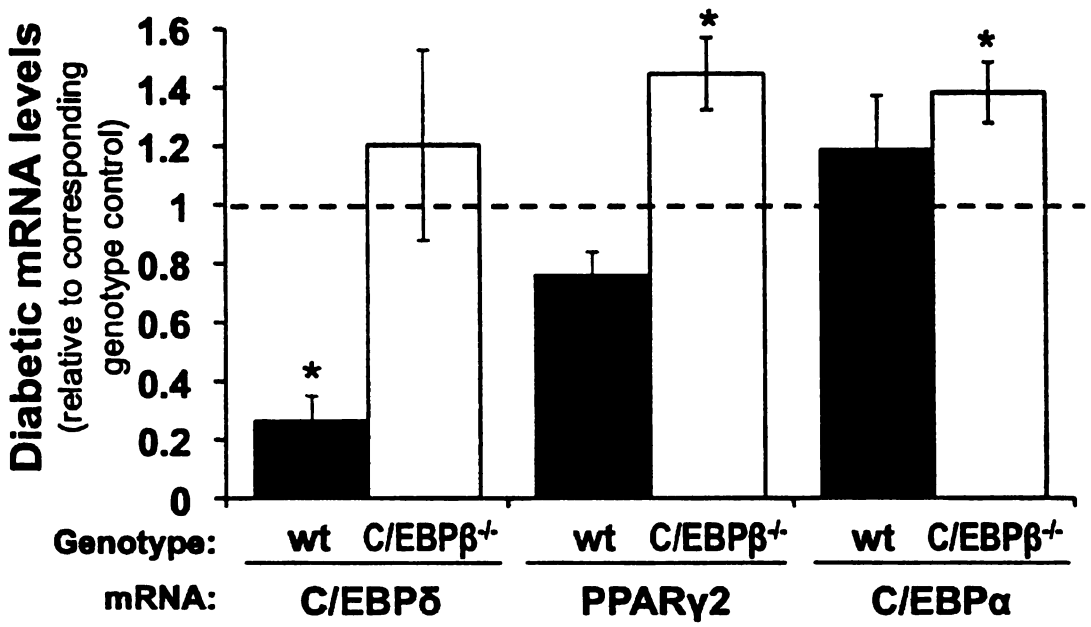

Figure 21. **Adipogenic transcription factors are elevated in diabetic C/EBPβ$^{-/-}$ compared to wild type diabetic bone.** mRNA was extracted from frozen tibias and was made into cDNA with a reverse transcriptase reaction. cDNA was amplified by RT-PCR with primers specific to C/EBPδ, PPARγ2 and C/EBPα. Diabetic levels were expressed relative to controls for the corresponding genotype. Bars represent mean ± standard error of diabetic wild type (gray bars) and diabetic *C/EBPβ*$^{-/-}$ (white bars) bone. *$p<0.05$ compared to genotype-matched control by student's t-test. $N \geq 5$ per condition.

Next, we examined bone density parameters in the tibia of these mice to determine if C/EBPβ-deficiency had an impact on the diabetic bone phenotype. We scanned tibias with a μCT and examined the trabecular bone immediately distal to the proximal growth plate (Table 5 and Figure 22A). Control C/EBPβ KO mice had significantly lower BMC, BMD, BVF, and Tb.N. than control wild type mice, similar to recent findings (7, 44). Diabetes caused trabecular bone loss in both wild type and KO mice. Specifically, trabecular BMC, BMD, BVF and Tb.Th. were lower (Table 5). Thus, diabetic bone loss was not prevented by C/EBPβ-deficiency. The amount of loss, however, was greater in diabetic *C/EBPβ*$^{-/-}$ mice compared to diabetic wild type mice. Specifically, BMD was further decreased (a reduction of 66 mg/cc versus 39 mg/cc, 31% versus 15% in KO versus wild type mice, respectively). Diabetes also caused BMC to be reduced 31% in KO and only 15% in wild type mice. BVF loss was 48% in diabetic KO mice, while only 22% in diabetic wild type mice (Table 5, Figure 22A and 22B). Trabecular thickness decreased 38% in diabetic KO mice versus 20% in diabetic wild type mice. Trabecular spacing trended to be higher ($p<0.1$) in the diabetic KO mice, but it did not change in the diabetic wild type mice. Similarly, although trabecular number was unchanged in the diabetic wild type mice compared to control wild type mice, it was significantly lower (27% decrease) in the diabetic KO mice compared to control KO mice (Table 5).

Table 5. Trabecular bone μCT measurements from the tibia of 28 day diabetic and untreated wild type and C/EBPβ$^{-/-}$ mice.

	wild type		C/EBPβ$^{-/-}$	
	Control (n=5)	Diabetic (n=9)	Control (n=9)	Diabetic (n=12)
BMC (mg)	0.75 ± 0.04	0.64 ± 0.02*	0.62 ± 0.03^	0.43 ± 0.03*^
BMD (mg/cc)	251 ± 12	212 ± 8*	214 ± 11^	148 ± 10*^
BVF (%)	37 ± 3	29 ± 2*	27 ± 3^	14 ± 2*^
Tb.Th. (μm)	65 ± 5	52 ± 2*	58 ± 7	36 ± 2*^
Tb.Sp. (μm)	174 ± 16	204 ± 31	298 ± 33^	369 ± 25^{a}^
Tb.N.	6.4 ± 0.2	6.0 ± 0.3	5.2 ± 0.3^	3.8 ± 0.3*^

Abbreviations: BMC, bone mineral content; BMD, bone mineral density; BVF, bone volume fraction; Tb, trabecular; Th, thickness; Sp, spacing; N, number.

*$p < 0.05$ compared to genotype-matched control.

^$p < 0.05$ compared to treatment-matched wild type.

$^{a}p < 0.1$ compared to genotype-matched control.

Figure 22. **Absence of C/EBPβ exacerbated T1-diabetic bone loss without altering osteocalcin expression.** A: Representative 3-dimensional isosurface μCT images were taken in a cylindrical region of interest (1 mm diameter x 1 mm length) immediately distal to the proximal growth plate of the tibia. B: Bone volume fraction was measured by μCT in fixed tibias immediately distal to the proximal growth plate. C: mRNA was extracted from frozen tibias and was made into cDNA with a reverse transcriptase reaction. cDNA was amplified by RT-PCR with primers specific to osteocalcin (an osteoblast marker) and values expressed relative to HPRT, a housekeeping gene control. Bars represent mean ± standard error of control (C, white bars), diabetic (D, gray bars) wild type and *C/EBPβ*$^{-/-}$ mice. *$p<0.05$ by student's t-test. $N \geq 5$ per condition.

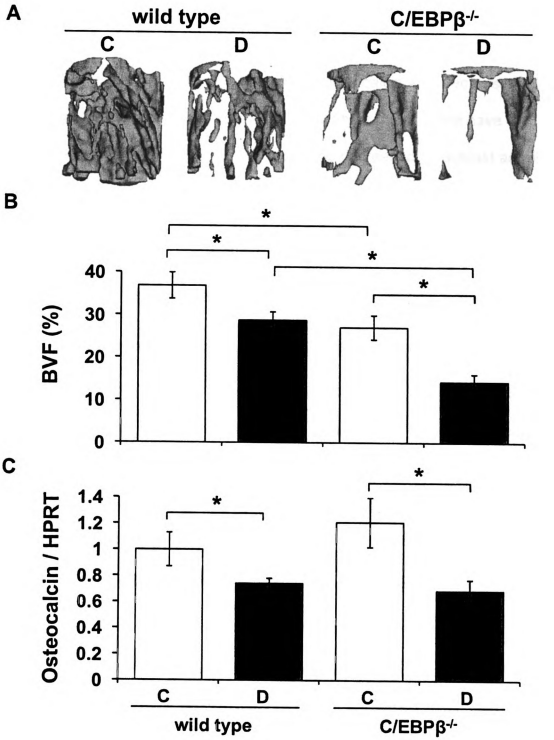
A
wild type
C/EBPβ-/-
C
D
C
D
B
BVF (%)
40
30
20
10
0
*
*
*
*
C
Osteocalcin / HPRT
1.4
1.2
1
0.8
0.6
0.4
0.2
0
*
*
C
D
C
D
wild type
C/EBPβ-/-

To determine if C/EBPβ deficiency affects diabetes-induced changes in osteoblast and osteoclast gene markers, we examined expression of osteocalcin and TRAP5, respectively. Tibia expression of osteocalcin was decreased 26% in diabetic wild type mice compared to control wild type mice, as we have demonstrated previously (16, 38, 40), indicating decreased osteoblast activity with diabetes (Figure 22C). Although control *C/EBPβ*$^{-/-}$ mice had less bone than control wild type mice, osteocalcin expression was unchanged. Diabetic *C/EBPβ*$^{-/-}$ mice also had a decrease in osteocalcin expression (43%) compared to control *C/EBPβ*$^{-/-}$ mice, however diabetic KO mice levels were not significantly lower than those of diabetic wild type mice. Since knockout of C/EBPβ did not alter diabetic changes in osteocalcin expression, we examined osteoclast parameters to determine if resorption was increased. Tibia RNA levels of TRAP5 and cathepsin K, markers of osteoclast activity, were unchanged in diabetic wild type mice compared to wild type controls (Figure 23A), which is similar to our previous findings (16, 40). TRAP5 expression was 1.5-fold higher in control *C/EBPβ*$^{-/-}$ mice compared to wild type controls (while cathepsin K expression was unchanged), indicating a potential role for increased resorption in *C/EBPβ*$^{-/-}$ bone. Similar to wild type mice, TRAP5 expression was unchanged but trended to decrease ($p = 0.07$) in diabetic KO bone. In contrast, cathepsin K mRNA was elevated 2-fold in diabetic KO mice compared to control KO mice. In order to account for the enhanced bone loss and clarify the status of bone resorption in

the diabetic KO mice, acid phosphatase-positive osteoclasts were measured (Figure 23B). We determined that osteoclast surface area (when expressed as a percent of total surface area) was 73% higher in diabetic KO mice than control KO mice. This is consistent with elevated cathepsin K mRNA levels and thus we concluded that the enhanced bone loss in diabetic *C/EBPβ*$^{-/-}$ mice is likely due to increased resorption.

Figure 23. **C/EBPβ knockout causes increased bone resorption in type 1 diabetes.** A: mRNA was extracted from frozen tibias and was made into cDNA with a reverse transcriptase reaction. cDNA was amplified by RT-PCR with primers specific to TRAP5 and cathepsin K (osteoclast markers) and expressed relative to HPRT, a housekeeping gene control. B: Decalcified tibia sections were stained for TRAP activity in order to identify osteoclasts. Trabecular bone surface in contact with osteoclasts was measured and expressed relative to the total bone surface examined. Bars represent mean ± standard error of control (C, white bars), diabetic (D, gray bars) wild type and *C/EBPβ*$^{-/-}$ mice. *$p<0.05$ by student's t-test. N ≥ 5 per condition.

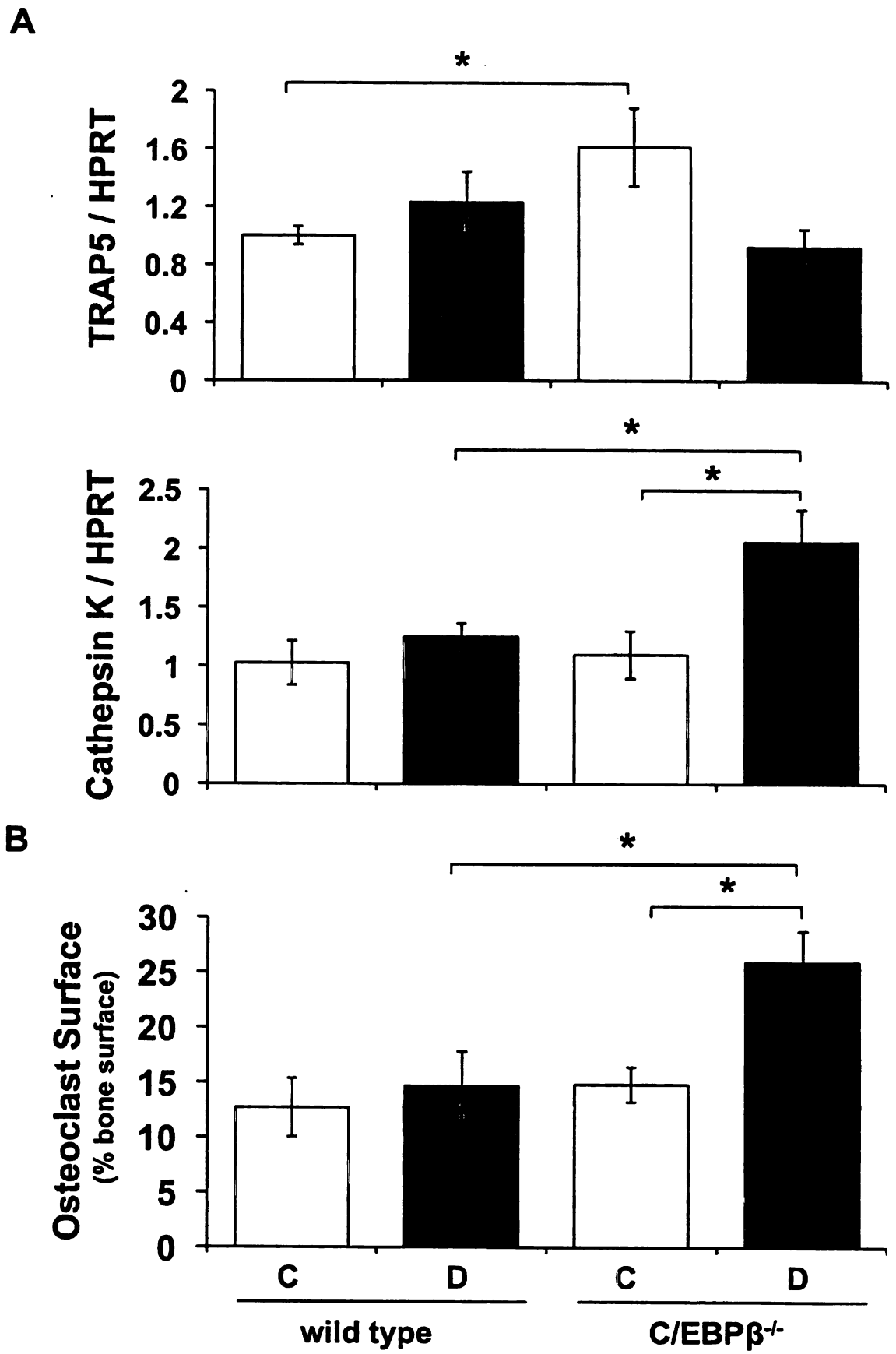
A
TRAP5 / HPRT
2
1.6
1.2
0.8
0.4
0
*
Cathepsin K / HPRT
2.5
2
1.5
1
0.5
0
*
*
B
Osteoclast Surface
(% bone surface)
30
25
20
15
10
5
0
*
*
C
D
C
D
wild type
C/EBPβ-/-

4.5. DISCUSSION

T1-diabetes results in decreased bone formation and increased marrow adiposity, which could be caused by mesenchymal stem cell lineage selection preference for the adipocyte rather than the osteoblast lineage (16, 45). The initial aim of this study was to determine if absence of C/EBPβ could prevent the altered lineage selection, thus preventing T1-diabetic bone marrow adipocyte accumulation and bone loss. Rather, we found the opposite effect: *C/EBPβ*$^{-/-}$ mice have enhanced bone marrow adiposity and bone loss in response to T1-diabetes.

Although many studies have demonstrated the importance of C/EBPβ for adipocyte differentiation *in vitro* (1, 2, 4, 5), and have demonstrated reduced *in vivo* peripheral adiposity in *C/EBPβ*$^{-/-}$ mice (6-8), bone marrow adiposity has not been extensively examined. Here, we find no significant change in marrow adipocyte numbers between wild type and *C/EBPβ*$^{-/-}$ mice (Figure 20), which is consistent with a recent study (44). Expression of the adipocyte marker, aP2, is slightly, but significantly, decreased in KO control mice compared to control wild type mice (Figure 20C). Contrary to our hypothesis, the loss of C/EBPβ enhanced T1-diabetic bone marrow adiposity (Figure 20). This could be explained by altered expression of other adipogenic transcription factors. We observed the maintenance of C/EBPδ expression in diabetic C/EBPβ KO mice

(Figure 21) and this may be sufficient for the modest increase in C/EBPα and PPARγ2 expression that we observed (Figure 21). C/EBPδ expression has previously been reported to be IFN-γ/LPS inducible in C/EBPβ KO, but not wild type, macrophages (46). We have previously reported inflammatory effects of T1-diabetes in bone (40). While most inflammatory effects were observed at diabetic onset, elevated IL-1α expression was observed at later times. IL-1 is known to stimulate C/EBPδ expression (47-51), as well as enhance its activity (52). As both C/EBPα (53) and PPARγ2 (54) transcription can be directly regulated through C/EBP transcription factors, a chain of events where IL-1 stimulates C/EBPδ expression and activity, which in turn stimulates C/EBPα and PPARγ2 expression to promote adipogenesis is plausible in the diabetic C/EBPβ KO animals.

Despite the enhanced marrow adiposity, C/EBPβ diabetic KO mice lost the same percentage of peripheral fat as diabetic wild types (Table 4). Bone marrow adipocytes and peripheral adipose depots often have reciprocal phenotypes. T1-diabetes generally induces a loss of peripheral and visceral fat, but this is accompanied by an increase of fat in the bone marrow (16). This reciprocal relationship between peripheral/visceral fat and marrow adiposity is also present in models of alcohol consumption (55) and aging (56). Here, however, the enhanced adiposity of the bone marrow in the diabetic knockout mice was not accompanied by enhanced peripheral fat loss, suggesting independent regulation of the two depots in the C/EBPβ KO mice. This idea is also supported by the fact that control C/EBPβ KO mice have less peripheral fat

with no significant change in bone marrow adiposity compared to their wild type counterparts. Perhaps under normal conditions, C/EBPβ plays an important role in adipose deposition in the periphery, but not in the marrow. In contrast, our study indicates that C/EBPβ is important in regulating diabetic marrow fat accumulation, while having no effect on diabetic peripheral fat loss.

It is important to address the fact that we do not observe elevated PPARγ2 expression in diabetic wild type bone compared to control wild type bone (Figure 21), as we have seen in our past studies (16). Despite this discrepancy in PPARγ2 expression, we do observe increased marrow adiposity and aP2 mRNA levels. It is possible that adiposity may be dependent upon the severity of diabetes-induction, which can vary between experiments using streptozotocin (43), and that more severe diabetes would produce detectable increases in PPARγ2 expression concurrent with aP2 and marrow adiposity.

Upon examination of the bone phenotype of C/EBPβ KO mice, we found that KO mice had significantly lower bone density. However, absence of C/EBPβ did not alter osteoblast parameters in control mice. This is consistent with a recent study indicating bone loss, but unchanged bone formation parameters (osteoblast surface and osteoblast number) in femurs of 12-week old *C/EBPβ*$^{-/-}$ mice compared to wild type littermates (44). However, another study found reduced mineral apposition rate (MAR) and bone formation rate/bone surface (BFR/BS) in 8-week old *C/EBPβ*$^{-/-}$ mice suggesting C/EBPβ-deficiency suppresses osteoblast function (57). As our study was started in mice that were 14-weeks old, this apparent discrepancy may be due to the age of the mice, with

C/EBPβ being an essential regulator of osteoblasts during development (57, 58), but not during adult remodeling (44). Our finding that diabetic suppression of osteocalcin expression is not altered in the knockout mice indicates that factors other than C/EBPβ alone are necessary for reduced osteoblast activity in T1-diabetes.

Because bone formation markers were unchanged by C/EBPβ-deficiency, we examined bone resorption parameters (TRAP5, cathepsin K and osteoclast surface). Recent studies have demonstrated that loss of C/EBPβ enhances osteoclast differentiation, likely through absence of LAP-induced suppression of MafB (57). That study demonstrated increased expression of TRAP5 and cathepsin K in *C/EBPβ*$^{-/-}$ osteoclasts *in vitro*, and increased TRAP staining *in vivo* (specifically, larger osteoclasts were observed, with no change in osteoclast number in 8-week old knockout mice) (57). Here, we demonstrate increased TRAP5 expression with C/EBPβ-deficiency *in vivo* (Figure 23A), however we did not observe any change in cathepsin K (Figure 23A), percentage osteoclast surface (Figure 23B), or in osteoclast number (not shown) in control KO bone compared to control wild type bone. Another study using 12-week old wild type and knockout mice had a similar result (no change in osteoclast parameters), but did not examine serum or RNA markers of resorption (44). Upon induction of diabetes, we observed no change in osteoclast parameters (TRAP5 and cathepsin K mRNA, percentage OC surface) in wild type mice (consistent with previous studies), but found increases in cathepsin K expression and in percentage OC surface in diabetic KO mice compared to control KO mice

(Figure 23). TRAP5 expression, however, tended to decrease, but this was not statistically significant. Taken together, our osteoclast data indicates that C/EBPβ may be preventing increased resorption from occurring in T1-diabetic wild type bone.

Because C/EBPβ-deficiency was unable to prevent diabetic adipocyte accumulation, we cannot draw conclusions from the present study as to whether altered lineage selection is indeed a mechanism of diabetic bone loss. Our previous studies that have prevented diabetic marrow adiposity, but not bone loss (with BADGE and leptin treatment), suggest altered lineage selection is not the only contributing factor to decreased osteoblast activity in diabetes (29, 38). Additionally, we found that more severe diabetes (induced by increased STZ dose) increases marrow adiposity, while leaving bone volume fraction unchanged (compared to normal STZ doses), which also suggests that the two may not be linked in T1-diabetes (43). Certainly, in this study, we did observe that more marrow adiposity was associated with more bone loss. However, our data suggest that the bone loss in the *C/EBPβ*$^{-/-}$ mice occurred through increased osteoclast activity, rather than suppressed bone formation. It is possible that the enhanced osteoclast activity is a direct result of the absence of C/EBPβ in osteoclasts, or that it is secondary to the increased marrow fat because adipocytes can secrete factors like TNF-α that induce osteoclastogenesis (59, 60).

In summary, we demonstrated that the absence of C/EBPβ enhanced the diabetic bone phenotype. Contrary to our original hypothesis, absence of C/EBPβ

actually enhanced diabetes-induced expression of PPARγ2 and C/EBPα, and subsequent marrow adiposity. However, unlike marrow fat, we have shown that diabetic peripheral fat changes are not dependent on C/EBPβ, which speaks to the complexity and location dependence of fat depots. Increased marrow adiposity was concurrent with reduced bone density, but osteoblast activity markers were not further suppressed. In fact, osteoclast activity was increased in diabetic C/EBPβ KO mice, which is contrary to the classic mechanism of bone loss from T1-diabetes. Our findings add to the work of others that recently have suggested a role for C/EBPβ in the inhibition of osteoclast differentiation. Finally, we conclude that C/EBPβ alone is not responsible for the bone versus fat phenotype switch observed in T1-diabetes, and that therapeutic treatments suppressing its levels may further bone loss by increasing bone resorption.

4.6. ACKNOWLEDGEMENTS

The authors thank Pete Johnson (NCI) for providing breeder *C/EBPβ*$^{-/-}$ mice, Sandra Haslam and Jeffery Leipprandt (MSU) for breeding, genotyping and backcrossing the *C/EBPβ*$^{-/-}$ mice into the BALB/c strain, Regina Irwin for technical expertise and critical review of the manuscript, and Lindsay Martin for critical review of the manuscript. This work was funded by grants from the National Institutes of Health (RO1DK061184) and the American Diabetes Association (7-07-RA-105) to LRM. The authors have no financial conflicts.

4.7. REFERENCES

1. **Darlington GJ, Ross SE, MacDougald OA** 1998 The role of C/EBP genes in adipocyte differentiation. J Biol Chem 273:30057-30060

2. **Cao Z, Umek RM, McKnight SL** 1991 Regulated expression of three C/EBP isoforms during adipose conversion of 3T3-L1 cells. Genes Dev 5:1538-1552

3. **Ramji DP, Foka P** 2002 CCAAT/enhancer-binding proteins: structure, function and regulation. Biochem J 365:561-575

4. **Yeh WC, Cao Z, Classon M, McKnight SL** 1995 Cascade regulation of terminal adipocyte differentiation by three members of the C/EBP family of leucine zipper proteins. Genes Dev 9:168-181

5. **Wu Z, Xie Y, Bucher NL, Farmer SR** 1995 Conditional ectopic expression of C/EBP beta in NIH-3T3 cells induces PPAR gamma and stimulates adipogenesis. Genes Dev 9:2350-2363

6. **Millward CA, Heaney JD, Sinasac DS, Chu EC, Bederman IR, Gilge DA, Previs SF, Croniger CM** 2007 Mice with a deletion in the gene for CCAAT/enhancer-binding protein beta are protected against diet-induced obesity. Diabetes 56:161-167

7. **Staiger J, Lueben MJ, Berrigan D, Malik R, Perkins SN, Hursting SD, Johnson PF** 2009 C/EBPbeta regulates body composition, energy balance-related hormones and tumor growth. Carcinogenesis 30:832-840

8. **Schroeder-Gloeckler JM, Rahman SM, Janssen RC, Qiao L, Shao J, Roper M, Fischer SJ, Lowe E, Orlicky DJ, McManaman JL, Palmer C, Gitomer WL, Huang W, O'Doherty RM, Becker TC, Klemm DJ, Jensen DR, Pulawa LK, Eckel RH, Friedman JE** 2007 CCAAT/enhancer-binding protein beta deletion reduces adiposity, hepatic steatosis, and diabetes in Lepr(db/db) mice. J Biol Chem 282:15717-15729

9. **Tanaka T, Yoshida N, Kishimoto T, Akira S** 1997 Defective adipocyte differentiation in mice lacking the C/EBPbeta and/or C/EBPdelta gene. EMBO J 16:7432-7443

10. **Gutierrez S, Javed A, Tennant DK, van Rees M, Montecino M, Stein GS, Stein JL, Lian JB** 2002 CCAAT/enhancer-binding proteins (C/EBP) beta and delta activate osteocalcin gene transcription and synergize with Runx2 at the C/EBP element to regulate bone-specific expression. J Biol Chem 277:1316-1323

11. **Harrison JR, Huang YF, Wilson KA, Kelly PL, Adams DJ, Gronowicz GA, Clark SH** 2005 Col1a1 promoter-targeted expression of p20 CCAAT enhancer-binding protein beta (C/EBPbeta), a truncated C/EBPbeta isoform, causes osteopenia in transgenic mice. J Biol Chem 280:8117-8124

12. **Levin ME, Boisseau VC, Avioli LV** 1976 Effects of diabetes mellitus on bone mass in juvenile and adult-onset diabetes. N Engl J Med 294:241-245

13. **Auwerx J, Dequeker J, Bouillon R, Geusens P, Nijs J** 1988 Mineral metabolism and bone mass at peripheral and axial skeleton in diabetes mellitus. Diabetes 37:8-12

14. **Kemink SA, Hermus AR, Swinkels LM, Lutterman JA, Smals AG** 2000 Osteopenia in insulin-dependent diabetes mellitus; prevalence and aspects of pathophysiology. J Endocrinol Invest 23:295-303

15. **Szkudelski T** 2001 The mechanism of alloxan and streptozotocin action in B cells of the rat pancreas. Physiol Res 50:537-546

16. **Botolin S, Faugere MC, Malluche H, Orth M, Meyer R, McCabe LR** 2005 Increased bone adiposity and peroxisomal proliferator-activated receptor-gamma2 expression in type I diabetic mice. Endocrinology 146:3622-3631

17. **Hamada Y, Kitazawa S, Kitazawa R, Fujii H, Kasuga M, Fukagawa M** 2007 Histomorphometric analysis of diabetic osteopenia in streptozotocin-induced diabetic mice: a possible role of oxidative stress. Bone 40:1408-1414

18. **Shires R, Teitelbaum SL, Bergfeld MA, Fallon MD, Slatopolsky E, Avioli LV** 1981 The effect of streptozotocin-induced chronic diabetes mellitus on bone and mineral homeostasis in the rat. J Lab Clin Med 97:231-240

19. **Krakauer JC, McKenna MJ, Buderer NF, Rao DS, Whitehouse FW, Parfitt AM** 1995 Bone loss and bone turnover in diabetes. Diabetes 44:775-782

20. **McCracken M, Lemons JE, Rahemtulla F, Prince CW, Feldman D** 2000 Bone response to titanium alloy implants placed in diabetic rats. Int J Oral Maxillofac Implants 15:345-354

21. **Shyng YC, Devlin H, Sloan P** 2001 The effect of streptozotocin-induced experimental diabetes mellitus on calvarial defect healing and bone turnover in the rat. Int J Oral Maxillofac Surg 30:70-74

22. **Botolin S, McCabe LR** 2007 Bone loss and increased bone adiposity in spontaneous and pharmacologically induced diabetic mice. Endocrinology 148:198-205

23. **Bouillon R, Bex M, Van Herck E, Laureys J, Dooms L, Lesaffre E, Ravussin E** 1995 Influence of age, sex, and insulin on osteoblast function: osteoblast dysfunction in diabetes mellitus. J Clin Endocrinol Metab 80:1194-1202

24. **Goodman WG, Hori MT** 1984 Diminished bone formation in experimental diabetes. Relationship to osteoid maturation and mineralization. Diabetes 33:825-831

25. **Martin LM, McCabe LR** 2007 Type I diabetic bone phenotype is location but not gender dependent. Histochem Cell Biol 128:125-133

26. **Nuttall ME, Patton AJ, Olivera DL, Nadeau DP, Gowen M** 1998 Human trabecular bone cells are able to express both osteoblastic and adipocytic phenotype: implications for osteopenic disorders. J Bone Miner Res 13:371-382

27. **Verma S, Rajaratnam JH, Denton J, Hoyland JA, Byers RJ** 2002 Adipocytic proportion of bone marrow is inversely related to bone formation in osteoporosis. J Clin Pathol 55:693-698

28. **Ahdjoudj S, Lasmoles F, Holy X, Zerath E, Marie PJ** 2002 Transforming growth factor beta2 inhibits adipocyte differentiation induced by skeletal unloading in rat bone marrow stroma. J Bone Miner Res 17:668-677

29. **Botolin S, McCabe LR** 2006 Inhibition of PPARgamma prevents type I diabetic bone marrow adiposity but not bone loss. J Cell Physiol 209:967-976

30. **Sterneck E, Tessarollo L, Johnson PF** 1997 An essential role for C/EBPbeta in female reproduction. Genes Dev 11:2153-2162

31. **Vengellur A, LaPres JJ** 2004 The role of hypoxia inducible factor 1alpha in cobalt chloride induced cell death in mouse embryonic fibroblasts. Toxicol Sci 82:638-646

32. **Phan J, Peterfy M, Reue K** 2004 Lipin expression preceding peroxisome proliferator-activated receptor-gamma is critical for adipogenesis in vivo and in vitro. J Biol Chem 279:29558-29564

33. **Li J, Takaishi K, Cook W, McCorkle SK, Unger RH** 2003 Insig-1 "brakes" lipogenesis in adipocytes and inhibits differentiation of preadipocytes. Proc Natl Acad Sci U S A 100:9476-9481

34. **Kast-Woelbern HR, Dana SL, Cesario RM, Sun L, de Grandpre LY, Brooks ME, Osburn DL, Reifel-Miller A, Klausing K, Leibowitz MD** 2004 Rosiglitazone induction of Insig-1 in white adipose tissue reveals a novel interplay of peroxisome proliferator-activated receptor gamma and sterol regulatory element-binding protein in the regulation of adipogenesis. J Biol Chem 279:23908-23915

35. **Ontiveros C, McCabe LR** 2003 Simulated microgravity suppresses osteoblast phenotype, Runx2 levels and AP-1 transactivation. J Cell Biochem 88:427-437

36. **Wiren KM, Zhang XW, Toombs AR, Kasparcova V, Gentile MA, Harada S, Jepsen KJ** 2004 Targeted overexpression of androgen receptor in osteoblasts: unexpected complex bone phenotype in growing animals. Endocrinology 145:3507-3522

37. **Yoshimatsu M, Shibata Y, Kitaura H, Chang X, Moriishi T, Hashimoto F, Yoshida N, Yamaguchi A** 2006 Experimental model of tooth movement by orthodontic force in mice and its application to tumor necrosis factor receptor-deficient mice. J Bone Miner Metab 24:20-27

38. **Motyl KJ, McCabe LR** 2009 Leptin treatment prevents type I diabetic marrow adiposity but not bone loss in mice. J Cell Physiol 218:376-384

39. **Fowlkes JL, Bunn RC, Liu L, Wahl EC, Coleman HN, Cockrell GE, Perrien DS, Lumpkin CK, Jr., Thrailkill KM** 2008 Runt-related transcription factor 2 (RUNX2) and RUNX2-related osteogenic genes are down-regulated throughout osteogenesis in type 1 diabetes mellitus. Endocrinology 149:1697-1704

40. **Motyl KJ, Botolin S, Irwin R, Appledorn DM, Kadakia T, Amalfitano A, Schwartz RC, McCabe LR** 2009 Bone inflammation and altered gene expression with type I diabetes early onset. J Cell Physiol 218:575-583

41. **Lane MD, Tang QQ, Jiang MS** 1999 Role of the CCAAT enhancer binding proteins (C/EBPs) in adipocyte differentiation. Biochem Biophys Res Commun 266:677-683

42. **Liu S, Croniger C, Arizmendi C, Harada-Shiba M, Ren J, Poli V, Hanson RW, Friedman JE** 1999 Hypoglycemia and impaired hepatic glucose production in mice with a deletion of the C/EBPbeta gene. J Clin Invest 103:207-213

43. **Motyl K, McCabe LR** 2009 Streptozotocin, Type I Diabetes Severity and Bone. Biol Proced Online

44. **Zanotti S, Stadmeyer L, Smerdel-Ramoya A, Durant D, Canalis E** 2009 Misexpression of CCAAT/enhancer binding protein beta causes osteopenia. J Endocrinol 201:263-274

45. **McCabe LR** 2007 Understanding the pathology and mechanisms of type I diabetic bone loss. J Cell Biochem 102:1343-1357

46. **Gorgoni B, Maritano D, Marthyn P, Righi M, Poli V** 2002 C/EBP beta gene inactivation causes both impaired and enhanced gene expression and inverse regulation of IL-12 p40 and p35 mRNAs in macrophages. J Immunol 168:4055-4062

47. **Massaad C, Paradon M, Jacques C, Salvat C, Bereziat G, Berenbaum F, Olivier JL** 2000 Induction of secreted type IIA phospholipase A2 gene

transcription by interleukin-1beta. Role of C/EBP factors. J Biol Chem 275:22686-22694

48. **Akira S, Isshiki H, Sugita T, Tanabe O, Kinoshita S, Nishio Y, Nakajima T, Hirano T, Kishimoto T** 1990 A nuclear factor for IL-6 expression (NF-IL6) is a member of a C/EBP family. EMBO J 9:1897-1906

49. **Harrison JR, Kelly PL, Pilbeam CC** 2000 Involvement of CCAAT enhancer binding protein transcription factors in the regulation of prostaglandin G/H synthase 2 expression by interleukin-1 in osteoblastic MC3T3-E1 cells. J Bone Miner Res 15:1138-1146

50. **Tengku-Muhammad TS, Hughes TR, Ranki H, Cryer A, Ramji DP** 2000 Differential regulation of macrophage CCAAT-enhancer binding protein isoforms by lipopolysaccharide and cytokines. Cytokine 12:1430-1436

51. **Greenwel P, Tanaka S, Penkov D, Zhang W, Olive M, Moll J, Vinson C, Di Liberto M, Ramirez F** 2000 Tumor necrosis factor alpha inhibits type I collagen synthesis through repressive CCAAT/enhancer-binding proteins. Mol Cell Biol 20:912-918

52. **Svotelis A, Doyon G, Bernatchez G, Desilets A, Rivard N, Asselin C** 2005 IL-1 beta-dependent regulation of C/EBP delta transcriptional activity. Biochem Biophys Res Commun 328:461-470

53. **Legraverend C, Antonson P, Flodby P, Xanthopoulos KG** 1993 High level activity of the mouse CCAAT/enhancer binding protein (C/EBP alpha) gene promoter involves autoregulation and several ubiquitous transcription factors. Nucleic Acids Res 21:1735-1742

54. **Clarke SL, Robinson CE, Gimble JM** 1997 CAAT/enhancer binding proteins directly modulate transcription from the peroxisome proliferator-activated receptor gamma 2 promoter. Biochem Biophys Res Commun 240:99-103

55. **Maddalozzo GF, Turner RT, Edwards CH, Howe KS, Widrick JJ, Rosen CJ, Iwaniec UT** 2009 Alcohol alters whole body composition, inhibits bone formation, and increases bone marrow adiposity in rats. Osteoporos Int

56. **Kirkland JL, Tchkonia T, Pirtskhalava T, Han J, Karagiannides I** 2002 Adipogenesis and aging: does aging make fat go MAD? Exp Gerontol 37:757-767

57. **Smink JJ, Begay V, Schoenmaker T, Sterneck E, de Vries TJ, Leutz A** 2009 Transcription factor C/EBPbeta isoform ratio regulates osteoclastogenesis through MafB. EMBO J 28:1769-1781

58. **Tominaga H, Maeda S, Hayashi M, Takeda S, Akira S, Komiya S, Nakamura T, Akiyama H, Imamura T** 2008 CCAAT/enhancer-binding protein beta promotes osteoblast differentiation by enhancing Runx2 activity with ATF4. Mol Biol Cell 19:5373-5386

59. **Xu J, Wu HF, Ang ES, Yip K, Woloszyn M, Zheng MH, Tan RX** 2009 NF-kappaB modulators in osteolytic bone diseases. Cytokine Growth Factor Rev 20:7-17

60. **Cawthorn WP, Sethi JK** 2008 TNF-alpha and adipocyte biology. FEBS Lett 582:117-131

CHAPTER 5

5. MICE WITH OVEREXPRESSION OF WNT10B ARE RESISTANT TO BONE LOSS BUT NOT MARROW ADIPOSITY FROM TYPE 1 DIABETES

5.1. ABSTRACT

Osteoporosis is a severe complication of type 1 diabetes, leaving patients and at risk for fracture and impaired bone healing. Bone loss from diabetes is primarily due to an osteoblast defect with no change or reduced osteoclast activity, and is accompanied by increased marrow fat. Increased osteoblast apoptosis and/or reduced osteoblast differentiation and maturation are likely involved in the diabetic bone pathology. Reduced osteoblast differentiation may be coupled to increased marrow adiposity because osteoblasts and adipocytes arise from the same precursor: mesenchymal stem cells. Wnt/β-catenin signaling is a potent regulator of lineage selection: it induces osteoblast differentiation and prevents adipocyte differentiation. Here, we examined bone expression levels of Wnt10b, which causes increased bone mass when overexpressed and reduced bone mass when deleted. We found that in diabetes and leptin treatment (which also causes bone loss itself and does not prevent diabetic bone loss) Wnt10b levels were suppressed. Alternately, PTH treatment, which increases bone formation (even in diabetic animals) promoted Wnt10b expression. We therefore examined the ability of overexpression of Wnt10b itself to prevent diabetic bone

changes. Interestingly, overexpression of Wnt10b in osteoblasts (from the osteocalcin promoter, OC-Wnt10b) prevented femur trabecular bone density changes induced by diabetes, suggesting lower Wnt10b in diabetic bone levels may be responsible for diabetic osteoporosis. However, diabetic OC-Wnt10b mice were not protected from diabetic marrow adiposity, which could be due to the localization of Wnt10b even though it is a secreted protein. Despite the prevention of bone loss, we still observed suppressed osteoblast markers (serum and mRNA) in the diabetic OC-Wnt10b mice compared to untreated OC-Wnt10b mice. This suggests that bone loss may still occur in the OC-Wnt10b mice but at a much slower rate that was not detectable after 40 days. Nonetheless, we advocate that agonizing the Wnt10b/β-catenin signaling pathway is a worthwhile therapeutic target for osteoporosis from type 1 diabetes.

5.2. INTRODUCTION

Type 1 diabetes (T1-diabetes) is a chronic condition in which the pancreas ceases to produce insulin, and the resulting hyperglycemia must be controlled with insulin injections. Despite well-controlled blood glucose (as determined by glycated hemoglobin levels, Hb_{A1C}), many patients do have complications from T1-diabetes, including osteoporosis. Young people diagnosed with T1-diabetes have reduced growth, which correlates with the level of glycemic control (1, 2). In addition to affecting adolescents, diabetes can cause bone loss at all stages of life, leaving patients at greater risk for bone loss, fracture and impaired fracture

healing (3-5). Serum osteocalcin, a marker of bone formation (osteoblast activity) is significantly reduced in diabetic patients of all ages (6). Additionally, diabetic patients have unchanged or decreased markers of resorption, suggesting that increased osteoclast activity is not responsible for bone loss (7).

Rodent models of T1-diabetes have a bone phenotype similar to that of humans. One pharmacologic agent used to induce diabetes in mice is streptozotocin (STZ). STZ is a glucose mimetic that diffuses into insulin secreting pancreatic β-cells through the non-insulin responsive glucose transporter GLUT2 (8). The effects of STZ include DNA damage and subsequent β-cell death (8). In both STZ-mice and rats, T1-diabetes causes bone loss and impaired bone healing (9-15). Non-obese diabetic (NOD) mice are susceptible to development of autoimmune T1-diabetes and display a similar bone phenotype to that of STZ-diabetic mice (16). Spontaneously diabetic BioBreeding (BB) rats also have bone loss due to decreased bone turnover (17, 18).

In addition to reduced bone formation and unchanged or reduced resorption in type 1 diabetic bone, STZ and NOD mice have an obvious increase in bone marrow adipocyte number (9, 16, 19-23). STZ mice have increased expression of peroxisome proliferator-activated receptor gamma (PPARγ) 2 in bone, a transcription factor important for adipocyte maturation (9). Because adipocytes are derived from the same stem cells that give rise to osteoblasts, the increased marrow adiposity suggests that differentiation of MSCs may be shunted away from the osteoblast lineage and toward the adipocyte lineage under diabetic conditions (9). It is also possible that adipocytes secrete factors

(i.e. tumor necrosis factor alpha (TNFα)) into the marrow microenvironment that reduce osteoblast differentiation or increase osteoblast apoptosis. Similarly, high marrow fat has been demonstrated in bone loss models of aging (24, 25) and unloading (26).

Several factors regulate both osteoblast and adipocyte lineage selection and could be involved in diabetic bone loss. We have demonstrated, however, that inhibition of PPARγ with bisphenol-A-diglycidyl ether (BADGE) in control and diabetic mice reduced diabetic marrow adiposity but did not prevent reduced bone formation (osteocalcin and runx2 expression) or reduced bone density from T1-diabetes (19). We have also prevented diabetic marrow adiposity with leptin treatment, but did not prevent bone loss (22). Both of these studies suggest that mature adipocytes in the bone marrow are not responsible for diabetic bone loss. It remains plausible, however, that lineage selection still favors the adipocyte lineage in these experiments, but that BADGE and leptin prevent maturation. Therefore, examining the effect of other osteoblast/adipocyte lineage regulators may provide insight into the mechanism of the diabetic bone phenotype.

Wnt/β-catenin signaling through TCF/LEF-induced transcription is a potent regulator of both bone formation and adipocyte differentiation (27, 28). Wnts are secreted ligands that bind low density lipoprotein receptor-related protein 5/6 (LRP5/6) and frizzled (Fzd) membrane receptors. Dimerization of the LRP and Fzd receptors in response to wnts initializes a signaling cascade that inhibits glycogen synthase kinase 3 beta (GSK3β). Without the wnt signal (or in the presence of endogenous pathway inhibitors such as dickkopf (Dkk) proteins),

GSK3β actively phosphorylates cytoplasmic β-catenin, targeting it for degradation. When GSK3β is inactive (as in the presence of a wnt ligand), transcriptionally active β-catenin (dephosphorylated on serine (Ser) 37 or threonine (Thr) 41) accumulates in the cytoplasm and translocates to the nucleus where it initiates transcription of genes with TCF/LEF binding sites, such as *Runx2* (29-31).

Mice null for LRP5 have low bone density and blindness, consistent with the rare recessive disorder, osteoporosis-pseudoglioma syndrome (OPPG), while gain of function of LRP5 results in high bone mass due to increased osteoblast activity (32-37). Although complete loss of function of LRP6 is fatal, loss of one allele causes more bone loss in mice deficient in LRP5 by exacerbating reduced bone formation (38). Similarly, modulation of Wnt10b affects only bone formation, not resorption (39). Wnt10b knockout (-KO) mice have low bone density while mice with overexpression of Wnt10b from the aP2 promoter have high bone density and low marrow adiposity (39). These mice also have attenuated bone loss from aging and ovariectomy (39). *In vitro* activation and inhibition of wnt signaling results in inhibition and activation of adipogenesis, respectively (40, 41), through regulation of expression of PPARγ and C/EBPα (42, 43). Wnt1, 5a and 7b have also been shown to promote osteoblast and/or suppress adipocyte differentiation (38). Endogenous agonists and antagonists can further regulate wnt signaling. Dally protein enhances the interaction between wnts and Fzds, while Dkks and secreted frizzled-related proteins (sFRP) antagonize it. Additionally, sclerostin, prevents the Fzd-LRP interaction. Targeted inhibition of

wnt agonists and antagonists is a relatively new and promising area of interest for treatment of osteosclerotic and osteoporotic diseases, respectively (28).

We therefore examined wnt pathway family member changes in diabetic bone and found that Wnt10b mRNA levels were significantly decreased. Because Wnt10b strongly promotes bone formation and inhibits adipogenesis (39, 44, 45), we also examined its levels with leptin treatment (which causes bone loss and prevents diabetic marrow adiposity) and PTH treatment (which promotes bone formation, but does not alter marrow adiposity in control or diabetic mice) (22)(Motyl, et al., *in preparation,* See Chapter 6). Consistent with the known effects of Wnt10b on bone density, we found mRNA levels decreased with leptin treatment and increased with PTH treatment (46). Therefore, we examined the effect of overexpression of Wnt10b itself on diabetic bone loss and marrow adiposity. Briefly, we determined that Wnt10b prevented trabecular bone phenotype changes in diabetes, but did not prevent the reduction of serum or mRNA osteoblast markers, suggesting bone loss may still occur, albeit at a slower rate. Consistent with previous reports, we found no changes in osteoclast surface measurements in any of the treatment groups. Interestingly, Wnt10b did not prevent adipocyte accumulation in the diabetic bone marrow. We concluded that because of the ability of Wnt10b to retard diabetic bone loss, Wnt10b/β-catenin signaling should be further explored as a therapeutic target for patients with T1-diabetic osteoporosis.

5.3. MATERIALS AND METHODS

5.3.1. Leptin and PTH treatment

All animal procedures were performed in accordance with Michigan State University Institutional Animal Care and Use Committee. Leptin treatment was performed as described previously (22). Briefly, 14-week old BALB/c mice (Harlan Sprague Dawley,Indianapolis, IN) were anesthetized with isofluorane and implanted subcutaneously with Alzet mini-osmotic pumps (model 2004, Durect Corporation, Cupertino, CA) that contained either 0.9% sterile saline vehicle or 1.3 mg/ml leptin (Amylin, San Diego, CA). Osmotic pumps delivered 6.6 mg leptin per mouse per day. Wounds were closed with staples and mice were given a one-time injection of 0.15 mg carprofen (Pfizer, New York, NY). Mice were harvested after 28 days.

Parathyroid hormone (PTH(1-34)) (Bachem, Torrance, CA) was stored in glass vials topped with argon gas (to prevent oxidation) at -80 °C as a 10^{-4} M stock in 4 mM HCl supplemented with 0.1% bovine serum albumin. PTH did not go through more than one freeze/thaw cycle. Immediately before injection, PTH was made up to 100 μl per mouse with ice cold 0.9% saline. At 14 weeks of age, BALB/c mice (Harlan Sprague Dawley,Indianapolis, IN) were subjected to daily subcutaneous injections of either 40 μg/kg PTH or an equivalent volume of saline vehicle. Mice were harvested after 40 days.

5.3.2. OC-Wnt10b mice and diabetes induction

C57BL/6 breeder mice with transgenic overexpression of Wnt10b from the osteocalcin promoter (OC-Wnt10b) were obtained from Ormond A. MacDougald (University of Michigan, Ann Arbor, MI) (44). Heterozygous transgenic mice were bred at Michigan State University with wild type C57BL/6J mice (Jackson Laboratories, Bar Harbor, ME). Mice were genotyped with genomic DNA isolated from an ear punch (DNAeasy Kit, Qiagen, Valencia, CA). DNA was amplified by real-time PCR with iQ SYBR Green Supermix (Biorad, Hercules, CA) and primers specific to the transgene synthesized by Integrated DNA Technologies (Coralville, IA) (44). All mice were maintained on a 12-hour light, 12-hour dark cycle at 23 °C, were given standard lab chow, and had food and water *ad libitum*. Diabetes was induced in female mice only, which have a diabetic bone phenotype similar to males (23) and at the age we are interested in, OC-Wnt10b mice have higher bone density (not shown). At 14 weeks of age, female wild type and transgenic mice were treated with either 50 mg/kg streptozotocin (to induce diabetes) or 0.1 M citrate buffer pH 4.5 vehicle (control) for five consecutive days. Diabetes was confirmed 12 days after the first injection (dpi, days post injection) with an AccuChek compact glucometer (Roche, Nutley, NJ) and a drop of blood collected from the saphenous vein. Blood glucose over 300 mg/dl was considered diabetic. Mice were harvested 4 weeks after diabetes was confirmed (at 40 dpi). Soft tissues were immediately weighed.

5.3.3. Micro-computed tomography (μCT) analyses

Bones were fixed in 10% formalin and transferred to 70% ethanol after 24 hours. Fixed femurs and tibias were scanned using a GE Explore Locus μCT system at a voxel resolution of 20 μm obtained from 720 views. Beam angle of increment was 0.5 and beam strength was set at 80 peak kV and 450 μA. Each run included bones from each treatment group and a calibration phantom to standardize grayscale values and maintain consistency. Based on autothreshold and isosurface analyses of multiple bone samples, a fixed threshold (800) was used to separate bone from bone marrow. Femur trabecular bone analyses were performed in a region of trabecular bone defined at 0.17 mm proximal to the growth plate of the distal femur extending 2 mm toward the diaphysis, and excluding the outer cortical shell. Tibia trabecular bone analyses were performed in a region of trabecular bone defined at 0.17 mm distal to the growth plate of the proximal tibia extending 2 mm toward the diaphysis, and excluding the outer cortical shell. Trabecular bone mineral content (BMC), bone mineral density (BMD), bone volume fraction (BVF), thickness (Tb Th), spacing (Tb Sp) and number (Tb N) values were computed by a GE Healthcare MicroView software application for visualization and analysis of volumetric image data. Trabecular isosurface images were taken from a cylindrical region in the tibia or femur where analyses were performed measuring 1.0 mm in length and 1.0 mm in diameter.

5.3.4. RNA analyses

Tibias were cleaned of muscle and connective tissue, snap frozen in liquid nitrogen and stored at -80°C. Frozen tibias were crushed under liquid nitrogen conditions with a Bessman Tissue Pulverizer (Spectrum Laboratories, Inc., Rancho Dominguez, CA). RNA was isolated with Tri Reagent (Molecular Research Center, Inc., Cincinnati, OH) and integrity was assessed by formaldehyde-agarose gel electrophoresis. cDNA was synthesized by reverse transcription with Superscript II Reverse Transcriptase Kit and oligo $dT_{(12-18)}$ primers (Invitrogen, Carlsbad, CA) and amplified by real-time PCR with iQ SYBR Green Supermix (Biorad, Hercules, CA) and gene-specific primers synthesized by Integrated DNA Technologies (Coralville, IA). Hypoxanthine guanine phosphoribosyl transferase (HPRT) mRNA levels do not fluctuate in diabetes, PTH treatment, leptin treatment, or overexpression of Wnt10b and were used as an internal control. HPRT was amplified using 5'-AAG CCT AAG ATG AGC GCA AG-3' and 5'-TTA CTA GGC AGA TGG CCA CA-3' (47). Wnt10b was amplified using 5'-TCT CTT TCA GCC CTT TGC TCG GAT-3' and 5'-ACA ACT GAA CGG AAG GAG AAG CCT-3' (48). Osteocalcin was amplified using 5'-ACG GTA TCA CTA TTT AGG ACC TGT G-3' and 5'-ACT TTA TTT TGG AGC TGC TGT GAC-3' (49). Runx2 was amplified using 5'-GAC AGA AGC TTG ATG ACT CTA AAC C-3' and 5'-TCT GTA ATC TGA CTC TGT CCT TGT G-3' (50). aP2 was amplified using 5'-GCG TGG AAT TCG ATG AAA TCA-3' and 5'-CCC GCC ATC TAG GGT TAT GA-3' (51). PPARγ2 was amplified using 5'-TGA AAC TCT GGG AGA TTC TCC TG-3' and 5'-CCA TGG TAA TTT CTT GTG AAG TGC-3' (52). Real time PCR was carried out for 40 cycles using the iCycler (Bio-Rad) and data

were evaluated using the iCycler software. Each cycle consisted of 95°C for 15 s, 60°C for 30 s (except for osteocalcin and runx2 which had an annealing temperature of 65°C), and 72°C for 30 s. cDNA-free samples, a negative control, did not produce amplicons. Melting curve and gel analyses (sizing, isolation, and sequencing) were used to verify single products of the appropriate base pair size.

5.3.5. Serum measurements

Blood was obtained from mice at the time of euthanasia and blood serum prepared from each sample by centrifugation for 10 min at 4,000 rpm. Serum was aliquoted and stored frozen at -20°C and did not go through more than one freeze/thaw cycle. Serum osteocalcin levels were measured using Mouse Osteocalcin EIA Kit (Biomedical Technologies, Inc., Stoughton, MA) according to manufacturer instructions.

5.3.6. Bone histology and histomorphometry

Fixed femur samples were processed on an automated Thermo Electron Excelsior tissue processor for dehydration, clearing and infiltration using a routine overnight processing schedule. Samples were then embedded in Surgipath embedding paraffin on a Sakura Tissue Tek II embedding center. Paraffin blocks were sectioned at 5 μm on a Reichert Jung 2030 rotary microtome. Slides were stained for tartrate-resistant acid phosphatase (TRAP) activity and counter

stained with hematoxylin according to manufacturer protocol (387A-1KT, Sigma, St. Louis, MO). Osteoclast surface was measured and expressed as a percentage of total bone surface in the femur trabecular region ranging from the distal growth plate to 2 mm proximal. Visible adipocytes, greater than 30 μm were counted in the same area.

5.3.7. Statistical Analyses

All measurements are presented as mean ± standard error. Statistically significant ($\alpha = 0.05$) effects were determined with a student's t-test.

5.4. RESULTS

T1-diabetic bone loss is caused by reduced bone formation with unchanged or reduced resorption. Reduced osteoblast differentiation is accompanied by increased marrow adiposity, suggesting a role for altered lineage selection. We measured wnt signaling family members and found that Wnt10b, a known regulator of osteoblast and adipocyte differentiation, was significantly suppressed in diabetic bone (Figure 24A). As we have recently demonstrated, PTH treatment promotes bone formation in diabetes, but does not alter marrow adiposity. Consistent with recent findings (46), we found that PTH induced Wnt10b mRNA levels (Figure 24B). Additionally, we have shown that leptin treated mice have bone loss, but are protected from diabetic marrow

adiposity (22). Here, for the first time, we show that leptin treatment reduced bone expression of Wnt10b (Figure 24C).

Figure 24. **Wnt10b mimics bone volume fraction changes in diabetes and in PTH and leptin treatments.** (**A**) Mice were treated with either 50 mg/kg streptozotocin daily for 5 days to induce diabetes (D) or vehicle (control, C). N = 6-10. (**B**) Mice were treated with either daily subcutaneous injections of 40 μg/kg PTH (P) or vehicle (control, C) for 40 days. N = 8-14. (**C**) Mice were implanted with osmotic minipumps containing either leptin (L) or saline vehicle control (C) such that leptin-treated mice received 6.6 μg leptin per day. N = 6-8. Fixed femurs (**A**) or tibias (**B,C**) were analyzed by μCT in order to determine bone volume fraction (BVF) of the trabecular bone immediately proximal to the distal growth plate of the femur, or immediately distal to the proximal growth plate of the tibia. Representative three-dimensional images were taken from the same area as BVF measurements. mRNA from frozen tibias was converted to cDNA by reverse transcriptase reaction and amplified with primers specific for Wnt10b and HPRT, a non-modulated housekeeping gene control. Bars represent mean ± standard error. *$p < 0.05$ by student's t-test.

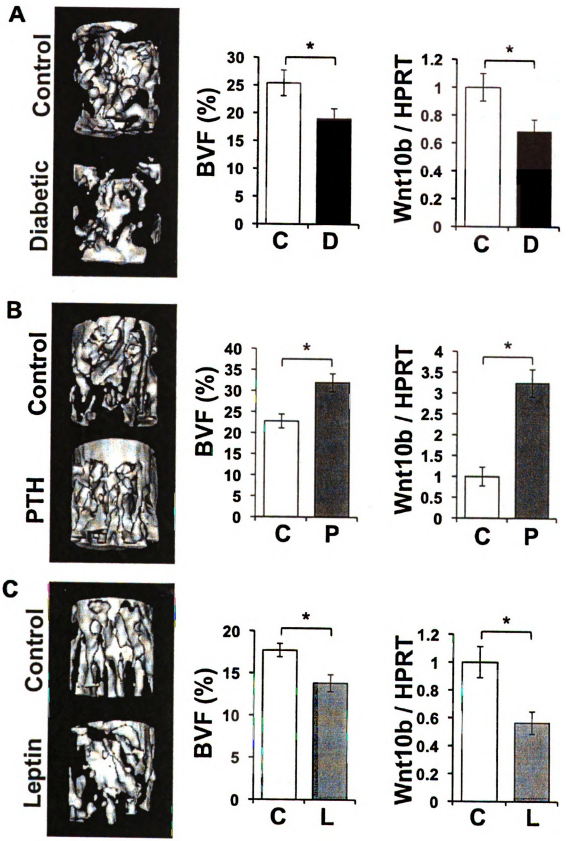
A
Control
Diabetic
BVF (%)
30
25
20
15
10
5
0
C
D
*
Wnt10b / HPRT
1.2
1
0.8
0.6
0.4
0.2
0
C
D
*
B
Control
PTH
BVF (%)
40
35
30
25
20
15
10
5
0
C
P
*
Wnt10b / HPRT
4
3.5
3
2.5
2
1.5
1
0.5
0
C
P
*
C
Control
Leptin
BVF (%)
20
15
10
5
0
C
L
*
Wnt10b / HPRT
1.2
1
0.8
0.6
0.4
0.2
0
C
L
*

Because we have found decreased Wnt10b levels in diabetes and in leptin treatment (which does not avert diabetic bone loss), and increased in PTH treatment (which promotes bone formation in diabetes) we wanted to determine whether overexpression of Wnt10b itself was sufficient to prevent diabetic bone loss and/or marrow adiposity. We bred mice with overexpression of Wnt10b from the osteocalcin promoter (OC-Wnt10b) (44), and determined bone density and Wnt10b expression levels in male and female, wild type and transgenic mice at 21 weeks of age, when we normally examine effects of diabetes one bone. At this age, the female OC-Wnt10b mice had higher trabecular bone parameters than males (not shown). We have previously shown that gender does not affect the diabetic bone phenotype (23), so we induced diabetes in only female OC-Wnt10b mice and wild type littermates.

Euglycemic wild type and OC-Wnt10b mice had similar blood glucose levels (Figure 25). Streptozotocin successfully induced diabetes in both genotypes, and glucose was not significantly different in diabetic OC-Wnt10b mice compared to diabetic wild type mice. Control OC-Wnt10b mice did not have significantly different body mass from wild type mice (Figure 25). We normally see significant weight loss in wild type mice after diabetes is induced, but in this case we did not. However, diabetes did induce significant weight loss in OC-Wnt10b transgenic mice. Consistent with no difference in body mass compared to wild type mice, OC-Wnt10b control mice did not have altered femoral fat pad or tibialis anterior muscle mass. Diabetic wild type mice did have significant fat and muscle mass loss compared to control wild type mice, as we and others

have demonstrated previously (9). OC-Wnt10b mice also had significant fat and muscle mass loss when made diabetic, and their levels did not differ from diabetic wild type mice. Mass changes in the visceral perirenal fat pad (not shown) mimicked those of the subcutaneous femoral fat pad.

We performed μCT analysis of trabecular bone immediately proximal to the distal growth plate of the femur (Figure 26, Table 6). As previously reported, control OC-Wnt10b mice had significantly elevated BMC, BMD, BVF, trabecular thickness, and trabecular number, and reduced trabecular spacing compared to control wild type mice (44). Consistent with the literature, diabetes induced a significant reduction in trabecular BMC, BMD, BVF, thickness and number, but had no statistically significant effect on trabecular spacing in wild type mice (9, 15). Interestingly, diabetes did not induce significant changes in any of the trabecular bone density parameters in OC-Wnt10b diabetic mice compared to OC-Wnt10b controls. Correspondingly, diabetic OC-Wnt10b mice had significantly higher BMC, BMD, BVF, trabecular thickness, and number, and lower trabecular spacing than diabetic wild type mice.

Figure 25. **Overexpression of Wnt10b did not prevent diabetes induction by streptozotocin.** Wild type (WT) and heterozygous OC-Wnt10b (TG) mice were treated with either streptozotocin to induce diabetes (D) or vehicle (control, C) and harvested at 40 dpi. Nonfasting blood glucose, body mass, femoral fat pad mass and tibialis anterior muscle mass were measured immediately. Bars represent mean ± standard error. N = 5-8 per group. *$p < 0.05$ by student's t-test.

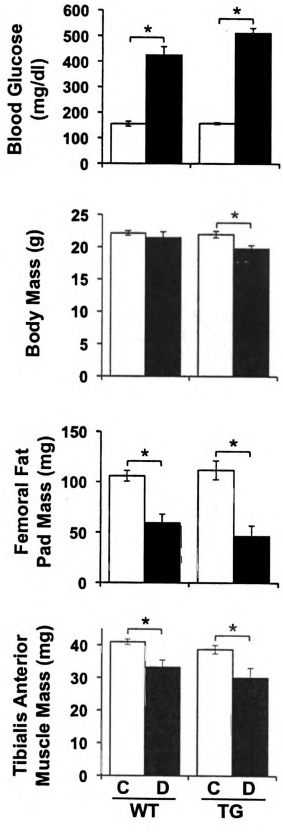
Blood Glucose (mg/dl)
600
500
400
300
200
100
0
*
*
Body Mass (g)
25
20
15
10
5
0
*
Femoral Fat Pad Mass (mg)
150
100
50
0
*
*
Tibialis Anterior Muscle Mass (mg)
40
30
20
10
0
*
*
C
D
C
D
WT
TG

Figure 26. **Mice with Wnt10b overexpression were protected from diabetes-induced trabecular bone loss.** Fixed femurs from control (C) and diabetic (D), wild type (WT) and OC-Wnt10b (TG) mice were analyzed by μCT. Representative three-dimensional images were taken from the volume of trabecular bone immediately proximal to the distal growth plate. Bone volume fraction (BVF) and bone mineral density (BMD) measurements were determined in similar region of interest, excluding the cortical bone. Bars represent mean ± standard error. N = 5-8 per group. *$p < 0.05$ by student's t-test.

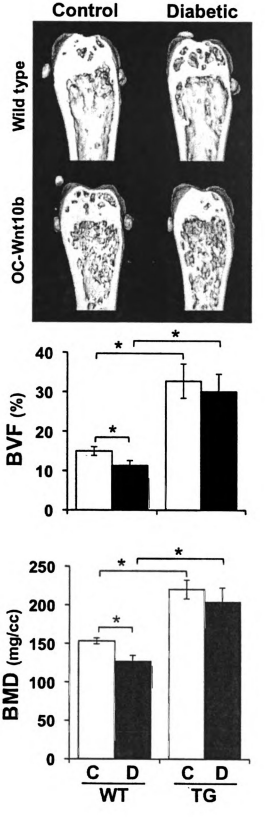
Control
Diabetic
Wild type
OC-Wnt10b
BVF (%)
40
30
20
10
0
*
*
*
BMD (mg/cc)
250
200
150
100
50
0
C
D
C
D
WT
TG

Table 6. Femur trabecular μCT measurements in control and diabetic, wild type and OC-Wnt10b mice.

	WT			OC-Wnt10b			*p* for WT vs. OC-Wnt10b	
	C (n = 8)	D (n = 8)	*p*	C (n = 6)	D (n = 5)	*p*	C	D
BMC (mg)	0.45 ± 0.01	0.37 ± 0.02	< 0.01*	0.66 ± 0.04	0.61 ± 0.05	0.45	< 0.01*	< 0.01*
BMD (mg/cc)	153 ± 4	127 ± 8	0.01*	220 ± 12	204 ± 19	0.46	< 0.01*	< 0.01*
BVF (%)	15.0 ± 1.0	11.3 ± 1.3	0.05*	32.8 ± 4.3	30.1 ± 4.5	0.68	< 0.01*	< 0.01*
Tb.Th. (μm)	45 ± 1	38 ± 2	0.02*	55 ± 5	50 ± 6	0.48	0.04*	0.05*
Tb.Sp. (μm)	294 ± 18	329 ± 16	0.17	152 ± 15	155 ± 10	0.88	< 0.01*	< 0.01*
Tb.N.	3.6 ± 0.2	3.0 ± 0.2	0.05*	6.1 ± 0.4	6.0 ± 0.3	0.90	< 0.01*	< 0.01*

Abbreviations: BMC, bone mineral content; BMD, bone mineral density; BVF, bone volume fraction; C, control; D, diabetic; N, number; Sp, spacing; Tb, trabecular; TG, transgenic; Th, thickness; WT, wildtype.
*Statistically significant based on student's t-test and $\alpha = 0.05$.

In order to determine how bone formation was affected by Wnt10b overexpression, we examined serum and mRNA markers of osteoblast activity. Serum osteocalcin was elevated in control OC-Wnt10b mice compared to wild type controls, which is consistent with higher bone formation (Figure 27A). Similar to previous findings, and consistent with low bone formation in diabetes, wild type diabetic mice had significantly lower serum OC levels than wild type controls. Despite protection from diabetic bone loss, OC-Wnt10b mice had reduced serum OC compared to control OC-Wnt10b mice, suggesting that bone formation was reduced. This finding was unusual because diabetes did not induce bone loss in these mice, so we examined mRNA markers of bone formation as well. The pattern of OC mRNA expression in bone was similar to that of serum OC levels. Runx2 levels, however, only tended toward higher levels in OC-Wnt10b control mice compared to wild type controls. Although Runx2 was significantly decreased in wild type diabetic mice compared to wild type controls, it only tended toward lower levels ($p = 0.07$) in diabetic OC-Wnt10b mice compared to OC-Wnt10b controls.

Despite the apparent reduced bone formation in the OC-Wnt10b mice, they did not have significantly decreased trabecular bone density, so we therefore measured bone resorption to gain an understanding of overall bone remodeling. TRAP5 positive osteoclast surface (% total) was not significantly altered by Wnt10b overexpression or diabetes (Figure 27C), which is consistent with previous reports (9, 44). Because osteoclast surface is dependent on total bone surface (which is markedly altered with both, diabetes and overexpression

of Wnt10b), unchanged % osteoclast surface is indicative of resorption changing proportionately to bone formation.

In order to address whether diabetic marrow adiposity was altered by overexpression of Wnt10b, we examined adipocytes in the marrow of femurs and measured tibia mRNA expression levels of adipocyte markers (Figure 28). Overexpression of Wnt10b from the OC promoter did not alter marrow adiposity in control mice (Figure 28A), while it did in mice with overexpression of Wnt10b from the aP2 promoter (39). As we have demonstrated in the past, T1-diabetes increased bone marrow adipocyte number in wild type mice. This increase in marrow adiposity was similar in diabetic OC-Wnt10b mice, suggesting that overexpression of Wnt10b in osteoblasts was not sufficient to alter adipogenesis in the marrow. We also measured mRNA markers of adiposity and found that aP2 expression coincided with adipocyte numbers (Figure 28B). PPARγ2 expression level were also unchanged in control OC-Wnt10b mice compared to control wild type mice. PPARγ2, however, only tended toward increases in both diabetic groups compared to their genotype matched controls, and diabetic wild type PPARγ2 levels were not different from those of diabetic OC-Wnt10b mice.

Figure 27. **Diabetes reduces bone formation in both wild type and OC-Wnt10b mice, but does not alter resorption.** (**A**) Total osteocalcin, a marker of bone formation, was measured with an ELISA in serum from control (C) and diabetic (D), wild type (WT) and OC-Wnt10b (TG) mice. (**B**) mRNA from frozen tibias was converted to cDNA by reverse transcriptase reaction and amplified with primers specific for osteocalcin, runx2 and HPRT, a non-modulated housekeeping gene control. (**C**) Fixed femurs sections were stained for TRAP activity counterstained with hematoxylin. Surface of bone in contact with TRAP5 positive osteoclasts was measured and expressed as a percent of the total bone surface. Bars represent mean ± standard error. N = 5-8 per group. *$p < 0.05$ by student's t-test.

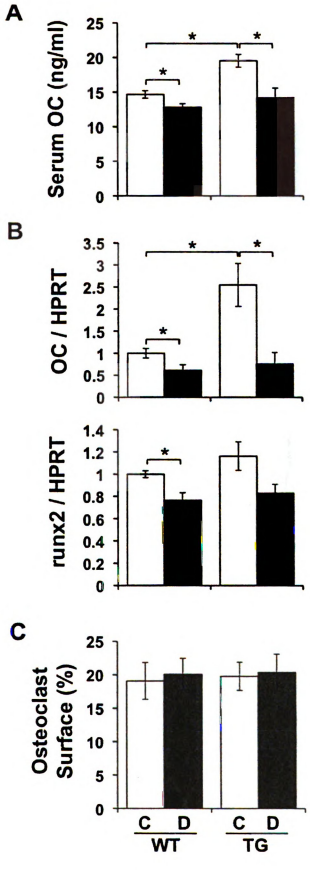
A
Serum OC (ng/ml)
25
20
15
10
5
0
*
*
*
B
OC / HPRT
3.5
3
2.5
2
1.5
1
0.5
0
*
*
*
runx2 / HPRT
1.4
1.2
1
0.8
0.6
0.4
0.2
0
*
C
Osteoclast Surface (%)
25
20
15
10
5
0
C
D
C
D
WT
TG

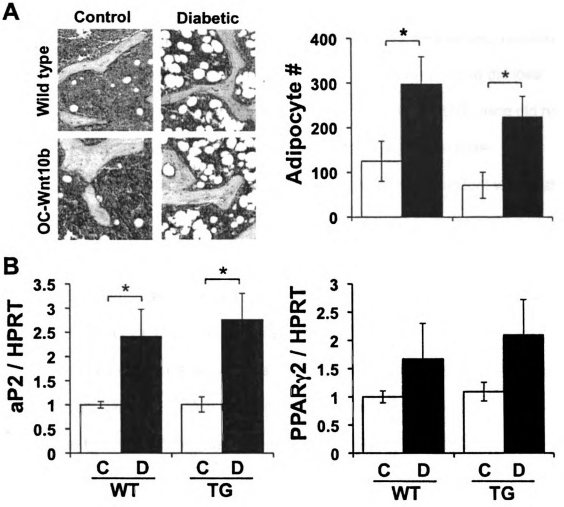

Figure 28. **Overexpression of Wnt10b did not alleviate diabetic marrow adiposity.** (**A**) Fixed femurs sections were stained for TRAP activity counterstained with hematoxylin. Visible adipocytes were counted in the femur trabecular area immediately proximal to the distal growth plate and extending 2 mm proximal. (**B**) mRNA from frozen tibias was converted to cDNA by reverse transcriptase reaction and amplified with primers specific for the adipocyte markers aP2 and PPARγ2, and for HPRT, a non-modulated housekeeping gene control. Bars represent mean ± standard error. N = 5-8 per group. *$p < 0.05$ by student's t-test.

5.5. DISCUSSION

To address the role of Wnt10b in diabetic bone loss we induced diabetes in wild type and OC-Wnt10b transgenic mice. Wild type diabetic mice did lose trabecular bone compared to controls, but interestingly, OC-Wnt10b mice did not lose bone. However, serum and RNA markers of bone formation were significantly reduced in diabetic mice from both genotypes. Consistent with past studies, osteoclast surface was not different in any of the treatment groups (9, 44). Additionally, despite the fact that Wnt10b is known to inhibit adipogenesis, OC-Wnt10b mice still accumulated marrow fat after diabetes was induced. We concluded that OC-Wnt10b mice are resistant to bone loss from diabetes and that reduced Wnt10b levels in diabetes may be a significant contributor to bone loss. Although diabetic OC-Wnt10b mice did have reduced bone formation markers, we believe that the positive effects of agonizing Wnt10b/β-catenin signaling could outweigh the negative effects of diabetes if this pathway was further explored as a treatment target for diabetic bone loss.

Here, we overexpressed Wnt10b in osteoblasts, which may not be the source of the reduced Wnt10b in diabetes. Since wnts are secreted, there are several cell types in bone that could be responsible for the reduction of Wnt10b levels. A very recent report indicates that the anabolic effects of intermittent PTH are dependent on T-lymphocyte derived expression of Wnt10b (46). Consistent with this finding, we found elevated Wnt10b expression in bone of PTH-treated mice (Figure 24B), and we determined that PTH is capable of promoting bone

formation in diabetes (Motyl, et al., *in preparation*, See Chapter 6). Additionally, recent work from our lab demonstrates that the cellular composition of the bone marrow is dramatically altered in response to diabetes (Martin, et al. 2010, *submitted*), and it will be incumbent upon us to determine how lymphocyte sub-populations are affected and how marrow derived Wnt10b is altered in diabetes.

Overexpression of Wnt10b from the osteocalcin promoter results in high expression levels in mature osteoblasts and osteocytes, but not preosteoblasts (which do not yet express OC). Therefore, if it is most important for Wnt10b to work in a paracrine/autocrine dependent manner in preosteoblasts to promote maturation, then overexpression of Wnt10b in only mature osteoblasts may not be able to fully prevent the diabetic bone phenotype of reduced osteoblast maturation (9, 15, 53).

In addition to reduced maturation, diabetic bone loss may likely result from increased osteoblast apoptosis as well. We have recently demonstrated elevated osteoblast apoptosis during diabetes onset in mice (Martin, et al., 2010, *submitted*). Wnt1 and Wnt3a have been demonstrated to prevent osteoblast death from serum starvation *in vitro* in a β-catenin dependent manner (54). Additionally, oxidative stress has been hypothesized to be involved in diabetic bone pathology (10, 55). Increased reactive oxygen species (ROS) induce FoxO transcription factors to bind β-catenin and activate FoxO target genes. This pulls β-catenin away from TCF/LEF-responsive genes and therefore antagonizes the end point of wnt signaling (56). Since wnt signaling regulates many of the wnt pathway members, increased oxidative stress could potentially be responsible for

reduced Wnt10b levels we have found in diabetes (57). Agonizing the wnt pathway with overexpression of Wnt10b may be sufficient to inhibit early osteoblast apoptosis from diabetes and is a topic of current examination in our laboratory.

We also found that Wnt10b expression was suppressed by chronic subcutaneous infusion of leptin (Figure 24C). To our knowledge, this is the first demonstration of leptin affecting Wnt10b levels in bone. The effect of leptin on bone density and Wnt10b in this case could be two-fold: through reduced body mass and mechanical load on bone, or through β2-adrenergic inhibition of bone formation. Leptin treatment reduces food intake and body mass, and changes in bone volume fraction are proportionate to body mass changes (21). Sclerostin, an endogenous wnt signaling antagonist, is secreted by osteocytes in response to unloading, then subsequently reduces β-catenin activity and bone formation in osteoblasts (58). Alternately, sclerostin levels are reduced in response to increased load (59). Interestingly, wnt/β-catenin signaling pathway members, and in particular Wnt10b levels, are elevated in response to increased mechanical load *in vivo* and *in vitro* in microstrained osteoblast cultures (60). It is unclear whether Wnt10b itself is reduced in response to unloading situations like hind limb suspension or simulated microgravity and whether this response would be maintained long term as in our experiment (22). Independent of body mass, leptin itself can reduce bone density through hypothalamic relay activation of β2-adrenergic receptor signaling (61). A previous study demonstrated that the β-blocker porpranolol was able to enhance osteogenic effects of intermittent PTH

therapy (62), which we now know is dependent on Wnt10b (46), suggesting that regulation of these pathways may not be entirely independent.

The fact that overexpression of Wnt10b from the osteocalcin promoter did not prevent diabetic marrow adiposity (Figure 28) is very interesting because aP2-Wnt10b mice have significantly reduced marrow and peripheral fat (39, 45). We did not detect differences in adipocyte numbers or gene expression between control wild type and OC-Wnt10b mice. This difference could be due to different levels of Wnt10b protein expression in aP2-Wnt10b versus OC-Wnt10b mice, or it is possible that as we hypothesized above with osteoblasts, the effect of Wnt10b in adipocytes is strongest when it is expressed locally.

Despite the fact that we observed reduced markers of mature osteoblasts in diabetic OC-Wnt10b mice, bone density loss induced by diabetes was prevented by overexpression of Wnt10b. Diabetic OC-Wnt10b mice had increased bone density compared to wild type mice (control and diabetic). This finding suggests that reduced Wnt10b levels in diabetic bone may be in part responsible for diabetic bone loss in wild type mice. Similarly, our findings warrant further exploration into agonizing the wnt/β-catenin signaling pathway as a treatment for diabetic osteoporosis.

5.6. ACKNOWLEDGEMENTS

The authors thank Amylin for providing the leptin and Laurie McCauley for assistance with the protocol for PTH treatment. We also thank Ormond

MacDougald for the OC-Wnt10b breeder mice. We thank Regina Irwin and Lindsay Martin for technical assistance and critical review of the manuscript. This work was funded by grants from the National Institutes of Health (RO1DK061184) and the American Diabetes Association (7-07-RA-105) to LRM. The authors have no financial conflicts.

5.7. REFERENCES

1. **Danne T, Kordonouri O, Enders I, Weber B** 1997 Factors influencing height and weight development in children with diabetes. Results of the Berlin Retinopathy Study. Diabetes Care 20:281-285

2. **Holl RW, Grabert M, Heinze E, Sorgo W, Debatin KM** 1998 Age at onset and long-term metabolic control affect height in type-1 diabetes mellitus. Eur J Pediatr 157:972-977

3. **Levin ME, Boisseau VC, Avioli LV** 1976 Effects of diabetes mellitus on bone mass in juvenile and adult-onset diabetes. N Engl J Med 294:241-245

4. **Auwerx J, Dequeker J, Bouillon R, Geusens P, Nijs J** 1988 Mineral metabolism and bone mass at peripheral and axial skeleton in diabetes mellitus. Diabetes 37:8-12

5. **Kemink SA, Hermus AR, Swinkels LM, Lutterman JA, Smals AG** 2000 Osteopenia in insulin-dependent diabetes mellitus; prevalence and aspects of pathophysiology. J Endocrinol Invest 23:295-303

6. **Bouillon R, Bex M, Van Herck E, Laureys J, Dooms L, Lesaffre E, Ravussin E** 1995 Influence of age, sex, and insulin on osteoblast function: osteoblast dysfunction in diabetes mellitus. J Clin Endocrinol Metab 80:1194-1202

7. **Schwartz AV, Sellmeyer DE** 2007 Diabetes, fracture, and bone fragility. Curr Osteoporos Rep 5:105-111

8. **Szkudelski T** 2001 The mechanism of alloxan and streptozotocin action in B cells of the rat pancreas. Physiol Res 50:537-546

9. **Botolin S, Faugere MC, Malluche H, Orth M, Meyer R, McCabe LR** 2005 Increased bone adiposity and peroxisomal proliferator-activated receptor-gamma2 expression in type I diabetic mice. Endocrinology 146:3622-3631

10. **Hamada Y, Kitazawa S, Kitazawa R, Fujii H, Kasuga M, Fukagawa M** 2007 Histomorphometric analysis of diabetic osteopenia in streptozotocin-induced diabetic mice: a possible role of oxidative stress. Bone 40:1408-1414

11. **Shires R, Teitelbaum SL, Bergfeld MA, Fallon MD, Slatopolsky E, Avioli LV** 1981 The effect of streptozotocin-induced chronic diabetes mellitus on bone and mineral homeostasis in the rat. J Lab Clin Med 97:231-240

12. **Krakauer JC, McKenna MJ, Buderer NF, Rao DS, Whitehouse FW, Parfitt AM** 1995 Bone loss and bone turnover in diabetes. Diabetes 44:775-782

13. **McCracken M, Lemons JE, Rahemtulla F, Prince CW, Feldman D** 2000 Bone response to titanium alloy implants placed in diabetic rats. Int J Oral Maxillofac Implants 15:345-354

14. **Shyng YC, Devlin H, Sloan P** 2001 The effect of streptozotocin-induced experimental diabetes mellitus on calvarial defect healing and bone turnover in the rat. Int J Oral Maxillofac Surg 30:70-74

15. **Fowlkes JL, Bunn RC, Liu L, Wahl EC, Coleman HN, Cockrell GE, Perrien DS, Lumpkin CK, Jr., Thrailkill KM** 2008 Runt-related transcription factor 2 (RUNX2) and RUNX2-related osteogenic genes are down-regulated throughout osteogenesis in type 1 diabetes mellitus. Endocrinology 149:1697-1704

16. **Botolin S, McCabe LR** 2007 Bone loss and increased bone adiposity in spontaneous and pharmacologically induced diabetic mice. Endocrinology 148:198-205

17. **Nyomba BL, Verhaeghe J, Thomasset M, Lissens W, Bouillon R** 1989 Bone mineral homeostasis in spontaneously diabetic BB rats. I. Abnormal vitamin D metabolism and impaired active intestinal calcium absorption. Endocrinology 124:565-572

18. **Verhaeghe J, Suiker AM, Nyomba BL, Visser WJ, Einhorn TA, Dequeker J, Bouillon R** 1989 Bone mineral homeostasis in spontaneously diabetic BB rats. II. Impaired bone turnover and decreased osteocalcin synthesis. Endocrinology 124:573-582

19. **Botolin S, McCabe LR** 2006 Inhibition of PPARgamma prevents type I diabetic bone marrow adiposity but not bone loss. J Cell Physiol 209:967-976

20. **McCabe LR** 2007 Understanding the pathology and mechanisms of type I diabetic bone loss. J Cell Biochem 102:1343-1357

21. **Motyl K, McCabe LR** 2009 Streptozotocin, Type I Diabetes Severity and Bone. Biol Proced Online

22. **Motyl KJ, McCabe LR** 2009 Leptin treatment prevents type I diabetic marrow adiposity but not bone loss in mice. J Cell Physiol 218:376-384

23. **Martin LM, McCabe LR** 2007 Type I diabetic bone phenotype is location but not gender dependent. Histochem Cell Biol 128:125-133

24. **Nuttall ME, Patton AJ, Olivera DL, Nadeau DP, Gowen M** 1998 Human trabecular bone cells are able to express both osteoblastic and adipocytic phenotype: implications for osteopenic disorders. J Bone Miner Res 13:371-382

25. **Verma S, Rajaratnam JH, Denton J, Hoyland JA, Byers RJ** 2002 Adipocytic proportion of bone marrow is inversely related to bone formation in osteoporosis. J Clin Pathol 55:693-698

26. **Ahdjoudj S, Lasmoles F, Holy X, Zerath E, Marie PJ** 2002 Transforming growth factor beta2 inhibits adipocyte differentiation induced by skeletal unloading in rat bone marrow stroma. J Bone Miner Res 17:668-677

27. **Moon RT** 2005 Wnt/beta-catenin pathway. Sci STKE 2005:cm1

28. **Baron R, Rawadi G** 2007 Targeting the Wnt/beta-catenin pathway to regulate bone formation in the adult skeleton. Endocrinology 148:2635-2643

29. **Clevers H** 2006 Wnt/beta-catenin signaling in development and disease. Cell 127:469-480

30. **Dong YF, Soung do Y, Schwarz EM, O'Keefe RJ, Drissi H** 2006 Wnt induction of chondrocyte hypertrophy through the Runx2 transcription factor. J Cell Physiol 208:77-86

31. **Gaur T, Lengner CJ, Hovhannisyan H, Bhat RA, Bodine PV, Komm BS, Javed A, van Wijnen AJ, Stein JL, Stein GS, Lian JB** 2005 Canonical WNT signaling promotes osteogenesis by directly stimulating Runx2 gene expression. J Biol Chem 280:33132-33140

32. **Gong Y, Slee RB, Fukai N, Rawadi G, Roman-Roman S, Reginato AM, Wang H, Cundy T, Glorieux FH, Lev D, Zacharin M, Oexle K, Marcelino J, Suwairi W, Heeger S, Sabatakos G, Apte S, Adkins WN, Allgrove J, Arslan-Kirchner M, Batch JA, Beighton P, Black GC, Boles RG, Boon LM, Borrone C, Brunner HG, Carle GF, Dallapiccola B, De Paepe A, Floege B, Halfhide ML, Hall B, Hennekam RC, Hirose T, Jans A, Juppner H, Kim CA, Keppler-Noreuil K, Kohlschuetter A, LaCombe D, Lambert M, Lemyre E, Letteboer T, Peltonen L, Ramesar RS, Romanengo M, Somer H, Steichen-Gersdorf E, Steinmann B, Sullivan B, Superti-Furga A, Swoboda W, van den Boogaard MJ, Van Hul W, Vikkula M, Votruba M, Zabel B, Garcia T, Baron R, Olsen BR, Warman ML** 2001 LDL receptor-related protein 5 (LRP5) affects bone accrual and eye development. Cell 107:513-523

33. **Boyden LM, Mao J, Belsky J, Mitzner L, Farhi A, Mitnick MA, Wu D, Insogna K, Lifton RP** 2002 High bone density due to a mutation in LDL-receptor-related protein 5. N Engl J Med 346:1513-1521

34. **Little RD, Carulli JP, Del Mastro RG, Dupuis J, Osborne M, Folz C, Manning SP, Swain PM, Zhao SC, Eustace B, Lappe MM, Spitzer L, Zweier S, Braunschweiger K, Benchekroun Y, Hu X, Adair R, Chee L, FitzGerald MG, Tulig C, Caruso A, Tzellas N, Bawa A, Franklin B, McGuire S, Nogues X, Gong G, Allen KM, Anisowicz A, Morales AJ, Lomedico PT, Recker SM, Van Eerdewegh P, Recker RR, Johnson ML** 2002 A mutation in the LDL receptor-related protein 5 gene results in the autosomal dominant high-bone-mass trait. Am J Hum Genet 70:11-19

35. **Kato M, Patel MS, Levasseur R, Lobov I, Chang BH, Glass DA, 2nd, Hartmann C, Li L, Hwang TH, Brayton CF, Lang RA, Karsenty G, Chan L** 2002 Cbfa1-independent decrease in osteoblast proliferation, osteopenia, and persistent embryonic eye vascularization in mice deficient in Lrp5, a Wnt coreceptor. J Cell Biol 157:303-314

36. **Babij P, Zhao W, Small C, Kharode Y, Yaworsky PJ, Bouxsein ML, Reddy PS, Bodine PV, Robinson JA, Bhat B, Marzolf J, Moran RA, Bex F** 2003 High bone mass in mice expressing a mutant LRP5 gene. J Bone Miner Res 18:960-974

37. **Holmen SL, Giambernardi TA, Zylstra CR, Buckner-Berghuis BD, Resau JH, Hess JF, Glatt V, Bouxsein ML, Ai M, Warman ML, Williams BO** 2004 Decreased BMD and limb deformities in mice carrying mutations in both Lrp5 and Lrp6. J Bone Miner Res 19:2033-2040

38. **Kubota T, Michigami T, Ozono K** 2009 Wnt signaling in bone metabolism. J Bone Miner Metab 27:265-271

39. **Bennett CN, Longo KA, Wright WS, Suva LJ, Lane TF, Hankenson KD, MacDougald OA** 2005 Regulation of osteoblastogenesis and bone mass by Wnt10b. Proc Natl Acad Sci U S A 102:3324-3329

40. **Bennett CN, Ross SE, Longo KA, Bajnok L, Hemati N, Johnson KW, Harrison SD, MacDougald OA** 2002 Regulation of Wnt signaling during adipogenesis. J Biol Chem 277:30998-31004

41. **Ross SE, Hemati N, Longo KA, Bennett CN, Lucas PC, Erickson RL, MacDougald OA** 2000 Inhibition of adipogenesis by Wnt signaling. Science 289:950-953

42. **Ross SE, Erickson RL, Gerin I, DeRose PM, Bajnok L, Longo KA, Misek DE, Kuick R, Hanash SM, Atkins KB, Andresen SM, Nebb HI, Madsen L, Kristiansen K, MacDougald OA** 2002 Microarray analyses during adipogenesis: understanding the effects of Wnt signaling on adipogenesis and the roles of liver X receptor alpha in adipocyte metabolism. Mol Cell Biol 22:5989-5999

43. **Kang S, Bennett CN, Gerin I, Rapp LA, Hankenson KD, Macdougald OA** 2007 Wnt signaling stimulates osteoblastogenesis of mesenchymal precursors by suppressing CCAAT/enhancer-binding protein alpha and peroxisome proliferator-activated receptor gamma. J Biol Chem 282:14515-14524

44. **Bennett CN, Ouyang H, Ma YL, Zeng Q, Gerin I, Sousa KM, Lane TF, Krishnan V, Hankenson KD, MacDougald OA** 2007 Wnt10b increases

postnatal bone formation by enhancing osteoblast differentiation. J Bone Miner Res 22:1924-1932

45. **Longo KA, Wright WS, Kang S, Gerin I, Chiang SH, Lucas PC, Opp MR, MacDougald OA** 2004 Wnt10b inhibits development of white and brown adipose tissues. J Biol Chem 279:35503-35509

46. **Terauchi M, Li JY, Bedi B, Baek KH, Tawfeek H, Galley S, Gilbert L, Nanes MS, Zayzafoon M, Guldberg R, Lamar DL, Singer MA, Lane TF, Kronenberg HM, Weitzmann MN, Pacifici R** 2009 T lymphocytes amplify the anabolic activity of parathyroid hormone through Wnt10b signaling. Cell Metab 10:229-240

47. **Vengellur A, LaPres JJ** 2004 The role of hypoxia inducible factor 1alpha in cobalt chloride induced cell death in mouse embryonic fibroblasts. Toxicol Sci 82:638-646

48. **Fox KE, Colton LA, Erickson PF, Friedman JE, Cha HC, Keller P, MacDougald OA, Klemm DJ** 2008 Regulation of cyclin D1 and Wnt10b gene expression by cAMP-responsive element-binding protein during early adipogenesis involves differential promoter methylation. J Biol Chem 283:35096-35105

49. **Ontiveros C, McCabe LR** 2003 Simulated microgravity suppresses osteoblast phenotype, Runx2 levels and AP-1 transactivation. J Cell Biochem 88:427-437

50. **Ontiveros C, Irwin R, Wiseman RW, McCabe LR** 2004 Hypoxia suppresses runx2 independent of modeled microgravity. J Cell Physiol 200:169-176

51. **Li J, Takaishi K, Cook W, McCorkle SK, Unger RH** 2003 Insig-1 "brakes" lipogenesis in adipocytes and inhibits differentiation of preadipocytes. Proc Natl Acad Sci U S A 100:9476-9481

52. **Kast-Woelbern HR, Dana SL, Cesario RM, Sun L, de Grandpre LY, Brooks ME, Osburn DL, Reifel-Miller A, Klausing K, Leibowitz MD** 2004 Rosiglitazone induction of Insig-1 in white adipose tissue reveals a novel interplay of peroxisome proliferator-activated receptor gamma and sterol regulatory element-binding protein in the regulation of adipogenesis. J Biol Chem 279:23908-23915

53. **Botolin S, McCabe LR** 2006 Chronic hyperglycemia modulates osteoblast gene expression through osmotic and non-osmotic pathways. J Cell Biochem 99:411-424

54. **Almeida M, Han L, Bellido T, Manolagas SC, Kousteni S** 2005 Wnt proteins prevent apoptosis of both uncommitted osteoblast progenitors and differentiated osteoblasts by beta-catenin-dependent and -independent signaling cascades involving Src/ERK and phosphatidylinositol 3-kinase/AKT. J Biol Chem 280:41342-41351

55. **Manolagas SC** From Estrogen-Centric to Aging and Oxidative Stress: A Revised Perspective of the Pathogenesis of Osteoporosis. Endocr Rev

56. **Almeida M, Han L, Martin-Millan M, O'Brien CA, Manolagas SC** 2007 Oxidative stress antagonizes Wnt signaling in osteoblast precursors by diverting beta-catenin from T cell factor- to forkhead box O-mediated transcription. J Biol Chem 282:27298-27305

57. **Nusse R** 2005 Wnt signaling in disease and in development. Cell Res 15:28-32

58. **Lin C, Jiang X, Dai Z, Guo X, Weng T, Wang J, Li Y, Feng G, Gao X, He L** 2009 Sclerostin mediates bone response to mechanical unloading through antagonizing Wnt/beta-catenin signaling. J Bone Miner Res 24:1651-1661

59. **Robling AG, Niziolek PJ, Baldridge LA, Condon KW, Allen MR, Alam I, Mantila SM, Gluhak-Heinrich J, Bellido TM, Harris SE, Turner CH** 2008 Mechanical stimulation of bone in vivo reduces osteocyte expression of Sost/sclerostin. J Biol Chem 283:5866-5875

60. **Robinson JA, Chatterjee-Kishore M, Yaworsky PJ, Cullen DM, Zhao W, Li C, Kharode Y, Sauter L, Babij P, Brown EL, Hill AA, Akhter MP, Johnson ML, Recker RR, Komm BS, Bex FJ** 2006 Wnt/beta-catenin signaling is a normal physiological response to mechanical loading in bone. J Biol Chem 281:31720-31728

61. **Bonnet N, Pierroz DD, Ferrari SL** 2008 Adrenergic control of bone remodeling and its implications for the treatment of osteoporosis. J Musculoskelet Neuronal Interact 8:94-104

62. **Pierroz DD, Bouxsein ML, Rizzoli R, Ferrari SL** 2006 Combined treatment with a beta-blocker and intermittent PTH improves bone mass and microarchitecture in ovariectomized mice. Bone 39:260-267

CHAPTER 6

6. OSTEOPOROSIS FROM TYPE 1 DIABETES IS REVERSED BY INTERMITTENT PARATHYROID HORMONE STIMULATION OF BONE REMODELING AND REDUCTION OF OSTEOBLAST APOPTOSIS

6.1. ABSTRACT

Type 1 diabetic osteoporosis results from impaired osteoblast activity and osteoblast death. Because diabetes does not affect or reduces resorption, antiresorptive bisphosphonates may not be the best therapy. Anabolic intermittent parathyroid hormone (PTH) stimulates bone remodeling and increases bone density. Here, we examined the ability of 8 μg/kg and 40 μg/kg intermittent PTH to counteract diabetic bone loss. We found significant elevation of trabecular bone density parameters with the 40 μg/kg dose in control mice and diabetic mice (compared to their metabolic-state matched vehicle treated controls), and elevation of trabecular bone parameters in diabetic 8 μg/kg treated mice. Increased bone density in diabetic PTH-treated mice was due to increased bone formation, mineral apposition, and osteoblast surface, all of which are defective in type 1 diabetes. Reduction of diabetes-induced osteoblast apoptosis could account for some of the bone-forming effects of PTH. We also determined that 40 μg/kg PTH treatment reversed preexisting bone loss from diabetes, which will be significant for clinical application. We conclude that intermittent PTH will

likely be an effective therapeutic for patients with type 1 diabetes and that its use in these subjects should be explored.

6.2. INTRODUCTION

Bone is a highly dynamic tissue that is constantly remodeling to maintain blood calcium homeostasis and to respond to altered demand for structural support. Osteoblasts (bone forming cells) and osteoclasts (bone resorbing cells) work simultaneously to repair microcracks and maintain bone density and strength. Certain diseases and conditions can alter the balance of bone formation and resorption and can often lead to osteoporosis in men and women, which can heighten bone loss from aging and menopause (1). One such disease is type 1 (T1-) diabetes, in which patients are hypoglycemic and hyperinsulinemic and have bone loss and increased fracture risk (2-6). As with secondary osteoporosis resulting from any disease, understanding the mechanism of T1-diabetic bone loss is necessary for choosing the best therapies. Osteoporosis from T1-diabetes is marked by decreased bone formation (and unchanged or decreased resorption) in both humans and animals (1, 7-13). Reduced bone formation markers in diabetes include reduced mRNA levels of osteocalcin (OC), runt-related transcription factor 2 (runx2), osterix and Dlx5 in bone, and reduced serum OC, suggesting impaired differentiation and maturation of osteoblasts. It has been suggested that reduced differentiation to the osteoblast lineage could be related to increased differentiation of adipocytes in the bone marrow (both

osteoblasts and adipocytes arise from mesenchymal stem cells (MSCs)) (8, 12-15). However, recent studies have demonstrated a disconnect between osteoblast and adipocyte differentiation in T1-diabetes. For example, we have demonstrated that inhibition of marrow adiposity with neither leptin nor the PPARγ inhibitor bisphenol-A-diglycidyl ether (BADGE) prevents bone loss from T1-diabetes (16, 17). In addition to reduced maturation, we have found that osteoblasts undergo apoptosis as early as 2 days after high blood glucose is detectable in the streptozotocin mouse model of T1-diabetes and at comparably early time points in the spontaneously diabetic *Ins2*$^{+/-Akita}$ mice (Martin et al., 2010, *submitted*). This osteoblast apoptosis remains detectable for several weeks. Thus, a treatment that could target osteoblasts (by promoting differentiation and/or preventing apoptosis) would be ideal for diabetic patients.

Most of the treatments for osteoporosis, however, are antiresorptive, meaning they work by inhibiting osteoclast activity. Bisphosphonates (the most widely used antiresorptive therapy) have a similar structure to inorganic pyrophosphate and are incorporated into bone (18). However, bisphosphonates are more stable than inorganic phosphate and can withstand exposure to bone resorbing acids secreted by osteoclasts (19). Therefore, when osteoclasts encounter bisphosphonates embedded in bone, resorption is halted, and osteoclasts often undergo apoptosis (20). This could present a problem for fracture repair and everyday remodeling of microcracks. In fact, recent clinical evidence suggests long-term bisphosphonate therapy could increase incidence of fracture (21-25). In diabetes, bone resorption is already suppressed (1); further

suppression of resorption with antiresorptive therapies may worsen impaired fracture healing in these patients. Additionally, one of the well-characterized side effects of bisphosphonates is osteonecrosis of the jaw (bisphosphonate-related osteonecrosis, BON) (26, 27). Diabetes appears to be a risk factor for BON: compared to the total patient population receiving bisphosphonates for osteoporosis, diabetic patients receiving bisphosphonates were nearly 5 times more likely to be diagnosed with BON (28). Other antiresorptive treatments for osteoporosis exist (including hormone replacement therapy and selective estrogen receptor modulators (SERMs), and calcitonin). However, because bone loss from T1-diabetes is due to reduced osteoblast bone formation, and not increased resorption, we maintain that anabolic therapies that target bone formation directly may be most appropriate.

Currently, the only anabolic treatment in use is truncated parathyroid hormone (PTH), also called teriparatide (29, 30). The mechanism of PTH action in bone is complex and dependent on dosing. Chronic PTH stimulation causes bone resorption and calcium release. However, when administered intermittently (daily subcutaneous injections) PTH causes a net increase in bone formation and reduction of fracture risk in humans and laboratory animals (31-35). PTH receptors are present on cells in the osteoblast lineage including preosteoblasts, osteoblasts, osteocytes and bone lining cells. Intermittent PTH promotes osteoblast differentiation and inhibits osteoblast and osteocyte apoptosis, perhaps through upregulation of runx2 (36). Additionally, *in vitro* PTH treatment activates the TCF/LEF-dependent transcription, which is activated by Wnt

signaling (37), a potent regulator of bone formation (38, 39). PTH may also inhibit production of sclerostin, which inhibits bone formation by inhibiting Wnt and bone morphogenic protein (BMP) signaling (40). A very recent report indicates that the anabolic effects of intermittent PTH are dependent on T-lymphocyte expression of Wnt10b (41). Because no PTH receptors are present on cells of the osteoclast lineage, net bone resorption from chronic PTH treatment is likely due to secreted osteoblast factors (RANKL and M-CSF) activating osteoclast activity.

There are no reports examining the efficacy of PTH treatment for T1-diabetic bone loss in humans. In laboratory animals, intermittent PTH treatment has proven to be anabolic (32), and is effective at increasing bone formation in models of unloading, ovariectomy, and alcohol consumption (34, 42-46). Additionally, 4-week intermittent PTH treatment of STZ-diabetic rats improves bone density parameters 4, 6 and 8 weeks after diabetes induction (47). Similarly, PTH related protein (PTHrP) treatment of streptozotocin-diabetic mice also enhances bone formation markers and bone density (48). However, the effects of the already commercially available intermittent PTH therapy on mouse models of T1-diabetes induced bone loss have not been determined.

While understanding exactly what diabetic characteristics (hyperglycemia, inflammation, oxidative stress) cause these bone changes, it is also important to utilize the therapeutic resources available to treat patients on an individualized basis. Therefore, here we examined the efficacy of intermittent PTH therapy on several aspects (bone formation, osteoblast apoptosis, and bone resorption) of bone loss in T1-diabetic mice. Briefly, we determined that daily subcutaneous

PTH (at both 8 μg/kg and 40 μg/kg doses) is sufficient to restore trabecular bone density of T1-diabetic mice back to untreated control levels. We demonstrated that this effect was primarily due to increased osteoblast maturity, viability and mineralization. We also found that PTH was capable of restoring diabetic bone density to normal levels even when initiated after bone loss had already occurred, which is crucial for PTH to be an effective clinical treatment of osteoporosis in T1-diabetic patients. Our findings are clinically relevant and warrant further exploration of the use of PTH in human diabetic subjects.

6.3. MATERIALS AND METHODS

6.3.1. Diabetes induction

BALB/c mice were obtained from Harlan Sprague Dawley (Indianapolis, IN). All mice were maintained on a 12-hour light, 12-hour dark cycle at 23 °C, were given standard lab chow, and had food and water *ad libitum*. At 14 weeks of age, mice were treated with either 50 mg/kg streptozotocin (to induce diabetes) or 0.1 M citrate buffer pH 4.5 vehicle (control) for five consecutive days. Diabetes was confirmed 12 days after the first injection (dpi, days post injection) with an AccuChek compact glucometer (Roche, Nutley, NJ) and a drop of blood collected from the saphenous vein. Blood glucose over 300 mg/dl was considered diabetic. Mice were harvested at 5, 20 or 40 dpi.

6.3.2. PTH Treatment

PTH (Bachem, Torrance, CA) was stored in glass vials topped with argon gas at -80 °C as a 10^{-4} M stock in 4 mM HCl supplemented with 0.1% bovine serum albumin. PTH did not go through more than one freeze/thaw cycle. Immediately before injection, PTH was made up to 100 μl per mouse with ice cold 0.9% saline. Control and diabetic mice were subjected to daily subcutaneous injections of each PTH dosing regimen: 1) daily vehicle treatment from 0 dpi until harvest, 2) daily 8 μg/kg PTH from 0 dpi until harvest, 3) daily 40 μg/kg PTH from 0 dpi until harvest, or 4) daily vehicle treatment from 0-19 dpi followed by daily 40 μg/kg PTH from 20-40 dpi. As stated above, mice were harvested at 5, 20 or 40 dpi, at which time serum was collected, tissues were weighed, and tissues and bones were either fixed in formalin or frozen in liquid nitrogen and stored at -80°C. Blood glucose was measured at the time of harvest with an AccuChek compact glucometer (Roche, Nutley, NJ). All animal procedures were performed in accordance with Michigan State University Institutional Animal Care and Use Committee.

6.3.3. Micro-computed tomography (μCT) analyses

Bones were fixed in 10% formalin and transferred to 70% ethanol after 24 hours. Fixed tibias were scanned using a GE Explore Locus μCT system at a voxel resolution of 20 μm obtained from 720 views. Beam angle of increment was

0.5 and beam strength was set at 80 peak kV and 450 μA. Each run included bones from each treatment group and a calibration phantom to standardize grayscale values and maintain consistency. Based on autothreshold and isosurface analyses of multiple bone samples, a fixed threshold (800) was used to separate bone from bone marrow. Cortical bone analyses were made in a defined 2 mm × 2 mm × 2 mm cube in the mid-diaphysis immediately proximal to the distal tibial-fibular junction, with the exception of cortical bone mineral density (BMD), which were made in a 0.1 mm × 0.1 mm × 0.1 mm cube. Trabecular bone analyses were performed in a region of trabecular bone defined at 0.17 mm (1% of the total length) distal to the growth plate of the proximal tibia extending 2 mm toward the diaphysis, and excluding the outer cortical shell. Trabecular bone mineral content (BMC), BMD, bone volume fraction (BVF), thickness (Tb Th), spacing (Tb Sp) and number (Tb N) and cortical BMD, moment of inertia (MOI), thickness, inner and outer perimeter, and marrow, cortical and total area values were computed by a GE Healthcare MicroView software application for visualization and analysis of volumetric image data. Trabecular isosurface images were taken from a cylindrical region in the tibia immediately distal to the proximal growth plate measuring 0.8 mm in length and 0.8 mm in diameter.

6.3.4. Bone histology and histomorphometry

Fixed femur samples were processed on an automated Thermo Electron Excelsior tissue processor for dehydration, clearing and infiltration using a routine

overnight processing schedule. Samples were then embedded in Surgipath embedding paraffin on a Sakura Tissue Tek II embedding center. Paraffin blocks were sectioned at 5 μm on a Reichert Jung 2030 rotary microtome.

Slides were stained for tartrate-resistant acid phosphatase (TRAP) activity and counter stained with hematoxylin according to manufacturer protocol (387A-1KT, Sigma, St. Louis, MO). Osteoclast surface area was measured and expressed as a percentage of total bone surface in the femur trabecular region ranging from the distal growth plate to 2 mm proximal. Osteoblasts were counted and expressed relative to total trabecular bone surface. Visible adipocytes, greater than 30 μm were counted and number was expressed relative to marrow area.

To detect cell death *in vivo*, the TACS•XL® Basic In Situ Apoptosis Detection Kit was used according to manufacturer protocol (Trevigen Inc., Gaithersburg, MD). Positive controls included slides incubated with nuclease. Five trabecular regions were examined for each femur slide. Total osteoblast number counted ranged between 45 and 150 per mouse.

For mineral apposition rate (MAR), mice were injected intraperitoneally with 200 μl of 10 mg/ml calcein (Sigma, St. Louis, MO, USA) dissolved in saline 9 and 2 days before harvest. Fixed L5 vertebrae were then embedded and sectioned at 5 μm on a Reichert Jung 2030 rotary microtome. Sections were photographed under fluorescent light and the distance between lines of calcein was measured. All photomicrograph measurements were performed with Image Pro Plus software (Media Cybernetics, Inc., Bethesda, MD).

6.3.5. RNA analyses

Tibias were cleaned of muscle and connective tissue, snap frozen in liquid nitrogen and stored at -80°C. Frozen tibias were crushed under liquid nitrogen conditions with a Bessman Tissue Pulverizer (Spectrum Laboratories, Inc., Rancho Dominguez, CA). RNA was isolated with Tri Reagent (Molecular Research Center, Inc., Cincinnati, OH) and integrity was assessed by formaldehyde-agarose gel electrophoresis. cDNA was synthesized by reverse transcription with Superscript II Reverse Transcriptase Kit and oligo $dT_{(12\text{-}18)}$ primers (Invitrogen, Carlsbad, CA) and amplified by real-time PCR with iQ SYBR Green Supermix (Biorad, Hercules, CA) and gene-specific primers synthesized by Integrated DNA Technologies (Coralville, IA). Hypoxanthine guanine phosphoribosyl transferase (HPRT) mRNA levels do not fluctuate in diabetes or with PTH treatment and were used as an internal control. HPRT was amplified using 5'-AAG CCT AAG ATG AGC GCA AG-3' and 5'-TTA CTA GGC AGA TGG CCA CA-3' (49). Osteocalcin was amplified using 5'-ACG GTA TCA CTA TTT AGG ACC TGT G-3' and 5'-ACT TTA TTT TGG AGC TGC TGT GAC-3' (50). TRAP5 was amplified using 5'-AAT GCC TCG ACC TGG GA-3' and 5'-CGT AGT CCT CCT TGG CTG CT-3' (51). Receptor activator of nuclear factor kappa-B ligand (RANKL) was amplified using 5'-TTT GCA GGA CTC GAC TCT GGA G-3' and 5'-TCC CTC CTT TCA TCA GGT TAT GAG-3' (52). OPG was amplified using 5'-GAA GAA GAT CAT CCA AGA CAT TGA C-3' and 5'-TCC ATA AAC

TGA GTA GCT TCA GGA G-3′ (53). Real time PCR was carried out for 40 cycles using the iCycler (Bio-Rad) and data were evaluated using the iCycler software. Each cycle consisted of 95°C for 15 s, 60°C for 30 s (except for osteocalcin which had an annealing temperature of 65°C), and 72°C for 30 s. cDNA-free samples, a negative control, did not produce amplicons. Melting curve and gel analyses (sizing, isolation, and sequencing) were used to verify single products of the appropriate base pair size.

6.3.6. Statistical Analyses

All measurements are presented as mean ± standard error. Statistically significant ($\alpha = 0.05$) main effects (of PTH dose or diabetes) as well as PTH x diabetes interaction (which would indicate diabetes altering PTH effects or visa versa) were determined using factorial analysis of variance (ANOVA) and one-way ANOVA with Tukey HSD post hoc test (where necessary) with SPSS statistical software (Chicago, IL). Student's t-test was also used to determine significance where necessary.

6.4. RESULTS

6.4.1. Diabetes induction and body composition

In order to assess the efficacy of anabolic PTH therapy for osteoporosis from T1-diabetes, we induced diabetes with streptozotocin in BALB/c mice while simultaneously beginning a PTH treatment regimen. Control and diabetic mice were injected daily with either vehicle for PTH, 8 μg/kg PTH, or 40 μg/kg PTH. Mice were harvested 40 days after the first injection (dpi). Statsitical analysis with ANOVA indicated a significant ($p < 0.05$) effect from diabetes on blood glucose (as we would expect) but no significant effect of PTH treatment on blood glucose of either non-diabetic (euglycemic) or diabetic mice. Similarly, ANOVA did not detect a significant interaction between PTH and diabetes, indicating that it did not interfere with diabetes induction (Table 7). Similar to previous findings, diabetic mice weighed 9% less than controls at the end of the study (16). Weight loss was due in part to muscle and fat loss: diabetic mice had 16% lower tibialis anterior mass, 41% lower femoral fat pad mass and 57% lower perirenal fat pad mass (Table 7). When analyzed by ANOVA, neither 8 nor 40 μg/kg PTH altered the diabetes-induced loss of total body, fat or muscle mass (Table 7). As others and we have previously demonstrated, loss of peripheral and visceral fat depots in diabetes was accompanied by increased bone marrow adiposity (Table 7). Diabetes induced a 3.3-fold increase in marrow adipocyte number in the distal femur of vehicle treated mice. Interestingly, 8 μg/kg PTH treatment doubled marrow adipocyte number in control mice, although this was not significant by ANOVA, and neither was the 1.5-fold increase in 40 μg/kg PTH treated controls. The level of adiposity in diabetic mice did not differ between PTH treatment groups.

Table 7. Blood glucose, muscle and fat composition of control and diabetic, vehicle and PTH treated mice at 40 dpi.

	Vehicle		8 μg/kg PTH		40 μg/kg PTH	
	C (n = 19)	D (n = 17)	C (n = 13)	D (n = 12)	C (n = 14)	D (n = 15)
Non-fasting glucose (mg/dl)	173 ± 8	491 ± 27*	151 ± 9	531 ± 14*	164 ± 13	534 ± 19*
Body mass (g)	27.9 ± 0.4	25.5 ± 0.5*	28.6 ± 0.4	25.6 ± 0.6*	29.0 ± 0.5	26.3 ± 0.5*
Tibialis anterior (mg)	50 ± 1	42 ± 3*	52 ± 1	43 ± 1*	52 ± 1	43 ± 1*
Femoral fat pad (mg)	133 ± 5	78 ± 7*	112 ± 8	76 ± 6*	114 ± 9	75 ± 6*
Perirenal fat pad (mg)	37 ± 3	16 ± 2*	31 ± 3	16 ± 2*	32 ± 4	14 ± 2*
Marrow adipocyte # (mm^{-2})[§]	6 ± 1	20 ± 3*	12 ± 1	23 ± 7	9 ± 2	17 ± 3*

Abbreviations: C, control; D, diabetic; dpi, days post injection; PTH, parathyroid hormone.

Significance: *$p < 0.05$ compared to treatment-matched control.

[§]n = 4-5 per group.

6.4.2. PTH Counteracted Diabetic Bone Loss

When analyzed by ANOVA, significant diabetes effects ($p < 0.05$) were found with BMC, BMD, BVF, trabecular thickness and trabecular number (Figure 29, Table 8). Significant PTH effects were found with all of the above parameters, in addition to trabecular spacing. No significant interaction between diabetes and PTH was found in any of the trabecular bone parameters. Significance between groups was determined with a post-hoc test (only after factorial ANOVA determined significance). Only high dose, 40 μg/kg, PTH significantly increased trabecular BMC, BMC, BVF, trabecular thickness, and trabecular number in euglycemic mice (Figure 29, Table 8). The increase in trabecular bone parameters observed in euglycemic mice treated with 8 μg/kg was not significant by ANOVA. As we have demonstrated in the past, diabetes significantly reduced tibia trabecular BMC, BMD, BVF, trabecular thickness, and trabecular number (Figure 29, Table 8) (8). Although diabetes still reduced all of these parameters in PTH treated mice, bone density did not decline to the level of vehicle treated diabetics, and, in the 40 μg/kg group, were more closely aligned with those of healthy untreated controls. Similar to the non-diabetic mice, all of the trabecular bone parameters were significantly elevated (with the exception of trabecular spacing, which was significantly decreased) in the diabetic 40 μg/kg PTH group compared to the vehicle treated diabetics. The increase in bone density in diabetic PTH treated mice (compare to vehicle treated diabetics) was higher with the 40 μg/kg dose of PTH than with the 8 μg/kg dose, but 8 μg/kg PTH still

produced a significant increase in BVF and trabecular number. For example, trabecular number increased 25% in 8 μg/kg PTH treated diabetics and 39% in 40 μg/kg PTH treated diabetics.

Cortical bone thickness was significantly affected by diabetes and PTH treatment, according to ANOVA, but there was no significant interaction between diabetes and PTH. Thickness was increased in 40 μg/kg PTH treated euglycemic controls (compared to vehicle treated controls), but not 8 μg/kg treated controls (Table 8). This can be attributed to an increase outer perimeter in the 40 μg/kg group, which consequently increased both cortical and total area, while 8 μg/kg PTH did not. Similar to our previous findings, diabetes did not induce any significant changes in cortical bone parameters in vehicle treated mice. However, diabetes did reduce cortical thickness and cortical area in 40 μg/kg PTH treated mice compared to 40 μg/kg PTH treated controls, but these parameters were not significantly different from healthy untreated controls. No significant changes were found in cortical BMD, MOI, inner perimeter or marrow area.

Figure 29. **PTH treatment counteracted trabecular bone loss from T1-diabetes.** Diabetes was induced with STZ at 14 weeks of age. At the same time, control (citrate buffer only) and diabetic mice were started on a daily regimen of subcutaneous injections of PTH (8 or 40 μg/kg) or saline vehicle. PTH treatment was continued for the remainder of the study. Mice were harvested at 40 dpi and tibias were analyzed by μCT. (A) Representative three-dimensional isosurface images of the trabecular bone of the proximal tibia of control and diabetic, vehicle and PTH treated mice. (B) BVF of control (white bars) and diabetic (gray bars), vehicle and PTH treated mouse tibias. Bars represent mean ± standard error. N ≥ 12 per group. Significance determined with ANOVA. $^{*}p < 0.05$ compared to treatment (vehicle, 8 or 40 μg/kg PTH) matched control. $^{\wedge}p < 0.05$ compared to vehicle-treated control. $^{\#}p < 0.05$ compared to vehicle-treated diabetic.

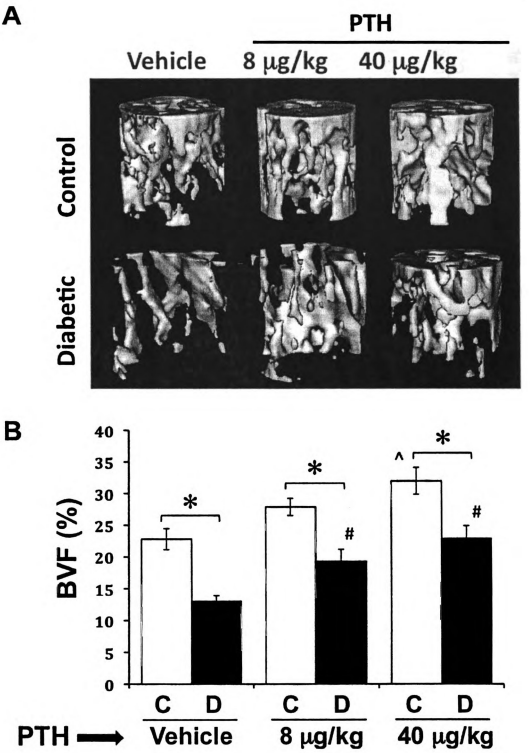
A
PTH
Vehicle
8 μg/kg
40 μg/kg
Control
Diabetic
B
BVF (%)
40
35
30
25
20
15
10
5
0
*
*
*
^
#
#
C
D
C
D
C
D
PTH
Vehicle
8 μg/kg
40 μg/kg

Table 8. μCT analysis of control and diabetic, vehicle and PTH treated mice at 40 dpi.

	Vehicle		8 μg/kg PTH		40 μg/kg PTH	
	C (n = 15)	D (n = 17)	C (n = 13)	D (n = 12)	C (n = 13)	D (n = 15)
TRABECULAR						
BMC (mg)	0.78 ± 0.03	0.62 ± 0.02*	0.84 ± 0.07	0.70 ± 0.04*	0.92 ± 0.06^	0.79 ± 0.05*#
BMD (mg/cm^3)	262 ± 9	208 ± 6*	283 ± 12	237 ± 13*	307 ± 17^	262 ± 14*#
BVF (%)	22.8 ± 1.7	13.0 ± 0.9*	27.9 ± 1.4	19.3 ± 1.2*#	32.0 ± 2.1^	22.9 ± 2.0*#
Tb Th (μm)	48 ± 2	36 ± 1*	54 ± 2	42 ± 2*	61 ± 4^	44 ± 2*#
Tb Sp (μm)	260 ± 19	277 ± 13	221 ± 23	247 ± 16	216 ± 18	227 ± 20#
Tb N (mm^{-1})	4.8 ± 0.3	3.6 ± 0.2*	5.4 ± 0.2	4.5 ± 0.2*#	5.6 ± 0.1^	5.0 ± 0.3*#
CORTICAL						
Th (μm)	328 ± 6	319 ± 7	344 ± 4	330 ± 7	360 ± 6^	329 ± 4*
MOI (mm^4)	0.091 ± 0.004	0.090 ± 0.004	0.087 ± 0.004	0.080 ± 0.005	0.102 ± 0.005	0.090 ± 0.006
Inner P (mm)	1.52 ± 0.03	1.55 ± 0.04	1.53 ± 0.04	1.48 ± 0.04	1.56 ± 0.04	1.61 ± 0.05
Outer P (mm)	3.72 ± 0.07	3.66 ± 0.05	3.82 ± 0.07	3.67 ± 0.07	3.95 ± 0.06^	3.86 ± 0.08
Mar. A (mm^2)	0.15 ± 0.01	0.16 ± 0.01	0.16 ± 0.01	0.15 ± 0.01	0.16 ± 0.01	0.17 ± 0.01
Cort. A (mm^2)	0.80 ± 0.02	0.77 ± 0.02	0.86 ± 0.02	0.79 ± 0.3	0.92 ± 0.02^	0.83 ± 0.03*
Total A (mm^2)	0.95 ± 0.03	0.93 ± 0.02	1.02 ± 0.03	0.93 ± 0.04	1.08 ± 0.03^	1.00 ± 0.04
BMD (mg/cm^3)	1071 ± 24	1042 ± 16	1086 ± 16	1071 ± 18	1065 ± 25	1060 ± 13

Abbreviations: A, area; BMC, bone mineral content; BMD, bone mineral density, BVF, bone volume fraction; C, control; Cort., cortical; D, diabetic; dpi, days post injection; Mar., marrow; MOI, moment of inertia; P, perimeter; PTH, parathyroid hormone; Sp, spacing; Tb, trabecular; Th, thickness.

Signficance: *$p < 0.05$ compared to treatment matched control; ^$p < 0.05$ compared to vehicle treated control; #$p < 0.05$ compared to vehicle treated diabetic.

6.4.3. PTH increased bone formation in a dose-dependent manner

PTH treatment of euglycemic control mice significantly (by factorial ANOVA) affected osteocalcin, such that there was a stepwise increase in expression that reached statistical significance in the 40 μg/kg PTH treated group (Figure 30A). Diabetes also had a significant effect on OC levels: diabetes reduced OC levels in untreated mice, consistent with previous findings, and that reduction remained evident in both PTH treated diabetic groups compared to PTH treated controls. However, as with the controls, PTH treatment increased osteocalcin in the diabetic mice compared to untreated diabetics, and this was significant with the 40 μg/kg dose. Furthermore, OC mRNA levels were not different in the diabetic 40 μg/kg mice compared to untreated controls, which suggests equivalent levels of bone formation in these two groups.

In order to address whether bone formation changes were due to altered osteoblast surface or rate of mineralization, we counted osteoblasts on the trabecular surface and examined the distance between calcein labels incorporated in to the bone. When expressed per mm bone surface, osteoblast number was not significantly elevated in either 8 or 40 μg/kg PTH treated control groups compared to untreated controls (Figure 30B). However, mineral apposition rate (MAR) was significantly increased in the 40 μg/kg PTH control group compared to untreated and 8 μg/kg PTH treated controls (Figure 30C), suggesting the increased bone formation was due to faster mineralization, rather than more bone forming surface. When made diabetic, untreated mice had

significantly less osteoblasts and reduced MAR, which is consistent with diabetic osteoporosis being primarily the result of an osteoblast defect. Interestingly, PTH treatment prevented any significant reduction in osteoblast number in diabetics compared to PTH treated controls (Figure 30B). Additionally, osteoblast number was significantly higher in PTH treated diabetic mice compared to untreated diabetic mice. MAR trended ($p = 0.08$) to be lower in the 8 μg/kg PTH treated diabetic mice compared to PTH treated controls (Figure 30C), which could still account for bone loss without altered osteoblast number. Similarly, MAR was significantly reduced in diabetic 40 μg/kg PTH treated mice compared to treatment-matched controls, but the value of MAR in 40 μg/kg PTH treated mice was not different from untreated control mice and was significantly higher than untreated diabetic mice. Taken together, high dose PTH appears capable of promoting bone formation in diabetic mice by preventing diabetes-induced loss of osteoblasts and by increasing MAR. Minor protection from bone loss in diabetic 8 μg/kg PTH treated mice was likely also due to improved osteoblast number and MAR.

Figure 30. **PTH promotes bone formation in diabetes.** (A) mRNA from frozen tibiae was converted to cDNA and amplified with primers specific for osteocalcin (OC) and the housekeeping gene HPRT. (B) Osteoblasts lining the surface of trabeculi in the distal femur were identified in hematoxylin stained slides based on morphology, counted, and expressed per mm bone surface. (C) The distance between calcein double labels was measured in undecalcified, unstained L5 vertebrae sections and expressed per day. Bars represent mean ± standard error of control (C, white bars) and diabetic (D, gray bars), vehicle, 8 μg/kg and 40 μg/kg PTH treated mice at 40 dpi. PTH treatment was daily from 0 to 40 dpi. N = 4-8 per group. Significance determined with ANOVA. $^{*}p < 0.05$ compared to treatment (vehicle, 8 or 40 μg/kg PTH) matched control. $^{\wedge}p < 0.05$ compared to vehicle treated control. $^{\wedge\wedge}p < 0.05$ compared to vehicle treated control and 8 μg/kg PTH treated control. $^{\#}p < 0.05$ compared to vehicle treated diabetic.

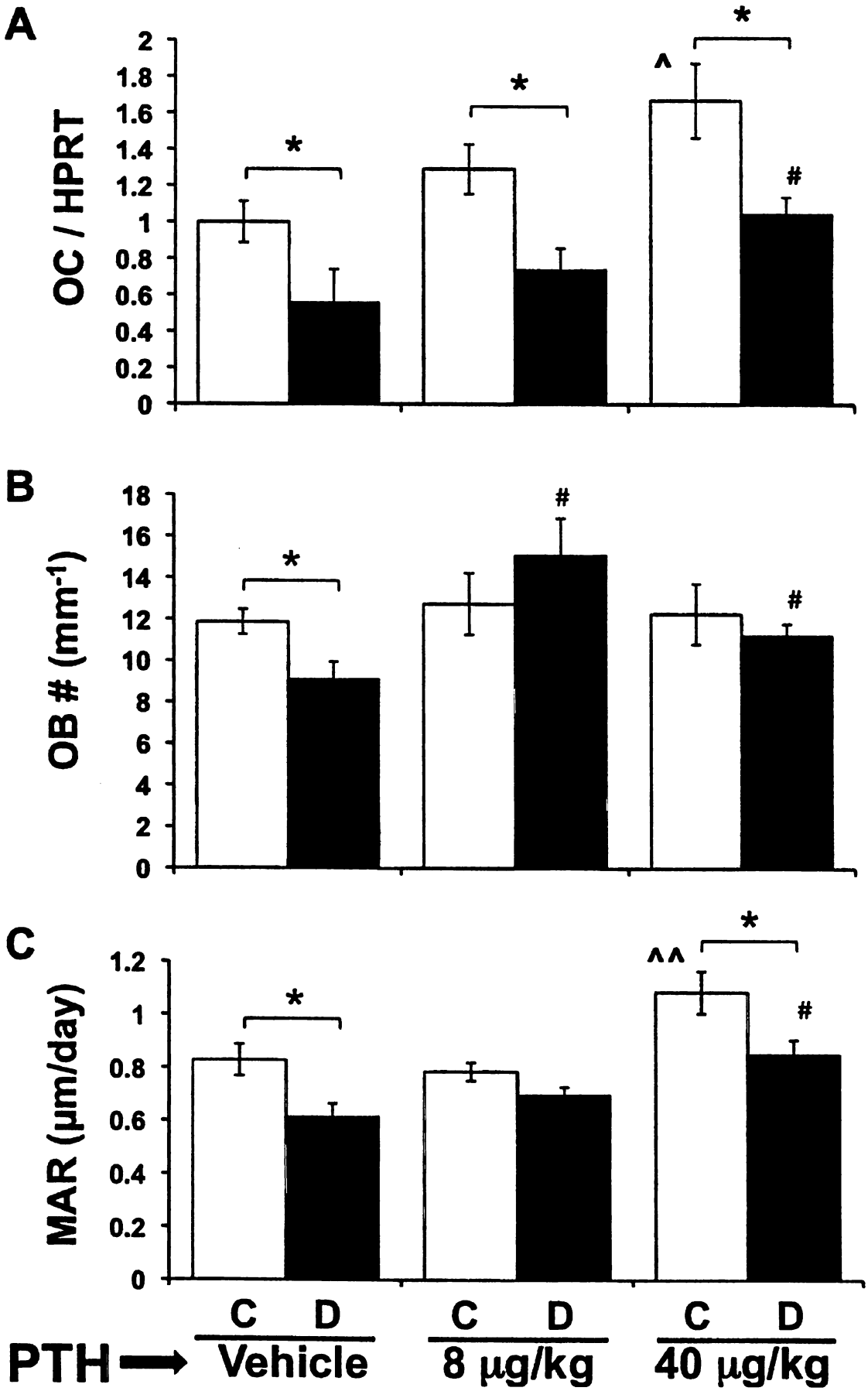
A
OC / HPRT
2
1.8
1.6
1.4
1.2
1
0.8
0.6
0.4
0.2
0
*
*
*
^
#
B
OB # (mm-1)
18
16
14
12
10
8
6
4
2
0
*
#
#
C
MAR (µm/day)
1.2
1
0.8
0.6
0.4
0.2
0
*
*
^^
#
C D C D C D
PTH
Vehicle
8 µg/kg
40 µg/kg

6.4.4. Effect of PTH on Bone Resorption

Total bone remodeling (as indicated by TRAP5 mRNA expression) was significantly elevated in the non-diabetic 40 μg/kg PTH treated group, but not in the 8 μg/kg group, compared to untreated controls (Figure 31A), which together with increased bone formation, is indicative of increased remodeling overall in the 40 μg/kg group. As we have demonstrated previously, diabetes did not alter total bone resorption in untreated mice, and this effect was consistent in the PTH treated groups. In agreement with overall increases in remodeling, the 40 μg/kg PTH treated diabetic mice had elevated TRAP5 expression compared to vehicle treated diabetic mice. We also examined osteoclast surface and did not find any significant diabetes or PTH effects, despite the increase in TRAP5 expression with the 40 μg/kg dose (Figure 31B). It is possible that there is more total resorption in these mice (since they have more bone surface), but when expressed as a function of total surface, it is unchanged. The fact that there is no change in osteoclast surface in diabetic vehicle treated mice compared to controls is consistent with our previous findings (8).

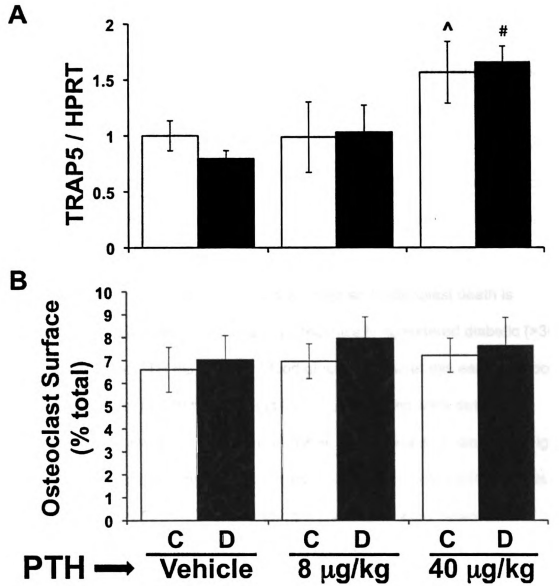

Figure 31. **High dose PTH promotes bone resorption in diabetic mice.** A) mRNA from frozen tibiae was converted to cDNA and amplified with primers specific for tartrate resistant acid phosphatase (TRAP5) and the housekeeping gene HPRT. (B) Osteoclasts were identified with TRAP5 staining in the distal femur. Length of trabecular bone surface covered by osteoclasts was measured and expressed as a percent of the total bone surface. Bars represent mean ± standard error of control (C, white bars) and diabetic (D, gray bars), vehicle, 8 μg/kg and 40 μg/kg PTH treated mice at 40 dpi. PTH treatment was daily from 0 to 40 dpi. N = 4-8 per group. Significance determined with ANOVA. $^{*}p < 0.05$ compared to treatment (vehicle, 8 or 40 μg/kg PTH) matched control. $^{\wedge}p < 0.05$ compared to vehicle-treated control. $^{\#}p < 0.05$ compared to vehicle-treated diabetic.

6.4.5. Osteoblast viability is improved by PTH treatment

We have previously demonstrated significantly elevated osteoblast death in diabetic mice throughout the time course of diabetes (Martin et al. 2010, *submitted*), which could account for the reduced osteoblast surface and MAR. In order to address the ability of PTH treatment to reduce diabetic osteoblast death, we induced diabetes as before, and simultaneously began treating control and diabetic mice with daily injections of 40 μg/kg PTH. We harvested the mice at 5 dpi, a time point shortly after blood glucose rises and osteoblast death is detectable (12), even though mice are not technically considered diabetic (>300 mg/dl) at this time. PTH did not alter blood glucose levels at this early time point (Figure 32B). No significant changes in RANKL/OPG ratio were detectable, which is consistent with no alterations in osteoclast activation in diabetes (Figure 32C). In order to address osteoblast activity, we measured tibia mRNA levels of osteocalcin (Figure 32D). PTH treatment trended to increase osteocalcin expression in non-diabetic mice ($p = 0.1$). As we have demonstrated in the past, osteocalcin was reduced nearly 5-fold in untreated diabetic mice compared to untreated controls (12). PTH-treated diabetic mice had significantly higher osteocalcin expression that untreated diabetics, which is consistent with our previous findings at 40 dpi (Figure 30). These results suggest that the early diabetes-induced reduction of bone formation can also be treated with PTH.

Because early bone changes have been demonstrated to be due to increased osteoblast apoptosis as well as reduced maturation, we examined

TUNEL-stained femur sections to quantify osteoblast death (Figure 32A and 32E). Consistent with our previous finding, TUNEL positive osteoblasts increased in untreated diabetic mice compared to controls. PTH-treatment of euglycemic mice significantly lowered baseline TUNEL staining. Although diabetes still induced osteoblast death in PTH-treated mice, the level of TUNEL staining was not different from untreated controls and trended to be lower than that in untreated diabetics. These results suggest that the mechanism of improved bone formation in PTH-treated diabetic mice could be reduced basal osteoblast apoptosis.

Figure 32. **PTH ameliorates diabetes-induced osteoblast death.** Mice were injected with either citrate buffer (control) or STZ to induce hyperglycemia. At the same time, control and diabetic mice were started on a daily regimen of subcutaneous injections of PTH (40 μg/kg) or saline vehicle. PTH treatment was continued until harvest at 5 dpi. (A) TUNEL stained trabecular bone in the distal femur. Dark brown nuclear stain (indicated by arrows) is positive for TUNEL label. (B) Blood glucose was measured at the time of harvest and was not significantly altered by PTH-treatment. mRNA from frozen tibiae was converted to cDNA and amplified with primers specific for RANKL or OPG (C) or with primers specific for OC and the housekeeping gene HPRT (D). (E) TUNEL positive osteoblasts were identified based on dark brown nuclear stain, counted and expressed relative to total osteoblasts. Bars represent mean ± standard error of control (C, white bars) and diabetic (D, gray bars), vehicle and 40 μg/kg PTH treated mice at 5 dpi. PTH treatment was daily from 0 to 5 dpi. N = 5-6 per group. Significance determined with student's t-test. $^{*}p < 0.05$ between bracketed bars.

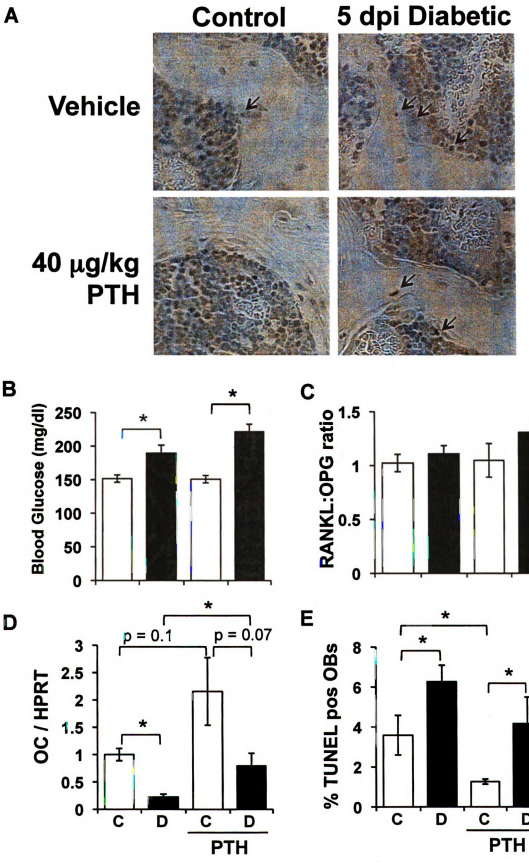
A
Control
5 dpi Diabetic
Vehicle
40 μg/kg PTH
B
Blood Glucose (mg/dl)
250
200
150
100
50
0
*
*
C
RANKL:OPG ratio
1.5
1
0.5
0
D
OC / HPRT
3
2.5
2
1.5
1
0.5
0
p = 0.1
p = 0.07
*
*
C
D
C
D
PTH
E
% TUNEL pos OBs
8
6
4
2
0
*
*
*
C
D
C
D
PTH

6.4.6. Diabetic bone loss can be reversed by PTH

Although PTH treatment was able to counteract bone loss when initiated simultaneously with diabetes induction (Figure 29 and Table 8), we recognize that diabetic patients will most likely not start treatment for bone loss when diagnosed with diabetes. Even if this were the case, diagnosis does not occur until after significant changes in blood glucose levels are evident, and based on our findings, after bone changes are initiated (12)(Martin et al., 2010, submitted). Therefore, we wanted to address whether PTH could improve bone density even after bone loss had already occurred.

We induced diabetes with streptozotocin as before. At 20 dpi, we either harvested control and diabetic mice, or treated control and diabetic mice with 40 μg/kg PTH or vehicle. At 20 dpi, diabetic mice had significantly lower BMD and showed a trend toward lower ($p = 0.07$) BVF (Figure 33A and 33B). Similarly, untreated diabetic mice at 40 dpi had lower BMD and BVF compared to untreated controls. Treating non-diabetic mice with 40 μg/kg PTH days 20-40 was not enough to induce a significant increase in BMD or BVF compared to untreated controls. However, treating diabetic mice with PTH days 20-40 increased BMD and BVF to levels not different from PTH-treated euglycemic controls, indicating short-term PTH imparts a stronger affect in diabetic mice than in controls.

To address the osteoblast/osteoclast phenotype in these mice we measured osteocalcin and TRAP5 mRNA levels (Figure 33C). We significantly

reduced osteocalcin levels at 20 dpi and 40 dpi in untreated diabetic bone compared to untreated controls. PTH treatment days 20-40 promoted osteocalcin expression in both control and diabetic mice, although the increase was not significant. However, osteocalcin levels in PTH-treated diabetic mice were not different from untreated controls. Similar to our previous findings, the resorption marker TRAP5 was unchanged or trended to decrease in diabetic mice at days 20 and 40, respectively. PTH treatment for the last 20 days of the experiment was not enough to increase TRAP5 levels in euglycemic mice. Similarly, TRAP5 expression tended toward increased levels in PTH-treated diabetic mice compared to untreated diabetic mice at 40 dpi, but this was not statistically significant. Fortunately, however, PTH is capable of restoring trabecular bone density to normal levels even after bone loss has already occurred.

Figure 33. **PTH promotes bone formation in diabetic mice when initiated after diabetic bone loss is detectable.** Mice were treated with streptozotocin to induce diabetes or citrate buffer (control). At 20 dpi, mice were either harvested, or treated with vehicle or 40 μg/kg PTH daily until harvest at 40 dpi. (A) Representative μCT isosurface images of trabecular bone immediately distal to the proximal growth plate. (B) Tibia bone mineral density (BMD) and bone volume fraction (BVF) from control (C, white bars) and diabetic (D, dark gray bars) untreated and PTH treated mice. (C) mRNA from frozen tibiae was converted to cDNA and amplified with primers specific for the bone formation marker osteocalcin or resorption marker TRAP5 and expressed relative to the housekeeping gene, HPRT. Bars represent mean ± standard error. $N \geq 6$ per group. Significance determined with student's t-test. $^{*}p < 0.05$ between bracketed bars.

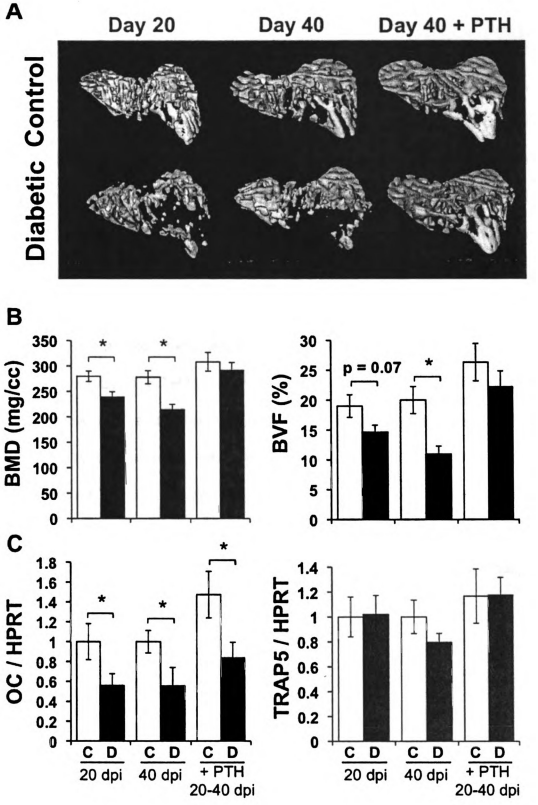
A
Day 20
Day 40
Day 40 + PTH
Diabetic Control
B
BMD (mg/cc)
350
300
250
200
150
100
50
0
*
*
BVF (%)
30
25
20
15
10
5
0
p = 0.07
*
C
OC / HPRT
1.8
1.6
1.4
1.2
1
0.8
0.6
0.4
0.2
0
*
*
*
TRAP5 / HPRT
1.4
1.2
1
0.8
0.6
0.4
0.2
0
C D
20 dpi
C D
40 dpi
C D
+ PTH
20-40 dpi

6.5. DISCUSSION

Osteoporosis is a severe complication of T1-diabetes that results from reduced bone formation, and unchanged or reduced resorption. Therefore, we wanted to determine whether anabolic, intermittent PTH therapy was capable of enhancing bone formation in T1-diabetes, and apropos, whether it would be an appropriate therapy for diabetic patients. Briefly, we found that 40 μg/kg PTH (and to a lesser extent 8 μg/kg PTH) counteracted trabecular bone changes when diabetic mice were treated daily for 40 days, starting at the same time as the diabetes-inducing streptozotocin injections. The higher dose of PTH was able to promote overall bone remodeling by increasing osteocalcin expression, MAR, osteoblast number and TRAP5 expression in diabetic mice. In addition, PTH treatment lowered basal osteoblast apoptosis, such that diabetes-induced osteoblast apoptosis levels were not different from apoptosis levels in control, untreated mice. Finally, we also determined that PTH treatment was capable of reversing diabetic bone loss after significant trabecular bone changes had already occurred, which makes PTH treatment in diabetic patients clinically relevant.

6.5.1. Both low and high dose PTH treats trabecular bone loss from diabetes

Although diabetes significantly reduced MAR and osteocalcin expression in 40 μg/kg PTH-treated mice, PTH treatment increased baseline levels of bone formation such that the values in diabetic PTH-treated mice did not differ from

those of untreated controls. This is consistent with the known PTH regulation of osteoblast proliferation and differentiation, and stimulation of Runx2 transcriptional activity (by which osteocalcin is regulated) (54, 55). Similarly, tail-suspended mice treated with 40 μg/kg PTH (5 days/wk) had increased bone formation rate, albeit to a lesser extent that control mice (42). Our finding that diabetic PTH treated bone parameters do not differ from untreated controls is extremely significant. Treating human diabetic patients with PTH may promote bone formation, and overall remodeling, to levels that are comparable to healthy age-matched subjects, which would be the ultimate goal of any therapy.

Low dose 8 μg/kg PTH did not significantly increase trabecular bone density in control mice, but there was a clear trend toward increased bone formation based on bone density measurements and tibia osteocalcin expression (Figure 29, Table 8, Figure 30). Interestingly, PTH appeared to be more capable of increasing bone density in the diabetic mice: 8 μg/kg PTH treated diabetic mice had significantly higher BVF, trabecular number and osteoblast number compared to untreated diabetic mice and did not have reduced MAR compared to 8 μg/kg PTH treated controls. In younger 9.5-week-old C57BL/6 mice, 10 μg/kg PTH modestly increased trabecular bone density parameters (56), suggesting that even a slightly higher dose might have had a significant effect in our euglycemic mice. In rats and after bone perturbations, effective doses of PTH appear to be much lower: 1 μg/kg PTH was capable of increasing bone density in hind-limb unloaded rats (57), although it was unclear whether this dose would have had an effect in healthy, load bearing rats in this study. Similarly, rats had

increased BMC, BMD, and fracture healing by day 21 of 30 mg/kg PTH treatment and by day 35 of 5 μg/kg PTh treatment (58). In another study 10 μg/kg PTH increased ultimate load to failure, BMD, BMC of rats by 28 days after fracture (59). Thus, it is possible that if our experiment had extended longer, we would have seen a significant effect with the 8 μg/kg dose in the control mice, and a stronger effect in the diabetic mice. Pettway, et al. demonstrated that the greatest increases in osteoblast proliferation occur after the first week of treatment (54). This idea, in combination with the fact that lower dose (8 μg/kg) PTH is capable of improving bone density (Table 8), suggests that an ideal treatment regimen might consist of an initial time period of high dose PTH to stimulate bone formation, followed by lower dose PTH to maintain bone density at a healthy level.

6.5.2. PTH restores bone density after it has occurred

We determined that PTH could restore bone density to normal levels even after bone loss had already occurred from diabetes (Figure 33), which is consistent with other bone loss conditions, but has not been demonstrated with diabetes. Sibonga, et al. demonstrated that 80 μg/kg PTH could restore preexisting bone density in rats fed alcohol, which, like diabetes reduces bone formation (46). Additionally, the same dose of PTH reverses bone loss from ovariectomy in rats (44). Lozano, et al. demonstrated increased bone formation in diabetic mice treated with PTHrP, which signals through the shared

PTH/PTHrP receptor, two weeks after diabetes was confirmed, a time point when bone loss should have been detectable (17, 48, 53). It was important to address this issue because pathways responsible for bone loss from T1-diabetes (which are not completely understood) could overlap with the pathways for PTH induced bone formation, and if this were the case, then PTH might not have been an effective therapeutic.

6.5.3. Diabetic response to PTH is stronger

Interestingly, we determined that PTH-treatment of diabetic mice during the 20-day period had a greater effect than PTH-treatment of control mice for 20 days (Figure 33). It is possible that the diabetes-induced suppression of resorption actually helped bone density increase faster in the diabetic group, although we did not detect a significant suppression of TRAP5 expression from diabetes ($p = 0.2$) in this case. Along the same lines, PTH did not increase osteoblast number per bone surface (Figure 30B) in control mice, but it did prevent a decrease after diabetes induction, suggesting a stronger response of osteoblasts to PTH in a diabetic environment.

Martin, et al. 2010 (submitted) demonstrated that bone marrow cell composition is altered at early time points during diabetes-induction, and could potentially be altered throughout the disease. This could account for increased expression of inflammatory cytokines we have observed in diabetic bone (12). Recent evidence suggests that intermittent PTH requires T-cell derived

expression of the potent osteogenic protein Wnt10b, and that its action is through canonical wnt signaling (41). However, it is unclear how important canconical wnt signaling is for PTH induced bone formation. The absense of LRP5 (a canonical wnt coreceptor) does not alter PTH-induced increases in bone density in male or female mice (60, 61). Similarly, LRP5 is not required for high bone remodeling caused by overexpression of PTH/PTHrP receptor in osteocytes, but it is required for the high bone mass phenotype in these mice (62). However, canonical wnt signaling can also work through LRP6. Interestingly, PTH is capable of activating TCF-dependent transcription by phosphorylating/inactivating GSK3β through the PKA/cAMP pathway (63). This could account for some of the observed effects of PTH on wnt pathway family members (37). There is also evidence that PTH works through Wnt4, a non-canonical wnt ligand that does not require LRP5/6 (64-66). Whether or not marrow alterations affect the potency of PTH treatment, the ability of PTH to stimulate bone formation faster in diabetic mice supports the notion that osteoporosis treatments should be tailored to etiology of the disease and warrants further investigation into the effects of PTH therapy in human subjects with T1-diabetes.

6.5.4. Reduction of osteoblast death: basal and diabetes induced

In addition to PTH-induced osteoblast differentiation and activity, there is ever-increasing evidence that PTH prevents osteoblast apoptosis. Bellido, et al.

demonstrated a significant reduction of osteoblast apoptosis with 10-300 μg/kg after 28 days in female Swiss-Webster mice (36). Here, we demonstrated that 40 μg/kg PTH reduced basal osteoblast apoptosis and reduced diabetes-induced increases in osteoblast apoptosis to a level comparable to that of untreated control mice (Figure 32). The mechanism of PTH protection against apoptosis may be dependent on Smad3 (67, 68). Recent evidence indicates that PTH promotes repair of DNA damage by increasing PCNA and Foxo3a (69).

6.5.5. Cortical bone effects

Although it appeared that trabecular effects of PTH were stronger in diabetes, we have some evidence that cortical effects of PTH were weakened by diabetes. We found that 40 μg/kg PTH treatment increased cortical bone thickness and outer perimeter in euglycemic mice. This is consistent with other studies in ovariectomized mice and rats (70, 71), however in our case, PTH could not increase cortical thickness in diabetic mice compared to diabetic controls (Table 8). This suggests that the mechanism of cortical bone accrual in PTH treated mice is affected by diabetes whereas the mechanism of trabecular bone accrual is not. Calvi, et al. demonstrated a similar phenomenon: when the PTH receptor was constitutively active, trabecular bone density increased while periosteal MAR and cortical thickness decreases (72), suggesting the mechanism of PTH action is location-dependent. Recently, Jilka, et al. found that although PTH has a profound anti-apoptotic effect in trabecular bone, cortical

bone accrual from PTH is more likely due to pro-differentiation effects on preosteoblasts because of the comparatively low levels of osteoblast apoptosis in the periosteum, coupled with fast (2 day) increases in periosteal osteoblast number after PTH treatment (73, 74). Levels of hyperglycemia equivalent to those in diabetes are known to have anti-differentiation as well as pro-apoptotic effects on osteoblasts (75)(Martin, et al. 2010) and it is likely that both differentiation and apoptosis play a role in the diabetic osteoblast phenotype.

6.6. SUMMARY

Our data indicate that PTH is an effective treatment for T1-diabetic bone loss in mice because it promotes remodeling and reduces diabetes-induced osteoblast apoptosis. Because of its ability to restore bone density to normal levels, even after bone loss has already occurred, it is likely to be an effective therapeutic in human patients. Intermittent PTH therapy might be a better option than the commonly used antiresorptive bisphosphonates because of its ability to promote bone formation and resorption, which are both depressed in diabetic patients.

6.7. ACKNOWLEDGEMENTS

The authors thank Laurie McCauley for her advice on PTH treatment. The authors thank Regina Irwin and Lindsay Martin for technical assistance and

critical review of the manuscript, and the MSU Investigative Histology Laboratory for technical assistance. This work was funded by grants from the National Institutes of Health (RO1DK061184) and the American Diabetes Association (7-07-RA-105) to LRM. The authors have no financial conflicts.

6.8. REFERENCES

1. **McCabe LR** 2007 Understanding the pathology and mechanisms of type I diabetic bone loss. J Cell Biochem 102:1343-1357

2. **Auwerx J, Dequeker J, Bouillon R, Geusens P, Nijs J** 1988 Mineral metabolism and bone mass at peripheral and axial skeleton in diabetes mellitus. Diabetes 37:8-12

3. **Kemink SA, Hermus AR, Swinkels LM, Lutterman JA, Smals AG** 2000 Osteopenia in insulin-dependent diabetes mellitus; prevalence and aspects of pathophysiology. J Endocrinol Invest 23:295-303

4. **Levin ME, Boisseau VC, Avioli LV** 1976 Effects of diabetes mellitus on bone mass in juvenile and adult-onset diabetes. N Engl J Med 294:241-245

5. **Gandhi A, Beam HA, O'Connor JP, Parsons JR, Lin SS** 2005 The effects of local insulin delivery on diabetic fracture healing. Bone 37:482-490

6. **Follak N, Kloting L, Wolf E, Merk H** 2004 Delayed remodeling in the early period of fracture healing in spontaneously diabetic BB/OK rats depending on the diabetic metabolic state. Histol Histopathol 19:473-486

7. **Bouillon R, Bex M, Van Herck E, Laureys J, Dooms L, Lesaffre E, Ravussin E** 1995 Influence of age, sex, and insulin on osteoblast function: osteoblast dysfunction in diabetes mellitus. J Clin Endocrinol Metab 80:1194-1202

8. **Botolin S, Faugere MC, Malluche H, Orth M, Meyer R, McCabe LR** 2005 Increased bone adiposity and peroxisomal proliferator-activated receptor-gamma2 expression in type I diabetic mice. Endocrinology 146:3622-3631

9. **Goodman WG, Hori MT** 1984 Diminished bone formation in experimental diabetes. Relationship to osteoid maturation and mineralization. Diabetes 33:825-831

10. **Holl RW, Grabert M, Heinze E, Sorgo W, Debatin KM** 1998 Age at onset and long-term metabolic control affect height in type-1 diabetes mellitus. Eur J Pediatr 157:972-977

11. **Danne T, Kordonouri O, Enders I, Weber B** 1997 Factors influencing height and weight development in children with diabetes. Results of the Berlin Retinopathy Study. Diabetes Care 20:281-285

12. **Motyl KJ, Botolin S, Irwin R, Appledorn DM, Kadakia T, Amalfitano A, Schwartz RC, McCabe LR** 2009 Bone inflammation and altered gene expression with type I diabetes early onset. J Cell Physiol 218:575-583

13. **Fowlkes JL, Bunn RC, Liu L, Wahl EC, Coleman HN, Cockrell GE, Perrien DS, Lumpkin CK, Jr., Thrailkill KM** 2008 Runt-related transcription factor 2 (RUNX2) and RUNX2-related osteogenic genes are down-regulated throughout osteogenesis in type 1 diabetes mellitus. Endocrinology 149:1697-1704

14. **Botolin S, McCabe LR** 2007 Bone loss and increased bone adiposity in spontaneous and pharmacologically induced diabetic mice. Endocrinology 148:198-205

15. **Martin LM, McCabe LR** 2007 Type I diabetic bone phenotype is location but not gender dependent. Histochem Cell Biol 128:125-133

16. **Motyl KJ, McCabe LR** 2009 Leptin treatment prevents type I diabetic marrow adiposity but not bone loss in mice. J Cell Physiol 218:376-384

17. **Botolin S, McCabe LR** 2006 Inhibition of PPARgamma prevents type I diabetic bone marrow adiposity but not bone loss. J Cell Physiol 209:967-976

18. **Tashjian AH, Jr., Gagel RF** 2006 Teriparatide [human PTH(1-34)]: 2.5 years of experience on the use and safety of the drug for the treatment of osteoporosis. J Bone Miner Res 21:354-365

19. **Russell RG, Rogers MJ** 1999 Bisphosphonates: from the laboratory to the clinic and back again. Bone 25:97-106

20. **Russell RG** 2006 Bisphosphonates: from bench to bedside. Ann N Y Acad Sci 1068:367-401

21. **Goh SK, Yang KY, Koh JS, Wong MK, Chua SY, Chua DT, Howe TS** 2007 Subtrochanteric insufficiency fractures in patients on alendronate therapy: a caution. J Bone Joint Surg Br 89:349-353

22. **Lenart BA, Lorich DG, Lane JM** 2008 Atypical fractures of the femoral diaphysis in postmenopausal women taking alendronate. N Engl J Med 358:1304-1306

23. **Neviaser AS, Lane JM, Lenart BA, Edobor-Osula F, Lorich DG** 2008 Low-energy femoral shaft fractures associated with alendronate use. J Orthop Trauma 22:346-350

24. **Kwek EB, Goh SK, Koh JS, Png MA, Howe TS** 2008 An emerging pattern of subtrochanteric stress fractures: a long-term complication of alendronate therapy? Injury 39:224-231

25. **Abrahamsen B, Eiken P, Eastell R** 2009 Subtrochanteric and diaphyseal femur fractures in patients treated with alendronate: a register-based national cohort study. J Bone Miner Res 24:1095-1102

26. **Migliorati CA, Schubert MM, Peterson DE** 2009 Bisphosphonate osteonecrosis (BON): unanswered questions and research possibilities. Rev Recent Clin Trials 4:99-109

27. **Mariotti A** 2008 Bisphosphonates and osteonecrosis of the jaws. J Dent Educ 72:919-929

28. **Khamaisi M, Regev E, Yarom N, Avni B, Leitersdorf E, Raz I, Elad S** 2007 Possible association between diabetes and bisphosphonate-related jaw osteonecrosis. J Clin Endocrinol Metab 92:1172-1175

29. **Vahle JL, Long GG, Sandusky G, Westmore M, Ma YL, Sato M** 2004 Bone neoplasms in F344 rats given teriparatide [rhPTH(1-34)] are dependent on duration of treatment and dose. Toxicol Pathol 32:426-438

30. **Vahle JL, Sato M, Long GG, Young JK, Francis PC, Engelhardt JA, Westmore MS, Linda Y, Nold JB** 2002 Skeletal changes in rats given daily subcutaneous injections of recombinant human parathyroid hormone (1-34) for 2 years and relevance to human safety. Toxicol Pathol 30:312-321

31. **Barnes GL, Kakar S, Vora S, Morgan EF, Gerstenfeld LC, Einhorn TA** 2008 Stimulation of fracture-healing with systemic intermittent parathyroid hormone treatment. J Bone Joint Surg Am 90 Suppl 1:120-127

32. **Dempster DW, Cosman F, Parisien M, Shen V, Lindsay R** 1993 Anabolic actions of parathyroid hormone on bone. Endocr Rev 14:690-709

33. **Neer RM, Arnaud CD, Zanchetta JR, Prince R, Gaich GA, Reginster JY, Hodsman AB, Eriksen EF, Ish-Shalom S, Genant HK, Wang O, Mitlak BH** 2001 Effect of parathyroid hormone (1-34) on fractures and bone mineral density in postmenopausal women with osteoporosis. N Engl J Med 344:1434-1441

34. **Burr DB, Hirano T, Turner CH, Hotchkiss C, Brommage R, Hock JM** 2001 Intermittently administered human parathyroid hormone(1-34) treatment increases intracortical bone turnover and porosity without reducing bone strength in the humerus of ovariectomized cynomolgus monkeys. J Bone Miner Res 16:157-165

35. **Jilka RL** 2007 Molecular and cellular mechanisms of the anabolic effect of intermittent PTH. Bone 40:1434-1446

36. **Bellido T, Ali AA, Plotkin LI, Fu Q, Gubrij I, Roberson PK, Weinstein RS, O'Brien CA, Manolagas SC, Jilka RL** 2003 Proteasomal degradation of Runx2 shortens parathyroid hormone-induced anti-apoptotic signaling in osteoblasts. A putative explanation for why intermittent administration is needed for bone anabolism. J Biol Chem 278:50259-50272

37. **Kulkarni NH, Halladay DL, Miles RR, Gilbert LM, Frolik CA, Galvin RJ, Martin TJ, Gillespie MT, Onyia JE** 2005 Effects of parathyroid hormone on Wnt signaling pathway in bone. J Cell Biochem 95:1178-1190

38. **Kang S, Bennett CN, Gerin I, Rapp LA, Hankenson KD, Macdougald OA** 2007 Wnt signaling stimulates osteoblastogenesis of mesenchymal precursors by suppressing CCAAT/enhancer-binding protein alpha and

peroxisome proliferator-activated receptor gamma. J Biol Chem 282:14515-14524

39. **Bennett CN, Ouyang H, Ma YL, Zeng Q, Gerin I, Sousa KM, Lane TF, Krishnan V, Hankenson KD, MacDougald OA** 2007 Wnt10b increases postnatal bone formation by enhancing osteoblast differentiation. J Bone Miner Res 22:1924-1932

40. **Keller H, Kneissel M** 2005 SOST is a target gene for PTH in bone. Bone 37:148-158

41. **Terauchi M, Li JY, Bedi B, Baek KH, Tawfeek H, Galley S, Gilbert L, Nanes MS, Zayzafoon M, Guldberg R, Lamar DL, Singer MA, Lane TF, Kronenberg HM, Weitzmann MN, Pacifici R** 2009 T lymphocytes amplify the anabolic activity of parathyroid hormone through Wnt10b signaling. Cell Metab 10:229-240

42. **Tanaka S, Sakai A, Tanaka M, Otomo H, Okimoto N, Sakata T, Nakamura T** 2004 Skeletal unloading alleviates the anabolic action of intermittent PTH(1-34) in mouse tibia in association with inhibition of PTH-induced increase in c-fos mRNA in bone marrow cells. J Bone Miner Res 19:1813-1820

43. **Liu CC, Kalu DN** 1990 Human parathyroid hormone-(1-34) prevents bone loss and augments bone formation in sexually mature ovariectomized rats. J Bone Miner Res 5:973-982

44. **Liu CC, Kalu DN, Salerno E, Echon R, Hollis BW, Ray M** 1991 Preexisting bone loss associated with ovariectomy in rats is reversed by parathyroid hormone. J Bone Miner Res 6:1071-1080

45. **Turner RT, Evans GL, Cavolina JM, Halloran B, Morey-Holton E** 1998 Programmed administration of parathyroid hormone increases bone formation and reduces bone loss in hindlimb-unloaded ovariectomized rats. Endocrinology 139:4086-4091

46. **Sibonga JD, Iwaniec UT, Shogren KL, Rosen CJ, Turner RT** 2007 Effects of parathyroid hormone (1-34) on tibia in an adult rat model for chronic alcohol abuse. Bone 40:1013-1020

47. **Tsuchida T, Sato K, Miyakoshi N, Abe T, Kudo T, Tamura Y, Kasukawa Y, Suzuki K** 2000 Histomorphometric evaluation of the recovering effect of human parathyroid hormone (1-34) on bone structure and turnover in streptozotocin-induced diabetic rats. Calcif Tissue Int 66:229-233

48. **Lozano D, de Castro LF, Dapia S, Andrade-Zapata I, Manzarbeitia F, Alvarez-Arroyo MV, Gomez-Barrena E, Esbrit P** 2009 Role of parathyroid hormone-related protein in the decreased osteoblast function in diabetes-related osteopenia. Endocrinology 150:2027-2035

49. **Vengellur A, LaPres JJ** 2004 The role of hypoxia inducible factor 1alpha in cobalt chloride induced cell death in mouse embryonic fibroblasts. Toxicol Sci 82:638-646

50. **Ontiveros C, McCabe LR** 2003 Simulated microgravity suppresses osteoblast phenotype, Runx2 levels and AP-1 transactivation. J Cell Biochem 88:427-437

51. **Wiren KM, Zhang XW, Toombs AR, Kasparcova V, Gentile MA, Harada S, Jepsen KJ** 2004 Targeted overexpression of androgen receptor in osteoblasts: unexpected complex bone phenotype in growing animals. Endocrinology 145:3507-3522

52. **Zhao S, Zhang YK, Harris S, Ahuja SS, Bonewald LF** 2002 MLO-Y4 osteocyte-like cells support osteoclast formation and activation. J Bone Miner Res 17:2068-2079

53. **Motyl K, McCabe LR** 2009 Streptozotocin, Type I Diabetes Severity and Bone. Biol Proced Online

54. **Pettway GJ, Meganck JA, Koh AJ, Keller ET, Goldstein SA, McCauley LK** 2008 Parathyroid hormone mediates bone growth through the regulation of osteoblast proliferation and differentiation. Bone 42:806-818

55. **Krishnan V, Moore TL, Ma YL, Helvering LM, Frolik CA, Valasek KM, Ducy P, Geiser AG** 2003 Parathyroid hormone bone anabolic action requires Cbfa1/Runx2-dependent signaling. Mol Endocrinol 17:423-435

56. **Niziolek PJ, Murthy S, Ellis SN, Sukhija KB, Hornberger TA, Turner CH, Robling AG** 2009 Rapamycin impairs trabecular bone acquisition from high-dose but not low-dose intermittent parathyroid hormone treatment. J Cell Physiol 221:579-585

57. **Turner RT, Evans GL, Lotinun S, Lapke PD, Iwaniec UT, Morey-Holton E** 2007 Dose-response effects of intermittent PTH on cancellous bone in hindlimb unloaded rats. J Bone Miner Res 22:64-71

58. **Alkhiary YM, Gerstenfeld LC, Krall E, Westmore M, Sato M, Mitlak BH, Einhorn TA** 2005 Enhancement of experimental fracture-healing by systemic administration of recombinant human parathyroid hormone (PTH 1-34). J Bone Joint Surg Am 87:731-741

59. **Nakajima A, Shimoji N, Shiomi K, Shimizu S, Moriya H, Einhorn TA, Yamazaki M** 2002 Mechanisms for the enhancement of fracture healing in rats treated with intermittent low-dose human parathyroid hormone (1-34). J Bone Miner Res 17:2038-2047

60. **Iwaniec UT, Wronski TJ, Liu J, Rivera MF, Arzaga RR, Hansen G, Brommage R** 2007 PTH stimulates bone formation in mice deficient in Lrp5. J Bone Miner Res 22:394-402

61. **Sawakami K, Robling AG, Ai M, Pitner ND, Liu D, Warden SJ, Li J, Maye P, Rowe DW, Duncan RL, Warman ML, Turner CH** 2006 The Wnt co-receptor LRP5 is essential for skeletal mechanotransduction but not for the anabolic bone response to parathyroid hormone treatment. J Biol Chem 281:23698-23711

62. **O'Brien CA, Plotkin LI, Galli C, Goellner JJ, Gortazar AR, Allen MR, Robling AG, Bouxsein M, Schipani E, Turner CH, Jilka RL, Weinstein RS, Manolagas SC, Bellido T** 2008 Control of bone mass and remodeling by PTH receptor signaling in osteocytes. PLoS One 3:e2942

63. **Suzuki A, Ozono K, Kubota T, Kondou H, Tachikawa K, Michigami T** 2008 PTH/cAMP/PKA signaling facilitates canonical Wnt signaling via inactivation of glycogen synthase kinase-3beta in osteoblastic Saos-2 cells. J Cell Biochem 104:304-317

64. **Bergenstock MK, Partridge NC** 2007 Parathyroid hormone stimulation of noncanonical Wnt signaling in bone. Ann N Y Acad Sci 1116:354-359

65. **Li X, Liu H, Qin L, Tamasi J, Bergenstock M, Shapses S, Feyen JH, Notterman DA, Partridge NC** 2007 Determination of dual effects of parathyroid hormone on skeletal gene expression in vivo by microarray and network analysis. J Biol Chem 282:33086-33097

66. **Li X, Qin L, Bergenstock M, Bevelock LM, Novack DV, Partridge NC** 2007 Parathyroid hormone stimulates osteoblastic expression of MCP-1 to recruit and increase the fusion of pre/osteoclasts. J Biol Chem 282:33098-33106

67. **Sowa H, Kaji H, Iu MF, Tsukamoto T, Sugimoto T, Chihara K** 2003 Parathyroid hormone-Smad3 axis exerts anti-apoptotic action and augments anabolic action of transforming growth factor beta in osteoblasts. J Biol Chem 278:52240-52252

68. **Tobimatsu T, Kaji H, Sowa H, Naito J, Canaff L, Hendy GN, Sugimoto T, Chihara K** 2006 Parathyroid hormone increases beta-catenin levels through Smad3 in mouse osteoblastic cells. Endocrinology 147:2583-2590

69. **Schnoke M, Midura SB, Midura RJ** 2009 Parathyroid hormone suppresses osteoblast apoptosis by augmenting DNA repair. Bone 45:590-602

70. **Fox J, Miller MA, Newman MK, Metcalfe AF, Turner CH, Recker RR, Smith SY** 2006 Daily treatment of aged ovariectomized rats with human parathyroid hormone (1-84) for 12 months reverses bone loss and enhances trabecular and cortical bone strength. Calcif Tissue Int 79:262-272

71. **Pierroz DD, Bouxsein ML, Rizzoli R, Ferrari SL** 2006 Combined treatment with a beta-blocker and intermittent PTH improves bone mass and microarchitecture in ovariectomized mice. Bone 39:260-267

72. **Calvi LM, Sims NA, Hunzelman JL, Knight MC, Giovannetti A, Saxton JM, Kronenberg HM, Baron R, Schipani E** 2001 Activated parathyroid hormone/parathyroid hormone-related protein receptor in osteoblastic cells differentially affects cortical and trabecular bone. J Clin Invest 107:277-286

73. **Jilka RL, O'Brien CA, Ali AA, Roberson PK, Weinstein RS, Manolagas SC** 2009 Intermittent PTH stimulates periosteal bone formation by actions on post-mitotic preosteoblasts. Bone 44:275-286

74. **Ogita M, Rached MT, Dworakowski E, Bilezikian JP, Kousteni S** 2008 Differentiation and proliferation of periosteal osteoblast progenitors are differentially regulated by estrogens and intermittent parathyroid hormone administration. Endocrinology 149:5713-5723

75. **Botolin S, McCabe LR** 2006 Chronic hyperglycemia modulates osteoblast gene expression through osmotic and non-osmotic pathways. J Cell Biochem 99:411-424